

Paleo-hydrogeographic reconstruction of the groundwater salinity in the Ayeyarwady Delta, Myanmar, using a 3D variable-density groundwater model



24 June 2020

Utrecht University
Faculty of Geosciences
Earth Surface and Water
Hydrology

Paleo-hydrogeographic reconstruction of the
groundwater salinity in the Ayeyarwady Delta,
Myanmar, using a 3D variable-density groundwater
model

24 June 2020



Utrecht University



ARCADIS

Design & Consultancy
for natural and
built assets

*In loving memory of my grandmother. Thank you for always being
there for me.*

~ Dorothea Geertruida de Vlaming, 1923 – 2020 ~

Abstract

English

River deltas, in general densely populated, facilitate the needs of a large part of the world's population. One of the underlying reasons is their inherent high quality and easily obtained fresh water supply, mostly in the form of groundwater. Considering their socio-economic status, securing groundwater as a natural resource for the future is therefore important.

To improve the understanding of imposed pressures that influence the groundwater regime, hydrogeological modelling can be an insightful tool. However, necessary input data to run such models are not always readily available.

In this MSc research, a previously constructed 3D variable-density groundwater flow model of the Ayeyarwady Delta was enhanced to serve the Regional Water Security Study (RWSS) in Myanmar. This RWSS study aims to formulate measures for the near future concerning freshwater security.

Using regionally collected and processed data, in combination with literature research and fieldwork, improvements were realized through the addition of a voxel model of the local hydrogeology and a groundwater extraction component, as well as the performance of a "paleo-reconstruction", considering the past 130 kyears during which sea levels fluctuations were inserted.

A comparison was made between the calculated changes in future hydraulic head and groundwater salinity for the expected changes in groundwater extractions and climate change induced sea level rise and recharge until 2050 to determine the Ayeyarwady Delta groundwater regime's relative sensitivity to these individual and combined climate and anthropogenic stresses.

The results indicate residual saline groundwater pockets from preceding transgression have been removed almost completely before reaching the sea level of 7000 BP (equal to present-day sea level). Subsequent modelling of a shortened paleo-reconstruction of 6425 year provided almost identical results, suggesting that paleo-reconstructive modelling is sufficiently accurate in predicting the initial salinity distribution when modelled from the moment the first transgression exceeds present-day sea level. Neglecting to include the effects of sea-level rise in modelling delta groundwater development resulted in an overestimation of the fresh groundwater supply by roughly 33% ($\approx 695 \text{ km}^3$) and therefore might be considered injudicious.

Within the foreseeable future, a decrease in recharge, a sea-level rise due to climate change and an increase in groundwater extraction due to population growth and increased agricultural development are expected. Modelling efforts suggest salinization will be largest through sea-level rise, affecting the entire coastal region up to 15 km inward, being most felt to the southwest of the Ayeyarwady Delta. Recharge reductions on the other hand are expected to be dominant land inwards, playing only a minor contributing role in salinization of fresh groundwater reserves when compared to sea-level rise. Effects of groundwater extractions are more localized to regions with drawdowns scattered throughout the middle and upper Ayeyarwady Delta and surrounding the cities of Myaungmya and Yangon. However, the intensity of modelled extractions was most likely underestimated when compared to well-log measurements (indicating drawdowns up to 20 meters and beyond) and literature estimates, thus potentially causing the dissociation with increased salinization of the modelling results.

Considering an estimated 50% of the population being dependent on groundwater, sustainable management is indispensable to safeguard fresh groundwater availability. Vital in establishing currently absent groundwater regulatory procedures will be appropriate legislation, improved data collection and especially the (public and open) availability thereof. Meanwhile, awaiting conclusive research with respect to extraction activities, prudence is required.

Keywords: Ayeyarwady Delta, Myanmar, groundwater, groundwater modelling, variable-density, 3D, saltwater intrusion, Regional Water Security Study, iMOD-WQ, iMOD

Dutch

Rivierdelta's, met name dichtbevolkte, faciliteren de behoeften van een groot gedeelte van de wereldpopulatie. Reden hiervoor is de inherent aan een delta hoge kwaliteit en toegankelijkheid van zoetwater, voornamelijk in de vorm van grondwater. Gezien hun socio-economische status is het daarom belangrijk deze natuurlijke bron van zoet water voor de toekomst te waarborgen.

Voor het verbeteren van het begrip van externe druk op grondwater bronnen kunnen hydrogeologische modellen een uitkomst bieden. Echter, de data daarvoor is niet altijd beschikbaar. In deze studie is een eerder ontworpen 3D dichtheidsafhankelijk grondwater model van de Irrawaddy Delta, in het kader van de 'Regional Water Security Study' in Myanmar, verbeterd met behulp van regionaal verkregen en verwerkte data, in combinatie met een literatuuronderzoek en veldwerk ten behoeve van het formuleren van maatregelen voor de toekomst betreffende een duurzame zoetwatervoorziening. Dit betrof: de toevoeging van een voxel-model van de lokale geologie, grondwateronttrekkingen en de uitvoering van een paleo-hydrogeografische reconstructie welke de historische zeespiegelstijging in acht neemt over de afgelopen 130.000 jaar. De berekende veranderingen in toekomstige stijghoogte in het watervoerend pakket en het zoutgehalte van het grondwater voor de verwachte veranderingen in grondwateronttrekkingen, klimaat gedreven zeespiegelstijging, en natuurlijke grondwateraanvulling tot en met het jaar 2050 zijn vervolgens vergeleken. Dit om de relatieve gevoeligheid van het grondwatersysteem van de Irrawaddy te bepalen voor deze individuele als wel de samengetrokken veranderende randvoorwaarden.

De resultaten laten zien dat achtergebleven zout grondwater, afkomstig van eerdere periodes van transgressie, bijna volledig is uitgespoeld alvorens 7000 BP het huidige zeeniveau wordt bereikt. Het modelleren van een verkorte paleo-reconstructie van 6425 jaar levert zo goed als identieke resultaten. Daaruit kan worden opgemaakt dat wanneer een zoet-zout grondwatersysteem paleo-hydrogeografisch wordt gemodelleerd, schattingen van de initiële zoet-zout verdeling in het grondwater goed genoeg zijn wanneer wordt gemodelleerd vanaf de eerste transgressie die de huidige zeespiegel overschrijdt. Het niet meenemen van de effecten van zeespiegelstijging tijdens het modelleren van de reconstructie van de zoet-zout grondwater verdeling in de delta resulteerde in een overschatting van de hoeveelheid zoet grondwater met zo'n 33% ($\approx 695 \text{ km}^3$); dit kan daarom beschouwd worden als onverantwoord.

In de voorzienbare toekomst wordt een afname in natuurlijke grondwateraanvulling, een toename in zeespiegelstijging ten gevolge van klimaatverandering en een toename in de hoeveelheid grondwateronttrekkingen door bevolkingsgroei en agrarische ontwikkelingen verwacht. Het modelleren van deze scenario's laat zien dat de zeespiegelstijging de grootste oorzaak van verzilting van het grondwatersysteem zal zijn. Dit zal langs de gehele kustzone plaatsvinden, tot wel 15 km landinwaarts en met name in het zuidwesten van de Irrawaddy delta. Een afname van de grondwateraanvulling zal daarentegen dominant zijn in het binnenland. Hier speelt immers de zeespiegelstijging een (zeer) geringe rol wat betreft de verzilting van het grondwatersysteem. Grondwateronttrekkingen leiden tot lokale dalingen van de stijghoogte, in het midden en noordelijke deel van de delta en met name in de omgeving van Myaungmya en Yangon. De intensiteit van de onttrekkingen in deze modelleringsstudie is waarschijnlijk onderschat indien vergeleken wordt met stijghoogte observaties (die dalingen van 20 meter en meer suggereren) en literatuurschattingen. In werkelijkheid zou derhalve verzilting van het grondwatersysteem wel eens ernstiger kunnen zijn.

Gegeven dat waarschijnlijk ongeveer 50% van de lokale bevolking afhankelijk is van grondwater in hun zoetwatervoorziening, is duurzaam beheer ervan evident. Hiertoe zou een goed reguleringssysteem kunnen helpen. Cruciaal bij het opzetten van de tot dusver afwezige reguleringsprocedures zal zijn: a. het opstellen van passende wetgeving, b. verbeteren van gegevensverzameling en in het bijzonder het beschikbaar maken van deze gegevens. Ondertussen, in afwachting van afdoende onderzoek met betrekking tot grondwaterwinning is voorzichtigheid geboden.

Expression of gratitude

Spending most of my time working on this thesis in Yangon, I would like to start this expression of gratitude with thanking my Burmese friends and my girlfriend, who were able to make my stay abroad a pleasant one. Therefore, thank you Daw Schwe Jue, Michael Saung Yieng, Ma Khaing Khin Oo and Jumjee Nammungkun.

I would not have been able to collect the amount of data that I did without the help of U Myint Thein. He was able to introduce me to relevant parties, providing a much needed foot-hold from which to start networking.

From the Irrigation and Water Utilization Management Department, I would like to thank U Thant Zin who has been most helpful and hospitable during my visit in Naypyidaw. I fondly remember our time together and I hope we will meet again someday.

From the Department of Rural Development, I would like to thank U Win Min Oo for sharing information regarding the subsurface of the Ayeyarwady Delta and being open minded with regards to collaboration.

I would like to express my gratitude towards Deltares for partially funding this research, but also to my father, whose contribution made it possible for me to not be uncomfortable during my internship and who was willing to serve as a soundboard providing political advice.

I would like to thank Arcadis for opening-up their office to me, providing me with a place to work.

Also, I want to hereby thank my supervisor Gualbert Oude Essink at Deltares and the Utrecht University, for providing me with the tools to conduct my research and the advice needed to construct the groundwater model used to investigate the groundwater quality and quantity of the Ayeyarwady Delta.

From Utrecht University, I would like to thank Niko Wanders for reading my paper as my second assessor.

Last, but not least, a special thanks goes to Jan de Bruin, who has showed much needed and appreciated interest in my research project and was so kind as to facilitate and finance the field work required, essential to verify that which was reported in literature.

Prelude

Having had the privilege to work on my master thesis in Bangkok, I was keen for another adventure abroad to conclude my master's degree. With my almost innate predilection for the orient (inherited from my father, who was born in Indonesia), a probably somewhat biased search led to a last-minute internship opportunity in Myanmar, the country formerly known as Burma.

After a short introduction on 3D variable-density groundwater flow and coupled salt transport modelling in the Netherlands at Deltares, I was sent for 5 months to Yangon, Myanmar's former capital and current financial centre, from November 2019 until April 2020. Having visited the country three years earlier, I already had some idea of what to expect. The warm weather was a welcome change from the depressing winter conditions back home and the thrill of a new environment was sure to shake things up a bit. However, I was soon to learn that, in this case, travelling and living somewhere are two completely different things. In retrospect, it sure did have its fair share of ups and downs. From staring at awe at a 112-meter tall, gold plated, diamond studded Schwedagon Pagoda, to slipping on one of the countless of roadkill rats ending up to my ankles in the cities open sewer. From enduring the almost daily city blackouts, the occasional earthquake and its suffocating traffic, to coming to my senses at an unspoiled, pristine and deserted island landscape, I was definitely in for another adventure.

Although not new to the difference in living standards, the change in scenery never stops to impress me. Everywhere in South-East Asia the social inequality can be large. This seemed especially true for Myanmar, where the gap between rich and poor at times was astounding. Nowadays, it is very well possible to live like royalty in Yangon. However, the price tag to do so can be high, even by Western standards.

Without ungrateful intent, at times it was a struggle to effectuate an acceptable standard of living within the limitations of an internship. In general, life in Yangon is 'get less for more' when compared to other major cities in South-East Asia. With prices seemingly directly coupled to the level of hygiene, this provided a challenge in almost all facets of living. Especially with regards to the real estate market. While there is no shortage of property for rent, the price/quality ratio can be incomprehensible, which undoubtedly had something to do with the fact that I was a foreigner.

After two weeks of frantic searching, an opportunity presented itself. Being the very first apartment, not too far from work, which was clean and did not require to pay everything up front, I look back at it as being one of the biggest comforts during my time in Yangon.

Being used to eat street food in Thailand, this was not always an option in Myanmar. Western intolerance for Burmese street food did not allow for a quick bite on every corner. It certainly required some level of caution and constant consideration to keep a healthy diet. Nevertheless, with time and exploration, there were always good and affordable alternatives to be found.

As a means of transportation, the obvious choice for a Dutchman was to go cycling. However, riding a bicycle in Yangon was not at all similar to riding a bicycle back home. Having been called courageous, cheap and just downright stupid, engaging Yangon on a bicycle was most certainly interesting and many a plight have led to nervous fits of laughter. Thinking back, it was almost exhilarating to go through morning rush hour traffic, but for anybody wanting to accept this challenge, please be advised: wear a helmet!

The primary reason for my presence in Yangon was the acquisition of local data, necessary to realize groundwater model improvements. However, being just a person of little distinction, getting a foot in the door is not at all self-evident. In addition, European business operations are not directly compatible within cultural boundaries and preferred methods most certainly do not provide results

overnight. Fortunately, Asian hospitality has never disappointed me and with some persistence, composure and respect, some relevant parties were included in a mutual beneficial collaboration. Taking the time and effort needed to stumble my way through the basic principles of Burmese turned out to be most fruitful and provided me with many wonderful opportunities that can, without a doubt, be called the highlights of my time in Myanmar. One such example was my visit to the Irrigation and Water Utilization Management Department (IWUMD) in the country's capital, Naypyidaw, being a breath of fresh air with respect to always buzzing Yangon. I got to present my research ideas, attaining their support, whilst getting a tour of the capital from the most hospitable IWUMD.

With the majority of my time and effort spend on the pivotal data collection, it did not seem justifiable to accept the data without question. However, my internship did not include the possibility to travel through the research area to verify the research data. Therefore, I was more than fortunate to meet Jan the Bruin, a retired Shell seismologist who used to work within the field of seismic acquisition in Myanmar. His much needed and appreciated interest in my research was a welcome change to my otherwise solitary pursuits. Caring enough to foot the bills, he provided me with the amazing opportunity to converse with the locals, who were most hospitable and open to conversation with us via our interpreter. They provided us with a wealth of essential information, proving that desk research alone does not cut it.

While these visits provided welcome intermissions, most of my time was spend in Yangon. Relative to other big cities in South-East Asia, Yangon has a small expat community with whom it proved difficult to connect. Additionally, establishing relations with locals were also complicated due to the, in general, poor English language proficiency. Nevertheless, I was able to find satisfaction in sports, where it was evident that no language is needed when a common denominator is in place. Furthermore, in the field of water science, at the university level, people were adept in English, providing good conversation and company. I joyfully remember one recently graduated PhD student in particular who gave me the honour of attending her wedding. A wonderful experience that will not be forgotten anytime soon.

Having returned to Yangon after partaking in the festivities of that wedding, I received the disenchanting news that my grandmother had passed away. Not at all untimely, as she was nearly 97, but sad nonetheless. A very brief, almost surreal, visit allowed me to attend the funeral in the Netherlands and provided me with the necessary solace to continue and complete my research mission in Yangon, at least, that is what I thought at the time. Who would have guessed that, nearing the end of my term, a pandemic would render the world inoperative? As soon as became clear that this novel virus was not going to pass quietly and with the prospect of being stranded in Myanmar, there was no other option than to return head over heels to the Netherlands and continue my research project at home.

Now, having the time to look back and reflect, I am content with the results. Without seeing a single day of rain in 5 months' time, compared to the otherwise perpetual greyness of the Dutch winter, I had collected the information necessary to accomplish my research goals.

While filled with great contrasts, I have had the opportunity to meet wonderful people, see amazing structures, learn the principles of a new language and find myself with a more consolidated appreciation for my privileged position. I got a glimpse of what to expect if I were to pursue a corporate career. Subsequently, I learned valuable lessons on collegiate solidarity, advocacy and elective affinity, all of which I will try to take into consideration with regards to career prospects and future endeavours.

Wouter Goofers, Voorburg, 24-06-2020

Abbreviations & Glossary

Abbreviation	Explanation
MOALI	Ministry of Agriculture, Livestock and Irrigation
IWUMD	Irrigation and Water Utilization Management Department
DRD	Department of Rural Development
YCDC	Yangon City Development Committee
SWL	Static Water Level
PWL	Pumping Water Level (water table elevation after pumping commenced)
RWSS	Regional Water Security Study
MIMU	Myanmar Information Management Unit
OSM	Open Street Map
IDF	iMOD Data File
IPF	iMOD Point File
BP	Before Present
DEM	Digital Elevation Model
OLI	Operational Landsat Imager
TVD	Total Variation Diminishing
FD	Finite-Difference

Concept	Explanation
Aquifer	A permeable medium through which groundwater can flow.
Permeability	An intrinsic property of a porous medium for permitting flow.
Hydraulic conductivity	A measure for how well a fluid flows through a porous medium.
Aquitard	A medium with a low hydraulic conductivity.
Voxel	A 3D pixel (VOLUME piXEL)
Closed-system	A groundwater system with a poor surface connectivity due to the presence of a confining layer restricting infiltration.
Transmissivity	The thickness of an aquifer multiplied by its hydraulic conductivity.
Eustacy	The cycle of oceanic transgression and regression phases.
Saltwater intrusion	The intrusion of salt water into freshwater aquifers.
Well-log	Throughout the instalment process of groundwater wells, the well's characteristics and in-situ lithological sequence are recorded in well-logs.
Discretization	A defined, finite period taken from a continues signal.
Stepsize	The duration of the period passed for each computation.
Timestep	The number of computations (steps) passed.

Table of contents

Abstract	ix
Expression of gratitude.....	xi
Prelude.....	xiii
Abbreviations & Glossary	xv
1. Introduction	19
1.1 Problem definition.....	19
1.2 Research question, objective and scope.....	19
1.3 Report Structure	20
2. Background information	20
2.1 Situational assessment: Myanmar socio-economics and water use	21
2.2 Field investigation water use and demand	23
3. Methods.....	25
3.1 Base model improvement.....	25
3.1.1 Geological model	25
3.1.2 Paleo-reconstruction.....	28
3.1.3 Groundwater extraction.....	34
3.2 Future scenarios	37
3.2.1 Component sea level rise	37
3.2.2 Component recharge	37
3.2.3 Component groundwater extraction	37
3.2.4 Combined scenarios.....	38
4. Results.....	38
4.1 Numerical considerations	39
4.2 Determining the initial salinity distribution	39
4.3 Extraction component.....	43
4.4 Scenarios	46
5. Discussion.....	50
6. Conclusion.....	53
7. Recommendations.....	54
References	55
Appendices.....	61
Appendix A: geographic positioning	61
Appendix B: field work.....	62
Appendix C: modelling characteristics.....	76
Appendix D: geo(hydro)logy.....	81
Appendix E: paleo-reconstruction	91
Appendix F: groundwater extraction.....	94
Appendix G: results.....	98
Appendix H: discussion	110
Appendix I: recommendations	111

1. Introduction

River deltas include some of the most populous regions on the planet. Relative to their size, they facilitate the needs of a large part of the world's population. Their fertility provides sustenance and their location is convenient for economic development. In general, they constitute high quality and easily obtained fresh water supply, mostly as groundwater, which is used for agricultural, industrial and domestic purposes (Van Weert et al. 2008). Considering their socio-economic status, securing fresh groundwater as a natural resource is important to prevent crop losses, the forced abandonment of extraction wells and other potentially monetary consequences. Therefore, sustainable management is required. However, deltaic groundwater resources are under pressure by both direct and indirect anthropogenic interference and by changes in the natural system. With an ever-growing population, fresh water demands and therefore groundwater extraction across the world's deltas is expected to intensify. Poldering and natural subsidence lower the surface elevation of the already low-lying deltas (Minderhoud et al., 2017) and Global Climate Change (GCC) has been predicted to intensify extreme weather events, induce Sea Level Rise (SLR) and cause changes in precipitation and evaporation regimes (Church et al., 2013). All these changes will affect both the quantity and quality of the available freshwater supply in the deltaic regions (Oude Essink et al., 2010; Weerasekera, 2017).

1.1 Problem definition

To better understand the impact of the different processes influencing a groundwater regime, hydrogeological modelling can be an insightful tool. However, a 3D variable density groundwater flow and coupled salt transport model, capable of investigating the individual parameters that alter the distribution of fresh and saline groundwater as well as head, requires a lot of input data.

Nowadays, researchers can turn to global databases for information on most parameters, e.g. Digital Elevation Model (DEM), precipitation and evaporation measurements, river network characteristics etcetera. However, this is not true for all input parameters. Often, hydrogeological data, describing the sequential lithological stratification of the unconsolidated subsurface, is not readily available.

Another unknown is the initial distribution of fresh and saline groundwater. Extensive measurements, needed to create a 3D-interpolation of the spatially (sometimes highly) variable salinity distribution, e.g. through Airborne ElectroMagnetic (AEM) surveys (Delsman et al., 2018), are almost always unavailable. Since coastal aquifers are in a constant state of flux due to the varying pressures imposed by ever-changing boundary conditions, the initial salinity groundwater distribution is dependent on their historical evolution. Therefore, steady-state modelling, using only current boundary conditions, is not a preferred method (Delsman et al., 2013; Larsen et al., 2017; Vallejos et al., 2018; Van Engelen et al., 2019; Van Pham et al., 2019; Worland et al., 2015). Delsman et al. (2013) showed that up to 60% of the present salinity distribution in a Dutch coastal region was to be attributed to the infiltration of sea water during historical periods of high sea level (compared to 17% due to saltwater intrusion alone). When ignored, the possibility exists that fresh groundwater reserve estimates are exaggerated up to three times the amount present (Mulder, 2018).

Furthermore, direct anthropogenic influence through groundwater extraction can have a major impact on a groundwater system. However, hardly any country currently registers, monitors and manages groundwater extraction activities. The omission of a comprehensive conspectus of this important component within a groundwater regime might lead to untruthful representations.

1.2 Research question, objective and scope

In a recent modelling study, six deltas were investigated: the Niger, Krishna, Orinoco, Nile, Shatt al Arab and Ayeyarwady delta (Mulder, 2018) using data from global databases and fictive hydrogeological scenarios. The design and consultancy firm Arcadis have contracted independent research institute Deltares to further enhance the Ayeyarwady groundwater model of Mulder as part of the Myanmar Regional Water Security Study (RWSS) project.

The RWSS project aims to formulate measures for the near future concerning the water security within the RWSS region in Myanmar, regarding floods, droughts and water quality. To complement the RWSS, insight will be provided in the mechanics of the Ayeyarwady Delta groundwater regime through a sensitivity analysis answering the following research question: ‘How sensitive is the Ayeyarwady Delta groundwater regime to possible future changes in recharge, sea level rise and groundwater extraction?’

To answer the research question, three improvements will be made to the existing 3D variable-density groundwater flow model, from now on referred to as the “base model”.

First, the hydrogeological scenarios representing the subsurface lithology will be replaced by a 3D hydrogeological model of the Ayeyarwady Delta, based on regionally collected and processed data.

Second, the initial salinity distribution will be estimated through the inclusion of relative sea level rise records found in literature in a similar fashion as done by Weerasekera (2017).

Third, the currently absent groundwater extraction component will be filled through the upscaling of assumptions derived from a field inventory of the number of extraction wells at multiple locations throughout the Ayeyarwady Delta and their general characteristics.

Other than modelling the possible future changes in groundwater salinity and hydraulic head as a result of the improvements mentioned above, it will be outside of the scope of this research to consider other confounding factors e.g. morphological changes throughout the modelling period, as well as the incorporation of saline geological formation. Also, water quality, other than salinity, will not be considered in the modelling process.

1.3 Report Structure

This report is structured to start with the provision of background information on the research area, after which the results of a field visit will be addressed shortly. The methodology for enhancing the base model is then discussed as well as the scenarios used for the sensitivity analysis. The ensuing modelling results will be presented and scrutinized accordingly, after which assumptions and implications will be discussed. Finally, conclusions will be drawn from the resulting computations to finalize an answer regarding the sensitivity of the Ayeyarwady Delta to future changes in recharge, sea level rise and groundwater extraction. Closing recommendations will then provide suggestions for further future model improvement. Since this research builds upon a previously constructed model, a brief exposition will be given on the core elements of the base model in the appendix (C1, 2).

2. Background information

The research window, as previously defined by Mulder (2018) is repeated here for ease of conduct (figure 1). Its relative position with regards to neighbouring countries is provided in Appendix A.

The deltaic area of interest’s administrative districts can be further subdivided:

- Ayeyarwady Division: Hinthada, Maubin, Labutta, Pathein, Pyapon, Myaungmy district.
- Yangon Region: Yangon North, South, East and West.
- Bago Region: East and West.

These administrative districts combined will be referred to as the Ayeyarwady Delta, while being comprised of both the Ayeyarwady and Bago Delta.

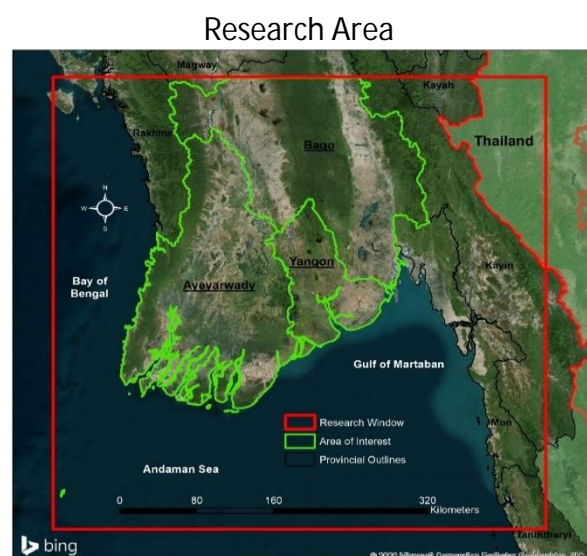


Figure 1: research window and area of interest

2.1 Situational assessment: Myanmar socioeconomics and water use

Within these administrative and spatial boundaries, this deltaic region is fertile enough to support the approximated 15 million people living there (Viossanges et al., 2017). Relative to the ~54.3 million people estimated to be living in Myanmar at this moment (Worldometers.info, 2020), the delta sustains 27.6 % of the population while comprising only 8% of the total land area (FAO, 2011; Viossanges et al., 2017). Historically, Myanmar's population has doubled over the last 50-years' time and is expected to increase by a little over 10% in the coming 15 years, equivalent to roughly five and a half million people (Worldometers.info, 2020). Using common sense, it would be acceptable to assume that a relatively large part of this expected increase in population will occur in the already relatively densely populated Ayeyarwady Delta.

Myanmar's population has a median age of 29 years and a life-expectancy of 68 years (Worldometers.info, 2020). With an urban population of 31.4 %, most of its residence still live in the countryside (Worldometers.info, 2020). The Gross Domestic Product (GDP) per capita is 1480 USD and 68 % of the people have to make do with less than 5.50 USD a day (World Bank, 2015). Ranking 145th out of 189 on the human development index of 2018 (UNDP, 2019), Myanmar classifies as one of the least developed countries in South-East Asia. Its economy used to be reliant on agriculture, 48.35% of the GDP in 2004 (FAO, 2011), but recent developments have seen this percentage drop to 26.2% in 2017, while industry (31.6%) and the service sector (42.2%) have become increasingly important for the national economy (World Bank, 2017). Nevertheless, 51.5% of the workforce still practices agriculture, compared to 16.7% in industry and 31.4% in service sector (World Bank, 2015).

Within the agricultural sector, annual crops represent 91% of all crops cultivated, while permanent crops (9%) play only a minor role (FAO, 2011). The dominant annual crop is rice, with the lion's share being cultivated in the Ayeyarwady Delta (FAO, 2011). Production is largest throughout the rainy season when crops are mostly rainfed. However, during the dry season, irrigation facilitates the continued cultivation of rice, be it at roughly 1/3rd of the production during the rainy season (FAO, 2011). Surface waters are the main source for irrigation (91%), but surface water storage is in many locations insufficient to also cultivate a dry season crop. As an addition to or substitute for surface waters, groundwater is being used for irrigation during the dry season (9%) (FAO, 2011).

Seemingly, groundwater contributes relatively little to the overall water consumption. However, it is important to note that 89 % of the country's total water use of an estimated 33 km³ per year is destined for agricultural sector (FAO, 2011). Thus, approximately 3 km³ of groundwater is used for agriculture alone every year. Furthermore, only 4% of all tube-wells are thought to be used for irrigation purposes (FAO, 2011). The vast majority of tube-wells are used for domestic purposes. Domestic consumption is responsible for approximately 10% of the total annual consumption. The percentage supplied by groundwater is highly variable per location, but on average is presumed to be around 50% (Thein, 2020), equal to roughly another 1.5 km³ of groundwater. Industry on the other hand only uses 1% of which the percentage supplied as groundwater is unknown (FAO, 2011).

Records of groundwater exploitation date back to the reign of the Burmese king around 1842, when dug wells were the only source of groundwater. Around the end of the 19th century, tube-wells started appearing, but their numbers only started to increase exponentially nearing the end of 20th century. Although surface waters are still the largest source of fresh water, fresh groundwater is becoming increasingly important every year (Thein, 2019a). This increased exploitation of and reliance on groundwater requires proper management to guarantee its worth for the years to come. However, with an estimated number of wells in Myanmar throughout the 21st century ranging from 400,000 to over half a million (Hulsman et al., 2013), the increasing strain on groundwater reservoirs can compromise their continued availability. Especially groundwater salinization has been pointed out to be a growing concern throughout the lower and middle Ayeyarwady Delta (Hulsman et al., 2013).

Multiple factors are responsible for the fresh/saline groundwater distribution in a delta, e.g. storm surges, tidal waves, eustacy and groundwater extraction, becoming increasingly important towards the coast, but are not limited to shallow coastal aquifers (Brakenridge et al., 2013; Yang et al., 2015). Near the shore, storm surges causes coastal flooding and consequently the infiltration of salt groundwater into the subsurface (Huizer et al., 2017; Smith and Turner, 2001; Xiao et al., 2019; Yang et al.; 2013, Yang et al., 2018), while tidal waves push saline water from the oceans upriver, increasing saltwater intrusion inland. An overview of the salinity front in shallow aquifers effected by salt water intrusion through these processes is provided by the National Water Resources Committee's (NWRC) "Ayeyarwady State of the Basin Assessment", which shows extensive shallow groundwater salinization in the southern reaches of the Ayeyarwady Delta that fluctuates with the seasons (Halcrow & Partners, 1983; Viossanges et al., 2017).

Away from the coast and the rivers, eustacy becomes increasingly important. Eustacy encompasses the cycle of transgression and regression of the world's seas, in other words, the rise and fall of sea level over long periods of time. During sea level rise large portions of a low-lying delta can be inundated, making it possible for saline transgression waters to infiltrate the subsurface (Minderhoud, 2017). When the sea retreats again in the regression phase, saline groundwater is not necessarily flushed out in later stages of delta development and can remain stagnant as "paleo-groundwater". With the increasing groundwater extraction experienced through agricultural expansion, industrialization and population growth, it is then possible to pull salt groundwater closer to the surface when pumping, reducing the potential fresh water yield. In more extreme cases, unsustainable use can even cause the forced abandonment of a well (Faneca et al., 2015).

There are two critical gaps in Ayeyarwady Delta groundwater management described by U Myint Thein, advisory member of the Myanmar National Water Resources Committee, that are responsible for the deterioration of groundwater resources in the Ayeyarwady Delta. The first being the absence of legislation and the second being a lack of documentation (Thein, 2019b).

At the time of writing, no legal framework is in place to regulate groundwater extraction throughout the Ayeyarwady Delta (FAO, 2011). The 1930 "Burma Underground Water Act" (Burma act IV, 1930), enacted by the British government, applied primarily to Yangon and is out of date with regards to current developments (Thein, 2019a). A "New Groundwater Act" has been submitted to parliament and has been awaiting approval for several years already.

Meanwhile, most groundwater wells are privately owned (FAO, 2011; Hulsman et al., 2013) and are not subjected to any restrictions with regards to how they are operated. Moreover, with groundwater availability declining and urban dependence growing, current reservoirs and efficiency of irrigation systems are suboptimal (10-50%) (Hulsman et al., 2013). This unregulated use has caused extensive drawdowns and groundwater quality deterioration due to over-exploitation, thus threatening communal availability (Drury, 2017; Thein, 2019b).

There are currently no national statistics neither on groundwater quality and quantity nor on its anthropogenic perturbations (Thein, 2019b). With the groundwater data quality and quantity available being described as "poor" and "critically lacking" (Hulsman et al., 2013), data on groundwater conditions throughout the research area are scarce, limited to the information collected during well construction and, often, not made readily available. Fortunately, efforts are being made to change these issues. Recently, a groundwater monitoring pilot has been successfully completed, and now a nationwide groundwater monitoring network is on its way (Zin, 2017). However, the fruits of such a network are currently still far away and building trust for gathering necessary data is time consuming. Furthermore, existing data, mostly hardcopy, is in Myanmar language and provides processing challenges and a barrier for researchers not skilled in Burmese. Therefore, to get a better understanding of the present-day status of groundwater conditions throughout the delta, a field trip was planned.

2.2 Field investigation water use and demand

In a three-day survey, from 12 to 14 February 2020, a total of 29 wells throughout the Ayeyarwady Delta were visited. These wells are, almost entirely, within the boundaries of the Maubin, Patheingyi and Hinthada district in the Ayeyarwady Region and are variable in their purpose, be it domestic, agricultural or industrial.

With the aid of a translator, the well characteristics and groundwater quality, quantity and changes over time were discussed with the owner(s) (or user(s)) of each well. An overview of the route relative to the research area is presented in Appendix B1a and a close-up, in which also the location of the specific wells visited can be seen, is presented in Appendix B1b. Further information on each individual well is provided in Appendix B1c. Finally, a transcript of conversations, including pictures, with the local population for each (group of) well(s) is provided in the appendix B2. What follows below is an overview of the information provided in that transcript and its resulting implications.

According to the information provided by the inhabitants of the areas along the survey route, the accessibility to (good quality) fresh groundwater has greatly improved over the last 20 years.

When surface waters are not near, people used to walk great distances to find water (which is still the case for the central dry-zone (Drury, 2017), either to the rivers, creeks and lakes or to a “dug well”, the oldest of which dating back roughly 100 years. However, this custom changed dramatically during the last 20 years with the arrival of “tube-wells”, which could reach deeper and more stable aquifers than dug wells and provided more protection from external sources of pollution. Either operated manually or automatically, using a diesel- or electrically-powered pump, the tube-wells provide a more conveniently located and more easily operated source of fresh water to be used for all kinds of domestic purposes, like washing, cooking, gardening and occasionally drinking.

A growing population and economy, combined with the coinciding increase in the demand for fresh water, resulted in exponential growth of the number of tube-wells, causing dug wells to be demoted to a subordinated function in their immediate vicinity. Only those who live close to surface waters or a (good quality) communal groundwater well and the very poorest of society do not need or cannot afford a private well.

Although having many benefits, the tube-well has its own drawbacks. The installation and operational costs provide a barrier to some, e.g. filter maintenance and fuel prices or the lack of electricity needed to operate tube-wells that use an electrical pump. At certain locations these issues even led to the abandonment of the well, a problem that can be avoided by the manually operated pumps, who were only occasionally spotted.

Besides these associated costs, also the quality of the water being produced is an important factor to consider. Only very few wells were reported to have an excellent water quality, good enough for drinking directly from the source. The majority of the tube-wells visited produce fresh groundwater with a rusty smell and, on a few occasions, was said to have a yellowish colour, indicating a high iron and/or manganese content. Common treatment methods used to purify the water include allowing the settlement of suspended materials with time, filtration (e.g. using cotton filters or a filter made from burned rice peels), the use of drinking water tablets or simply boiling the water. Only the drinking water production plant uses a more advanced UV-treatment method.

Regardless, bottled water, rainwater or (when superior) surface waters, in that order, are preferred for drinking. It is only during the dry season and when further away from surface waters, or when located in an aquifer with excellent water quality, that a groundwater well is the preferred source for drinking water. Unfortunately, water quality is not always properly analysed. While some water quality characteristics are clearly observable (smell, colour, taste), others are not. Water quality, on multiple locations, was determined to be spatially highly variable, especially regarding its arsenic content. On certain occasions, concentrations varied from 0 to over 80 micrograms per litre over a distance of less than 100 meters, a concentration high enough to warrant closing the well in question.

Sensitive locations, like a primary school, and wells installed by the DRD and the IWUMD have a water quality control test carried out before the well is taken into production. This is not the case for most of the wells visited. Some locations did conduct homeopathic water quality control tests, while others only had their groundwater quality tested to determine the amount of arsenic in the water.

Another noticeability is the construction of the homely septic tank 30 meters from the tube well. A development that could be countered with education, a reoccurring issue known by the local abbots. Interestingly, only one village has slightly saline (to the taste) dug wells, while a tube-well 30 meters from one of these dug wells produces only fresh groundwater from a depth roughly 20 meters deeper.

With the importance of groundwater in the domestic, industrial and agricultural sector growing every year, not only quality, but also quantity becomes more important. Nowadays, there is a private well for almost every house in the larger cities and in villages this number of wells is usually 1 to 4, besides having one or more communal wells placed upon request. This extensive and relatively quick increase in the strain put on groundwater resources could cause continuity problems. Neither registration obligations nor rules and regulations for private groundwater wells are in place to safeguard responsible groundwater conduct. The extent of the pressure already exerted on the available groundwater resources is therefore, unknown. Especially, during the dry season, when domestic reliance on groundwater is highest, insight in the size of the used reservoirs and the groundwater extraction rates is necessary to prevent depletion and the possibility of saltwater intrusion.

The amount of groundwater extracted was never measured directly and is almost always unknown. To get a feel for the relative strain on groundwater resources of the different sectors, being domestic, agricultural, industrial, the wells whose extraction rates could be estimated (very roughly) are compared on an hourly basis for a whole calendrical year. Calculations for the numbers presented here and in Appendix B1c, are provided in the transcript (appendix B2).

Domestically speaking, extraction rates vary between 11 and 214 L/hour per well, depending on the type of well and its purpose, while the industrial sector has a consumption rate between 250 and 833 L/hour per well and the agriculture sector 1184 L/hour.

When interpreting these numbers, not only the total volume, but also the total number of wells and the time of extraction needs to be considered. Taking the village of Oakshitkwin as an example, all the private wells of the village combined extract 1250L/hour for 300 houses spread over an entire year. These private wells are spaced out over the whole village and are placed at a variable depth, divided over multiple aquifers. Although having a large combined extracted volume, their drawdown is less likely to invite saltwater upconing or to cause groundwater depletion than a single industrial well that pumps-up 833 L/hour. Nevertheless, both the domestic sector and the industrial sector pale in comparison to the strain put on groundwater resources by the agricultural sector, specifically the paddy rice production. While the industrial sector might have a strong impact in a specific area, large scale industries requiring large amounts of fresh water, are far less common than the cultivation of paddy rice. Besides consuming as much water as a village of 300 houses for a single paddy rice field of 6 acres, almost all this water is extracted within a couple of months during the dry-season, when recharge from precipitation is negligible. This is a clear recipe for inviting saltwater intrusion and upconing, considering the already relatively large seasonal static water level fluctuation of 4 to 5 meters shown by most dug wells in the area. While changes between the seasons in the ease of pumping was only mentioned on two occasions to be more difficult during the dry season, the necessity to deepen the tube wells to reach the groundwater was reported by the farmer working the paddy rice fields in dry season, suggesting an overall drawdown of the water table. Possibly being correlated with the practice of double cropping, this does not mean that double cropping is unsustainable per se. Other, water stress resilient crops, like the 'black gram' bean, differ strongly from paddy rice in their need for water during the dry season. However, which crop is being grown is dependent on multiple external factors (e.g. financial market, land nutrient values, labour force etc.), which makes it difficult to get an overview of the distribution of water intensive agriculture.

3. Methods

Local data, used to improve upon the base model, was provided by the Myanmar government and processed in iMOD-WQ to create a baseline assessment of the current groundwater regime in the Ayeyarwady Delta. Sequentially, scenarios were designed to assess the delta's vulnerability to expected and possible changes in the near future.

3.1 Base model improvement

This research builds upon the base model by Mulder (2018) to increase the understanding of the impact of the different processes influencing the Ayeyarwady Delta groundwater regime and to provide a more accurate distribution of fresh and saline groundwater in this data scarce region.

While in this section, the focus lies on the improvements made to this model, a basic understanding of the underlying data is advised. Therefore, a brief summarization of the base model's design and the modelling software used is included in appendix C1, 2. If required, more detailed information can be found in Mulder (2018). Below follows a detailed discussion on how the base model was improved through the addition of a 3D geologic model, the performance of a paleo-reconstruction to approximate the initial salinity distribution and the addition of a groundwater extraction component. Alteration to other model components as a consequence of the model improvements referred to above are described in appendix C3 and include (extensive) changes with respect to the river network, DEM, drainage and starting heads.

3.1.1 Geological model

Previously, there was no existing measurements-based 3D model of the Ayeyarwady Delta's subsurface. To create the 3D medium of what through which to simulate groundwater flow, in-situ lithological sequences recorded in well-logs were gathered and processed for the Ayeyarwady and Yangon region.

These well-logs were provided by the Irrigation and Water Utilization Management Department (IWUMD) and the Department of Rural Development (DRD) under the Ministry of Agriculture, Livestock and Irrigation (MOALI) and the Yangon City Development Committee (YCDC). Examples are provided in Appendix D1a, b and c.

Unfortunately, being a separate administrative district, it was not possible to also obtain records for the Bago region due to administrative hurdles.

In Myanmar, the transition to a digitized information system is not yet completed. Therefore, the well-logs are only available as hardcopies, mostly in Myanmar language.

Well locations are described with coordinates and/or by administrative district credentials. Coordinates are in decimal degrees or degree, minute, seconds format in WGS-84 or in UTM-N46. Administrative districts are subdivided in regions, districts, village-tracts and villages. Within cities further sub-division is sometimes made through the distinction of quarters, compounds and finally, either specific buildings or street names. Most of these locations are not marked or easily found on conventional maps.

Occasionally, working with the registered well's coordinates proved to be challenging. Therefore, to get an indication on well locations, the village-tract and -name within the well-logs were coupled to their corresponding counterpart in the village-database of the Myanmar Information Management Unit (MIMU) (MIMU, 2019). Because there is no one correct way to transcribe Myanmar script into the roman alphabet, matching village-names from the well-logs with those in the MIMU database had to be done manually. Subsequently, Bing maps' aerial photographs (Bing Maps, 2020) were used in combination with OpenStreetMap (OSM) (OSM, 2020) to verify village locations, street names and buildings. Only those wells having plausible locations were then kept for modelling the Ayeyarwady Delta's subsurface.

Although well location accuracy had to be limited to a village resolution, the relatively small size of most villages is thought to provide coordinates that are in line with the model's 1 * 1 km resolution.

Using this approach 144 out of the 179 wells, from the well-logs provided by IWUMD and 38 out of 46 wells from the well-logs provided by the DRD, were located. While the YCDC provided 467 well-logs, their representation did not extent beyond the boundaries of Yangon City. Therefore, a limited 31 well-logs (one for each township, with 2 exemptions) were processed to be incorporated into the model, due to the relatively small area comprised by Yangon city compared to the research area. When combined, the wells amount to 213 points spread throughout the research area. A visual representation of the spatial distribution is presented in figure 2. A summary table of the number of wells per district per source is presented in Appendix D2.

Because iMOD uses a 6-digit maximum coordinate-system, the base model's EASE-Grid 2.0 projection was translated to start the lower left corner of the model with the coordinates 0.0, thereby reducing the coordinates used from 7 to 6 digits. A translation is therefore required to transfer the well locations to the model. The translation was assumed to be of the zeroth order and the values $X = -9024632$, $Y = -1831938$ were visually deduced using a reference point (landmark) in the DEM which could also be found in OpenStreetMap. All 213 well-log locations were re-projected in an EASE Grid 2.0 projection and translated to get matching positions within iMOD.

Sequentially, a database was constructed and coded per distributing governmental institution for either location, date of construction or a combination thereof. An overview explaining the coding systems is presented in Appendix D3a, b, c, d.

The information extracted from the well-logs (when available) includes: well number, Static Water Level (SWL), Pumping Water Level (PWL), screen depth(s), yield, date of completion and lithology.

Due to the unambiguous differentiation and indication of formations, lithological variability was reduced to two categories: aquifer and aquitard. These categories comprise the following lithologies specified in the well-logs:

- Aquifer: sand, gravel, aggregate.
- Aquitard: shale, slate and sandstone (unless specified as fractured), clay, mud and silt.

Any prefix specified was omitted in the process, thus sandy clay was reduced to clay and clayey sand was converted to sand.

Very little information on aquifer properties is known, due to (amongst other things) the limited number of pump-test that are carried out by private drilling companies. Therefore, aquifers and aquitards were assigned a horizontal and vertical hydraulic conductivity of 10 and 0.1 m/day and 0.001 and 0.0001 m/day, respectively.

Initially, well depths were set at "zero" and were registered in feet. To accommodate the model, feet were transformed to meters and rounded to integers. Sequentially, the starting elevation of the well's lithological sequence was adjusted to the elevation corresponding with the model's DEM for the well's specified location. Because well records are limited to a maximum depth of 298m, the remaining depth to bedrock, for which the lithological sequencing is unknown, was calculated for each well and grouped in a separate "unknown" category, which was given equal hydrological characteristics to that of the aquifer category.

Wells that extended beyond the depth suggested to be the maximum depth by the bedrock layer, were cut-off conform with depth to bedrock. A list of wells that fit this description is provided in Appendix D4.

A 3D visual of the wells' position throughout the Ayeyarwady Delta and their lithological sequencing are presented in Appendix D5a, b. Examples of the input .IPF-files and .TXT-files, which iMOD requires to interpret the wells' location and lithology, is provided in Appendix D6a, b.

Spatial distribution of wells used to create the 3D geological model

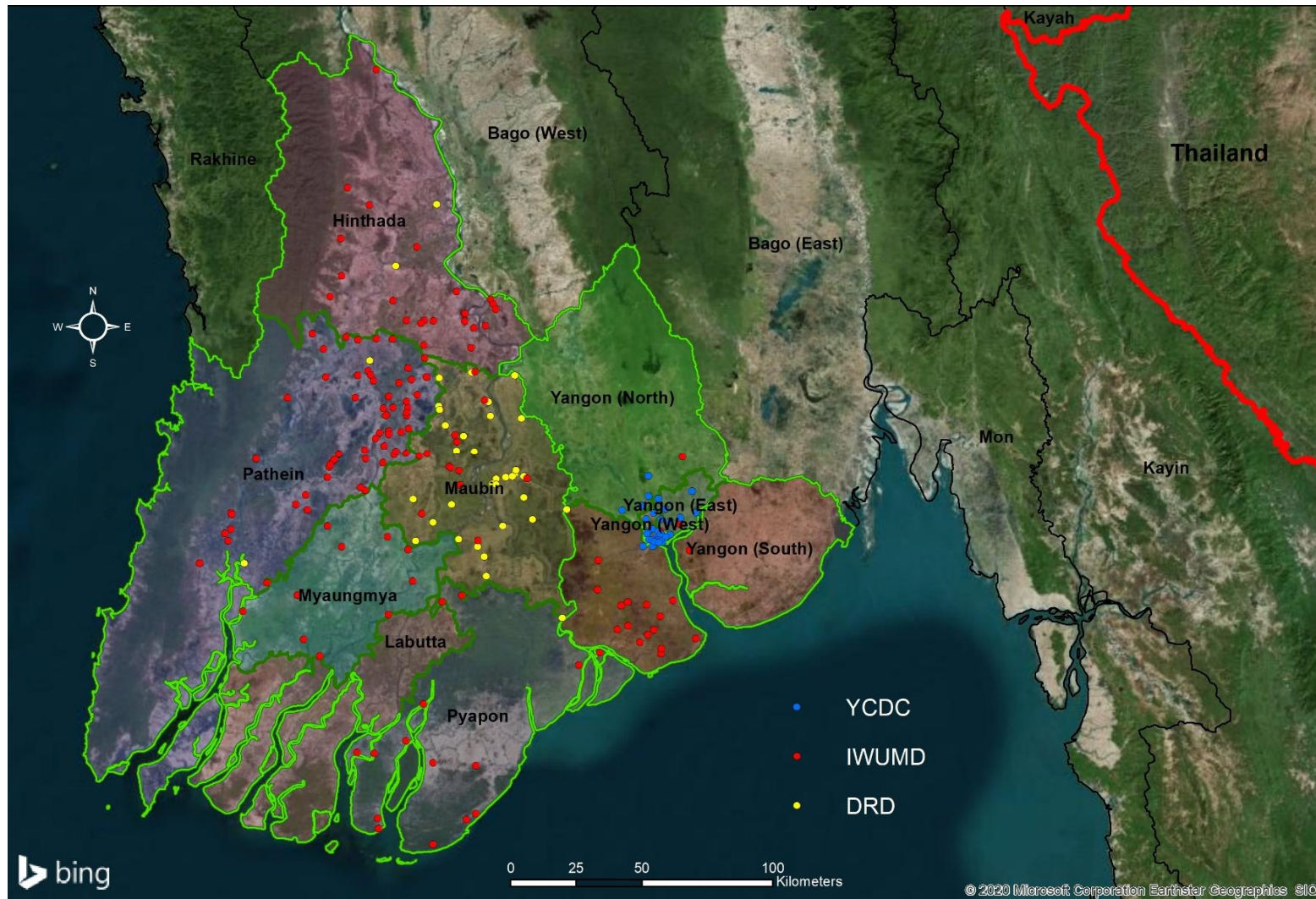


Figure 2: A spatial distribution of verified wells, derived from the well-logs provided by the Myanmar government, relative to the administrative districts of the research area. Well colours portray the source providing the well information, being either IWUMD (red), DRD (yellow) or YCDC (blue) (Bing Maps, 2020).

The manual determination of the connectivity between subsurface formations deals with a high degree of subjectivity, because wells are not drilled to equal depths, are irregularly spaced and lithological sequences are simplified. Also, similar sequences have, at times, big differences in their depth of occurrence and others differ in the differentiated number of layers. Therefore, it's challenging to establish connectivity between proposed layers in a reproducible manner. To work around this lack of objectivity the probability of occurrence of the specified categories was calculated. The final lithology used for a single cell is the lithology with the highest probability. Using an original kriging interpolation method to connect the digitized lithological records, a 3D-model of the Ayeyarwady Delta's supposed geology was computed within iMOD's Solid-Tool (Vermeulen et al., 2006).

The XYZTODF-(batch)function in iMOD was used to create two different 'voxel'-models for the Ayeyarwady Delta, both having their pros and cons.

The first model was constructed using constant vertical levels. While this model provides the freedom to easily adjust the resolution at depth, it does not follow the contours of the DEM and bedrock and requires a higher interpolation range to reach a similar extent.

The second model also contains variable vertical levels and follows preconstructed layers using the CREATELAYER (batch)function in iMOD. Creating high resolution in the top layers of the model, which follows the contours of the landscape, better preserve the confining clay-layer at the surface and covers the entire model for the same interpolation range. However, when there is a big difference in the progression of the thickness of the sedimentary basin, the resolution within a single layer can fluctuate substantially. Therefore, high resolution layers were created to be, individually, of uniform thickness, until a depth of 25 meters. Underneath, variable vertical levels were created until bedrock. Creating a decreasing resolution from the top down, the number of layers is limited by the shortest distance between the DEM and Bedrock. To warrant a regressive and sensible layer resolution progression, bedrock had to be of a minimum thickness throughout the entire model. Therefore, all locations with a difference between the DEM and bedrock of less than 50 meters were artificially deepened. The actively modelled area, affected by this adjustment, is presented in Appendix D7.

For both models, by default, the permeability suggested is that of the most common lithology. However, this default method, at certain locations, overlooks the confining clay-layer that is recorded to be present in the well-logs throughout the system. To preserve the strongly variable thickness of the top clay-layer, the permeability was calculated as the weighted sum of all individual permeability values within each vertical. This ensures that the model stays true to the Ayeyarwady Delta's 'closed-system' nature.

Cross-sections through the 3D geology of both models are presented in figures 3a, b and 4a, b and in Appendix D8a, b. The codes used to create both voxel models are available in Appendix D9.

3.1.2 Paleo-reconstruction

To incorporate eustacy effects, Sea Level fluctuations (SLR) has been considered through a transient modelling process referred to as a "paleo-reconstruction" used to simulate a plausible initial salinity distribution (Larsen et al., 2017; Van Engelen et al., 2019; Van Pham et al., 2019). The rise and fall of the world's oceans have been coupled to glacial and interglacial cycles and shows (on average) a return period of roughly 125.000 years. This pattern is clearly recognizable in PAGES (2016) whom have modelled the last 800.000 years of interglacials based on $\delta^{18}O$ estimates of benthic foraminifera.

The time it takes for the Ayeyarwady Delta to reach an equilibrium between fresh and saline groundwater volumes has been calculated to be between 30-90 Kyrs under constant conditions (Mulder, 2018). Therefore, modelling one full transgression-regression cycle is considered sufficient to estimate the initial salinity distribution.

Cross-sections through the 3D geology of both voxel models (N-S)

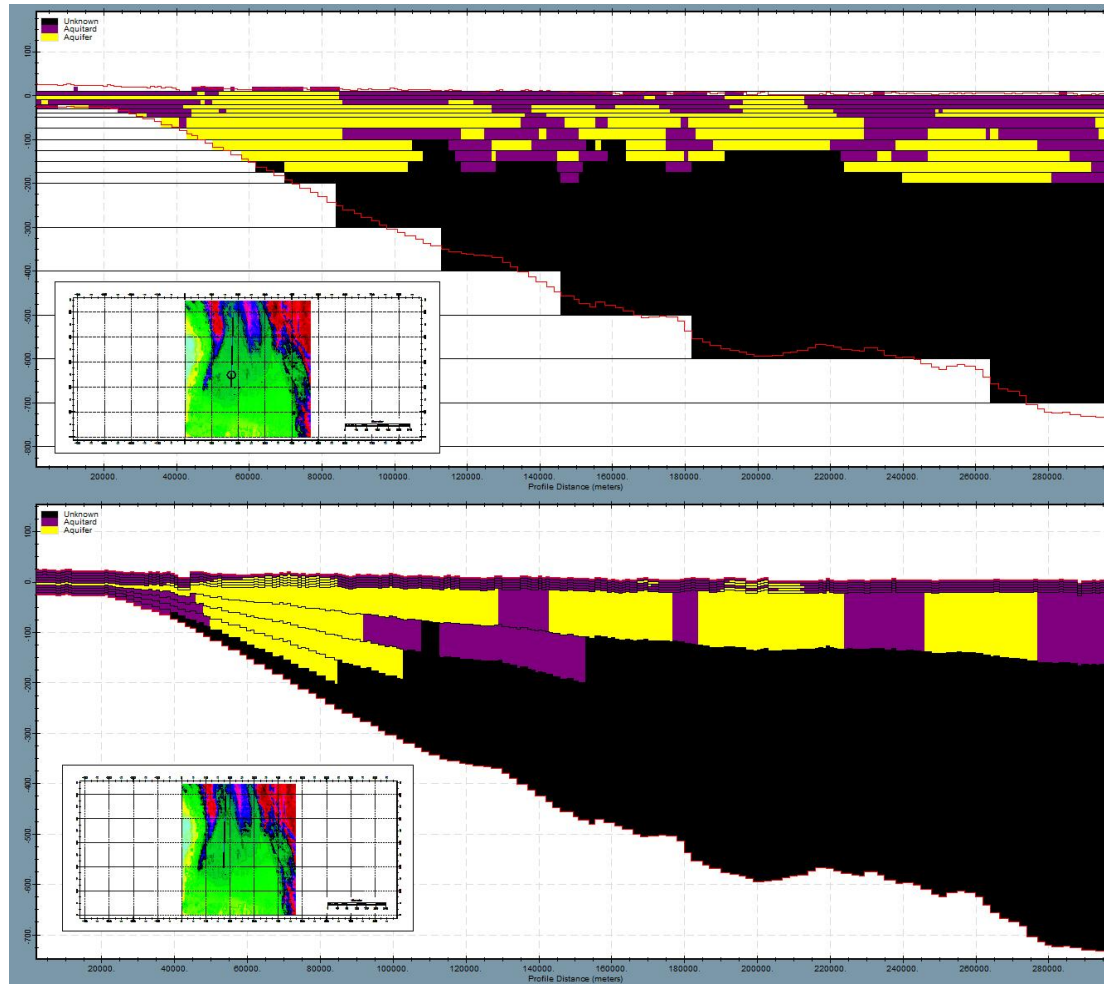


Figure 3a, b: identical cross sections from north to south through the Ayeyarwady Delta geological models. The top figure (figure 3a) represents the model with constant vertical levels, the bottom figure (figure 3b) represents the model also containing variable vertical levels. In the lower left corner, the plot survey shows the cross-section trajectory. The cross-section has been colour-coded, with yellow, purple and black representing aquifers, aquitards and undefined areas, respectively.

Cross-sections through the 3D geology of both voxel models (W-E)

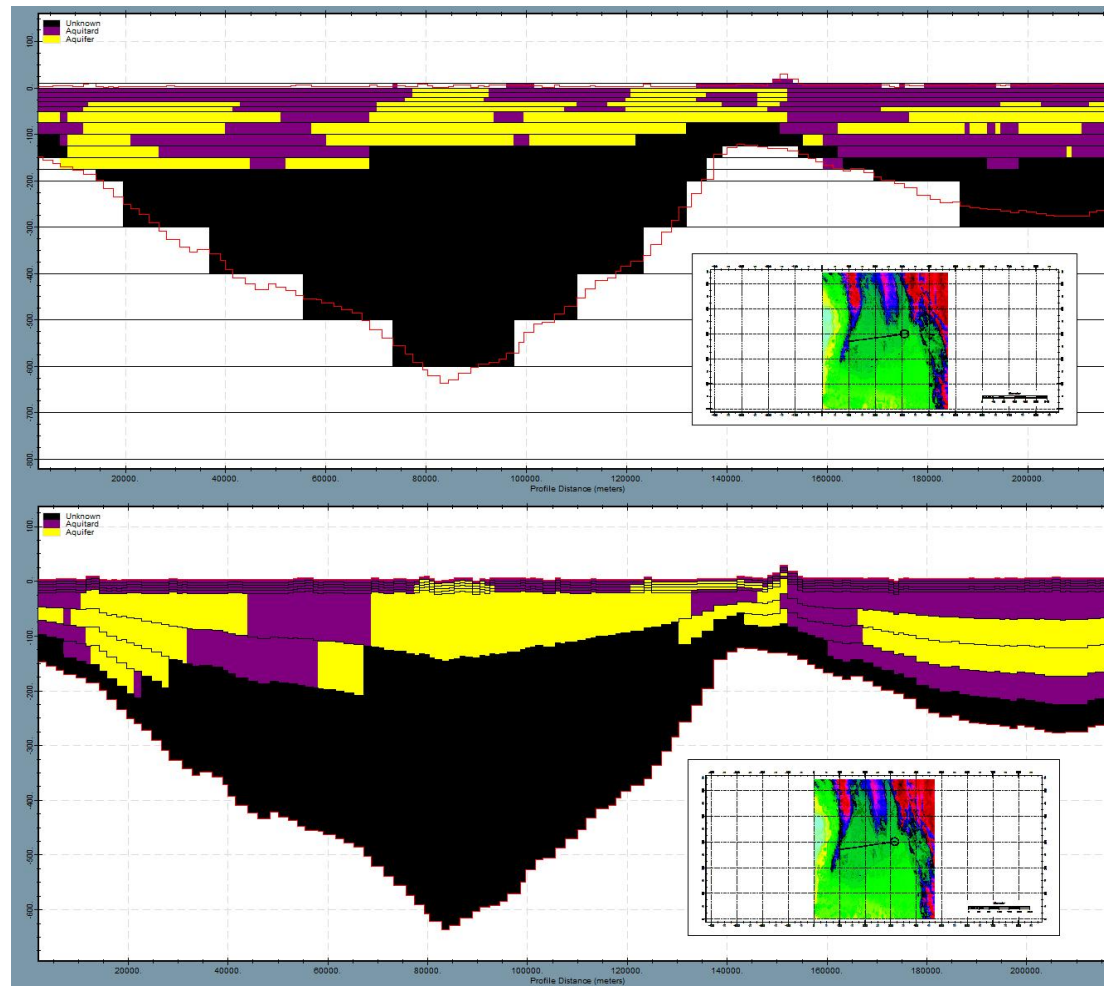


Figure 4a, b: identical cross sections from west to east through the Ayeeyarwady Delta geological models. The top figure (figure 4a) represents the model with constant vertical levels, the bottom figure (figure 4b) represents the model also containing variable vertical levels. In the lower right corner, the plot survey shows the cross-section trajectory. The cross-section has been colour-coded, with yellow, purple and black representing aquifers, aquitards and undefined areas, respectively.

There are many (composite) RSL curves available (Waelbroeck et al., 2002; Grant et al., 2012). Although they all show a similar eustacy pattern, they differ for which region they were constructed and in their resolution. Pirazzoli (1996) distinguished 5 zones globally for which RSLR estimates could potentially differ significantly. While there is no RSLR data available specific for Myanmar, a high resolution RSLR curve for the Holocene period for eastern India (Loveson & Nigam, 2019) is within the same zone described by Pirazzoli (1996) as the seas around Myanmar and therefore has been adopted as a substitute. However, Loveson & Nigam (2019) their timeframe is limited to 14500 years Before Present (BP) and therefore has been combined with another composite RSLR-curve provided by Grant et al. (2012) to represent a full transgression-regression cycle.

To model such a long timeseries, stress-periods had to be defined. Stress-periods are discretization's within the continuous RSL-curve for which conditions are set as constant. All SPs combined then represent a simplified version of the RSLR-curves. To prevent not capturing the full areal extent effected by eustacy, stress-periods were created in accordance with the minima and maxima of the transgression and regression phases. Starting at the moment that the historic sea-level rose above present sea level (approximately 130.000 years BP), four individual transgression-regression phases could be distinguished from Grant et al. (2012) before converging with the curve provided by Loveson & Nigam (2019) 14500 years BP, who defined another 5 stages. Since there was no measurement corresponding exactly to the start of the paleo-modelling, the first measurement before and after overstepping present-day sea level approximately 130.000 years BP were used to calculate the approximated year with RSL = 0, assuming a linear progression between the two measurements by Grant et al. (2012). To be able to combine the functions of RSLR by Grant et al. (2012) and Loveson & Nigam (2019), the same process was repeated for the data provided by Grant et al. (2012) approximately 14500 years BP, which marked the start of the Loveson & Nigam (2019) discretization.

The duration of a stress-period was then calculated to be half of the period between the next and previous extremes. Since the groundwater model describes elevations on an integer basis, floating values were rounded either above or below depending on their phase, transgression phase were rounded up, regression phase were rounded below. A graphical representation of the simplification of Grant et al. (2012) their RSLR-curve and its defined SPs is presented in Appendix E1 (130 kyears). The same has been done for Loveson & Nigam (2019) their RSLR-curve in Appendix E2a (14.5 kyears) and E2b (6.8 kyears). The results for both curves combined are presented in figure 5. A numerical overview of the resulting 24 stress-periods is provided in Appendix E3.

Due to eustacy the relative land area exposed differs between stress-periods, therefore the actively modelled area had to be adjusted accordingly. The Relative elevation's, adjoined to the individual discretization's, were used as boundary condition to isolate the exposed land area suggest by the DEM. In total eighteen indicator boundaries were differentiated. Consequently, the rasters were manually adjusted to further simplify the result. Any strayed pixels and intrusions of inactive cells within active model areas that were not interconnected and vice versa were assimilated by its adjacent pixels.

While for transgressions exceeding the present-day coastline inactive cells, representing mountainous terrain, indicated the limits of the actively modelled area to the west, no such boundary was available for regressions that exposed more than the present-day land area. Therefore, considering a classic delta shape, the DEM's contour lines were used to create an artificial continuation of the afore mentioned boundary. By doing so, the number of cells included during model calculations is kept to a minimum, preventing unnecessary retardation of the model's runtimes by adding areas that are not of interest.

A selection of the resulting indicator boundaries, showing the change in size of the Ayeyarwady Delta, is presented in figure 6.

Relative Sea Level Rise Discretization (130.000 years)

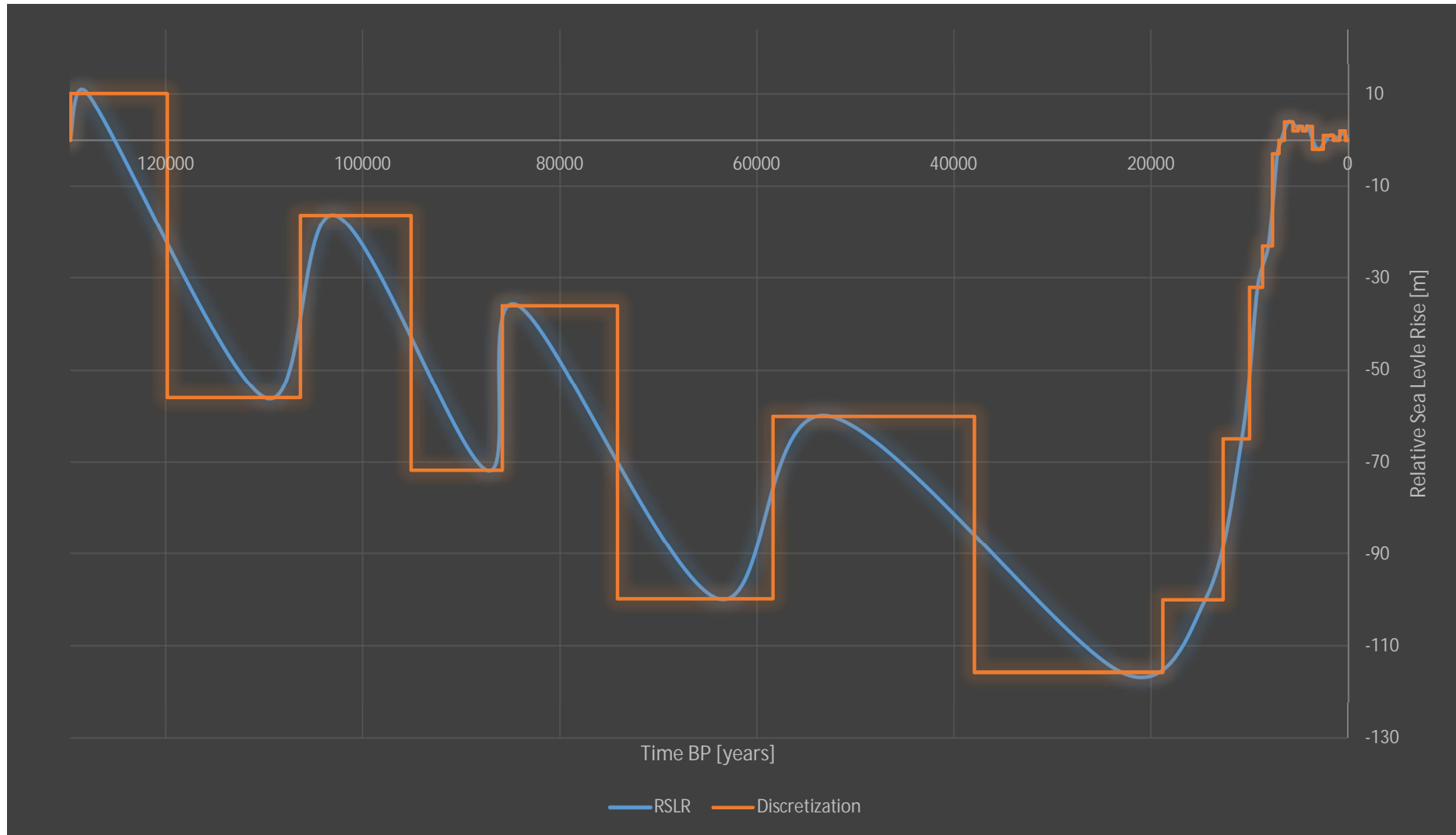


Figure 5: Combined Grant et al. (2012) and Loveson (2019) RSLR-curve discretizations. The blue line represents the simplified RSLR-curve. The orange line represents the discretised stress periods.

Relative Sea level, Ayeyarwady Delta, Myanmar

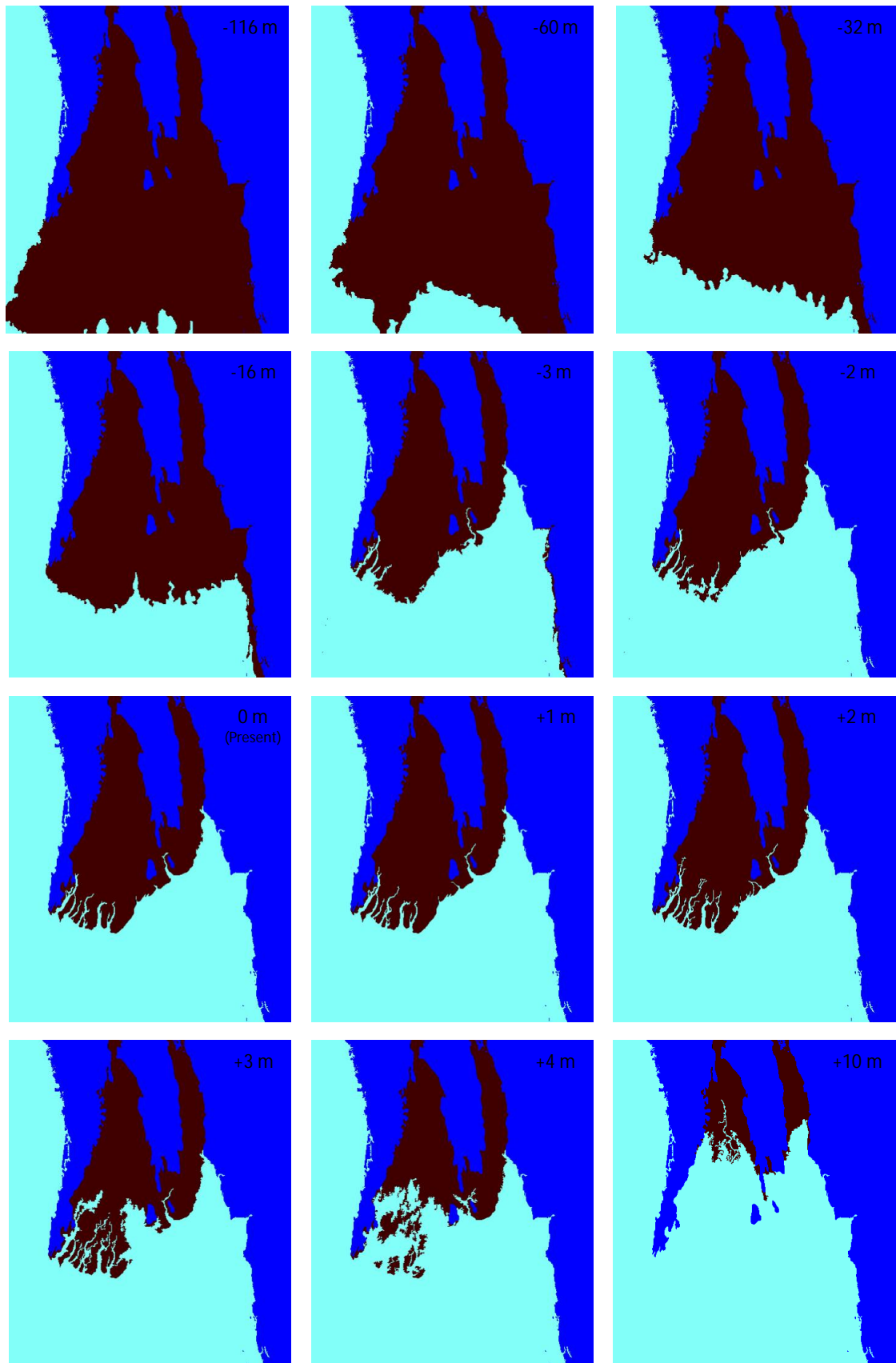


Figure 6: The evolution of the Ayeyarwady Delta presented here is not in chronological order, but in order of the lowest to the highest RSL experienced over the last 130-years. For an increasing RSL, consecutively, from the top left to the bottom right, the relative distribution of landmass (black) versus ocean (cyan) versus inactive model cells (dark blue) is shown.

When analysing the progression of eustacy, it is apparent that transgression waters have extended beyond current shore boundaries only relatively recently (starting from 6425 Years BP). Although the consideration of morphological changes is outside the scope of this research, it is during this period that the deposition of the clay particles responsible for the formation of the Holocene clay-layer referred to as the “alluvial formation” most likely took place (Larsen et al., 2017). Because of the alluvial formation’s significance for the delta’s infiltration capacity, the assumption was made that before 6800 years BP the concealing clay layer that gives the Ayeyarwady Delta it’s closed-off characteristics would not have been present. The clay-layer in question is of considerable variable thickness it is difficult to distinguish, but in general is estimated to be around 30 meters thick (Viossanges et al., 2017). Considering the model’s layering, as described in section 3.1.1, the top 5 layers were therefore given equal hydrogeological properties to that of the aquifer category until the first stress-period representing a present-day relative sea level.

3.1.3 Groundwater extraction

As became evident from fieldwork, only including governmentally registered groundwater wells would result in a severe underestimation of the actual groundwater extraction. Only a fraction of the existing wells is constructed by the government, a lot of them are installed by private companies whose administration is incomplete, not shared, or destroyed in bankruptcy. Therefore, the true number of wells is unknown.

To acquire a comprehensive and representative overview of the extraction regime, assumptious methods, based on the information collected in the field, are required. Depending on the sector, being either domestic, agricultural or industrial, groundwater extractions differ, both spatially and temporally. Therefore, a different approach is required for each sector to provide insight in their relative extent. Groundwater use for domestic purposes is widespread and practiced year-round, while agricultural extractions are more spatially diverse and concentrated around the dry-season. Both will be discussed separately in detail below. Although industry was identified to have the potential to exert a large pressure on the groundwater system locally, its importance throughout the Ayeyarwady Delta is relatively minor compared to the domestic and agricultural sector. Considering the complexity of locating and quantifying the water consumption of the broad variety of enterprises comprising the industrial sector, extractions related to industry were disregarded.

3.1.3.1 Domestic

To get an overview of urban development, all buildings currently registered in Open Street Map were extracted and assigned a well. Consequently, their numbers were reduced to those within the actively modelled area. Having noted the limited role of groundwater when surface waters are near, all wells within a 200-meter buffer zone around surface waters were removed. The map used to create this buffer zone was made by combining all surface water characteristics from OSM with a land use map of the Ayeyarwady and Salween Basin (IWMI, 2014). The result of this combination is visualized in Appendix F1.

While being the most comprehensive opensource mapping platform available, OSM does not provide a complete overview of all buildings present in the Ayeyarwady Delta. Taking the villages visited during field work as a reference, it is estimated that approximately 5/12th of the total number of buildings is represented in the OSM database. Therefore, with an estimate of one private well per every four houses, a correction factor was derived to approximate the total number of wells being used throughout the research area:

$$\text{Correction factor} = \text{number of buildings} / (5/12) * 0.25 = 0.6$$

The remaining wells were resampled as the sum of their parts to fit the groundwater model’s resolution. With an estimated groundwater consumption of 100 L per house per day and four houses

sharing a well, the average extraction rate is approximately 400 L/day per well. The summed number of wells per model cell were multiplied by this average extraction rate and converted to m³/day. Using this approach, a total of 373.168 domestic wells were combined into 21.361 model wells with a daily extracted volume ranging from 0,4 to 30 m³/day. Starting with the total number of buildings represented in OSM, the number of wells excluded for each consecutive step described in the methodology above is presented in Appendix F2.

3.1.3.2 Agricultural

While large scale governmentally supported groundwater irrigation schemes are ongoing in e.g. the central dry zone (Drury, 2017), no such project is currently implemented in the Ayeyarwady Delta according to the IWUMD. Therefore, all groundwater wells used for irrigation are privately owned and unregistered, making them practically invisible. Furthermore, crops irrigated during dry season have large differences in their water consumption and rotate depending on the market, making it next to impossible to obtain well locations and volumes of groundwater extracted for irrigational purposes. Nevertheless, extracted volumes for the cultivation of a single summer rice crop can equal the consumption of a small village for a year. Therefore, a groundwater model could not be made representable without including agricultural groundwater extractions.

Using the large difference in vegetation between the dry and rainy season visible on Landsat-8 OLI images (appendix F3a, b; Vermote et al., 2016), potentially irrigated areas were identified by calculating a Normalized Difference Vegetation Index (NDVI) and an Enhanced Vegetation Index (EVI) for dry season satellite scenes, whereas the latter showed slightly better results and is presented in appendix F4a, b. The methodology used to calculate NDVI/EVI values are presented in appendix F5.

With rice still being main cultivated crop and the almost complete absence of forest in the Ayeyarwady delta, it was assumed that all green areas identified with an EVI > 0.4 are irrigated rice fields.

Due to the preference of farmers for the use of surface waters, a distance of 2 km from the nearest surface waters was introduced, which is similar to the distance of the rice fields irrigated with groundwater that were visited during fieldwork.

With, on average, one groundwater well irrigating a plot of six acres, selected cells were grouped into clusters of equal size. Smaller clusters were omitted and larger clusters were divided into 6-acre plots. Each remaining plot was then assigned a well.

Subsequently, as was done for domestic wells, wells were resampled as the sum of their parts to fit the groundwater model's resolution and multiplied with the estimated extraction of (1184L * 24 = 28416 L/day =) 28 m³/day per well. Using this approach, a total of 15.524 agricultural wells were combined into 1956 model wells with a daily extracted volume ranging from 28 to 1392 m³/day.

3.1.3.3 Modelling

The presumed locations of all agricultural and domestic wells, relative to the provincial and modelling boundaries (as described in appendix C1), are presented in figure 7. Although providing a first indication of possible well locations, further refinement was required to simulate their impact on the groundwater table and the salinity distribution. The wells located using the methods described above do not make a distinction between aquifers and aquitards. Due to the impossibility of extracting water from an aquitard, all wells not situated within an aquifer had to be excluded to accommodate the model. With a depth range of the groundwater tube-wells throughout the Ayeyarwady Delta between 30 and 200 meters below the surface, model layer 1 to 5, with a depth ranging from 0 to 25 meters, did not qualify. Therefore, wells were assigned to the to the first water bearing model layer, starting from model layer 6 downwards. Wells that did not encounter an aquifer throughout the succession of layers were excluded from the modelling process.

The resulting selection of wells had the potential to simulate extractions from the subsurface, however with the model layers being of variable thickness, it did not yet exclude on a basis of depth.

Overview of all extraction wells incorporated in the groundwater model

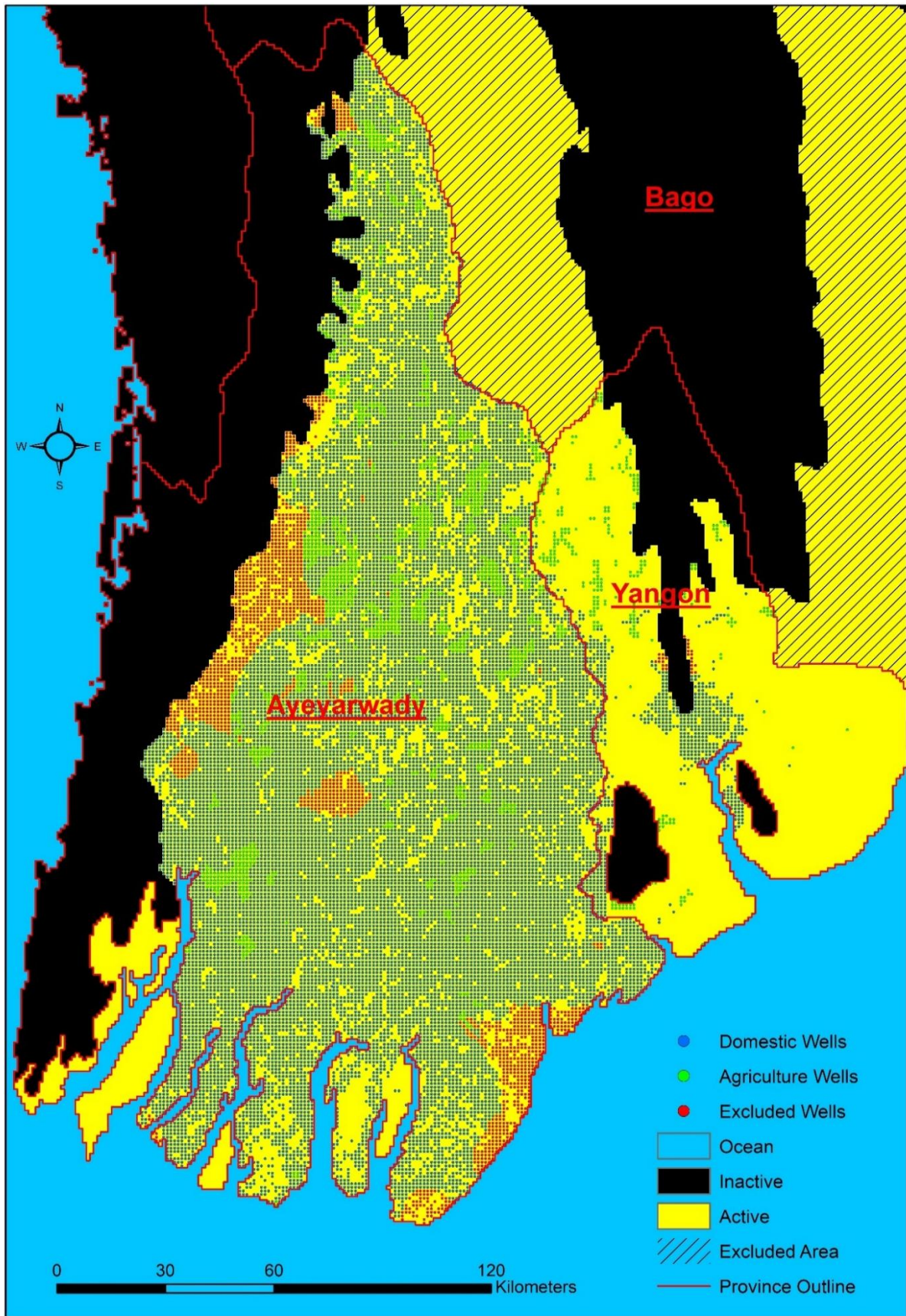


Figure 7: an overview of all domestic and agricultural wells' locations relative to the provincial and modelling boundaries. Wells were excluded either on the basis of depth or for not being situated in an aquifer.

At its most thin, the model reaches bedrock at a depth of 50 meters, therefore all model layers 6-10 have the potential to accommodate extraction well based on their relative depths. To ensure no wells exceeded the depth limit of 200 meters, all well locations that had the top of their consecutive layer in exceedance of 200 meters were also excluded from the modelling process.

This exclusion process resulted in a total number of 19709 and 1790 grouped domestic and agricultural wells, representing an estimate 349110 and 14044 of actual wells, assumed to be present throughout the Ayeyarwady Delta, respectively.

Because the number of tube-wells reported by local communities and in literature (section 2.1), have only started to increase exponentially over, approximately, the last 20 years, their importance and therefore their impact is assumed to be negligible before that time. Considering this development, groundwater extraction is only (statically) modelled for the last 20 years of the total runtime. While domestic use is considered equal year-round, seasonal extraction has been spread over a calendrical year to compute their combined impact on a yearly basis.

3.2 Future scenarios

With the paleo-reconstruction providing a baseline for the initial salinity distribution, the addition of the groundwater extraction component then concludes the starting point from which to model future scenarios. While there are many stresses thinkable that can potentially cause changes in the present-day groundwater regime, Global Climate Change (GCC) induced sea level rise and changes in recharge as well as an intensification of the groundwater extractions as a result of the predicted population growth and expected increase in agricultural practices were chosen to be investigated in further detail.

3.2.1 Component sea level rise

As a natural stressor, but indirectly also influenced by human action, GCC is expected to cause a rise in global mean sea level. The Church et al. (2013) describes a maximum 1-meter (rounded figure) increase in global mean sea level during this century for the more extreme Representative Concentration Pathway (RCP) scenarios. However, as regional sea level projection can differ significantly from the global mean, two scenarios are computed. The first scenario is run with a RSLR of 1 meter. The second, more extreme scenario, will induce an RSLR of 2 meters to prevent a possible underestimation of the regional SLR. Both scenarios were computed for a duration of 30 years, starting from 2020, during a single stress-period, with the increase in RSLR being in effect immediately.

3.2.2 Component recharge

Other examples of climate change effected variables are precipitation and evaporation. While the comparisons of the region's paleo-precipitation with current measurements suggest that the amount of precipitation has decreased over the past millennia, within the modelling timeframe, these changes will most likely not be significant. However, there is a theoretical expectation with regards to intensifying weather patterns, resulting in more severe droughts and more intense precipitation (Huntington, 2006). This can be expected to more frequently and severely overload the infiltration capacity of the top-soil, affecting the amount of runoff and therefore also recharge. Furthermore, the increasing urbanisation is thought to contribute to a reduction in recharge as well (Htun, 2015). To account for these possibilities, a 20% reduction in recharge will be modelled as from 2020, effective immediately, until 2050 during a single stress-period.

3.2.3 Component groundwater extraction

As a direct anthropogenic impact, as became evident from the discussion on the population dynamics of Myanmar over the last 50 years in section 2.1, relative to today, an 10% increase of the population can be expected in the coming 15 years. This figure can be expected to further increase to 15% in 2050 (Worldometers.info, 2020). While growth is thus slowing down, this increase in population will inevitably result in the increase of the fresh water demand. Recognizing the probability that a relatively large portion of this increase in population will occur in the densely populated Ayeyarwady

Delta, any ratio estimates would be highly speculative. Therefore, the 10% and 15% increase in population (relative to the population in 2020) will be directly translated to an equal percentual increase in extractions for all domestic wells defined in section 3.1.3. The changed extraction rates will be effective in an immediate fashion, starting with +10% in 2020 and +15% in 2035, modelled in two consecutive stress-periods.

Although agricultural water consumption has been mentioned to increase as well (FAO, 2011), its associated wells' extractions will remain unchanged due to the unavailability of substantiated estimates.

3.2.4 Combined scenarios

The overall changes in salinity, as well as the changes in hydraulic head, induced by all stresses mentioned above, are compared to the 2020 starting-point to provide insight in the sensitivity of the Ayeyarwady Delta to these parameters. Stresses are evaluated both individually and combined according to the different scenarios defined in table 1.

Scenario Matrix	No changes	SLR 1 +	SLR 2 +	Decreased recharge	Increased extraction	Decreased recharge & increased extraction
No changes	Starting-point	1S1	2S2	3R	4E	5RE
SLR 1 +	N/A	N/A	N/A	6S1R	7S1E	8S1RE
SLR 2 +	N/A	N/A	N/A	9S2R	10S2E	11S2RE

Table 1: Coding: S = sea level rise, 1 = 1-meter, 2 = 2-meter, R = recharge, E = Extraction, RE = Recharge & extraction. Prefix numbers are cumulative serial numbers.

4. Results

This results section consists of three parts. First, the initial salinity distribution and hydraulic head results are explored. Secondly, the extraction component is discussed. Thirdly, scenario results are investigated. Overarching all three parts is the underlying modelling process of which some key-details are provided in the paragraph below before presenting the results.

4.1 Numerical considerations

iMOD-WQ does not allow computation over time periods longer than 10,000 years. To remain within the software's limitations, as a precaution, transgression/regression phases exceeding 10,000 years were split into two periods of equal length. As explained in appendix C2, a finite-difference (FD) method was chosen to numerically solve the model's underlying partial differential equations. This method allowed a relatively large fixed "stepsize", while other solvers did not. Knowing the stepsize of each run in advance provides the possibility to pre-construct and string together the individual runfiles iMOD uses to specify the model's parameters. The output from one model run would then function as the input for the next. Within each runfile, stress periods (SPs) were given a maximum duration of 1,000 years. One year was defined as 365.25 days, thus a single SP of 1,000 years was specified as 365,250 days and was solved within 366 "timesteps".

Using the large stepsize of 1000 days to perform paleo-reconstructive modelling negatively affected the Courant number resulting in convergence issues. The stepsize of an iteration is limited by the model cells' characteristics, not allowing any particle to move more than one cell. Examining intermediate flow velocity results provided insight in the parameter adjustment necessary to optimize computational stabilization criteria, resolving non-convergence and reducing the model's runtime.

Test runs were also performed using a total variation diminishing discretization scheme (TVD-solver) to compare modelling results calculated using different solvers. However, the use of this method was quickly discontinued due to its significantly longer calculation times (up to 100 times slower than the FD-solver).

Because of the model's complexity, it is undesirable to discuss all model parameters individually. Therefore, to increase transparency and aid those wanting to work with the iMOD-WQ modelling

software, an exemplar sequential runfile is presented in appendix G1. For more information, regarding the code names of the parameters, the reader is referred to Verkaik & Janssen (2019).

The results presented below contain both 2D and 3D interpretations of the hydraulic head and salinity distribution of the Ayeyarwady Delta. To visualize the 3D modelling results, use was made of iMOD-WQ's option to write its output as .TEC-files, which was plotted using "TECPLOT".

4.2 Determining the initial salinity distribution

Groundwater salinity measurements throughout the Ayeyarwady Delta are scarce and hard to come by and were not made available. To provide an estimate of the initial salinity distribution, needed to calculate possible future scenario's, saltwater intrusions from past sea level fluctuations have been taken into consideration (Delsman et al, 2014; Van Engelen et al, 2019). Changes in relative sea level were imposed on the system by altering the extent of a fixed starting concentration and hydraulic head in the first model layer. Values for both variables in all subsequent model layers were then allowed to establish freely as a consequence of the model's top-layer. A visual representation of this concept is provided in appendix G2.

The paleo-reconstruction, spanning 129,705 years, consists of 32 consecutive runfiles and 160 SPs. To run it completely, it takes roughly 37 hours. The runtimes per runfile are presented in appendix G3. The paleo-reconstruction's 3D model outputs are presented in figure 8a, b, c, d, e, f. An enlarged 2D map of its proposed present-day hydraulic head of the first model layer can be found in appendix G4.

Figure 8a gives an overview of the present-day salinity distribution. Its top-layer provides a clear distinction between the Andaman Sea (red) and the Ayeyarwady Delta (blue) viewed from the south. To increase insightfulness, the model is split through the middle. Several tiers were then sawed into the multiple model layers to increase the visible surface area of the modelled salt concentrations throughout the system (figure 8b). The image suggests the presence of a classic saltwater wedge (referred to as a "toe") underneath the land surface. This lateral encroachment reaches further land inwards with increasing depth, as can be expected according to the Badon Ghijben-Herzberg principle (Drabbe & Badon Ghijben, 1889; Herzberg, 1901; Post et al., 2018). In between the freshwater recharge, imposed on the 1st model layer, and the saltwater intrusion toe, a concentration gradient developed, suggesting a thick transition zone of brackish/salty groundwater, becoming increasingly saltier with depth. Further inland, 2D cross-sections through the Ayeyarwady Delta show a density-inverted fingering process evolving downwards (figure 8c). At certain locations these freshwater fingers manage to reach bedrock relatively quickly (especially visible in the western part of the Ayeyarwady Delta freshwater), thereby creating isolated pockets of saline groundwater (figure 8d). The associated groundwater flow velocities confirm freshwater leakage within the domain of each freshwater lens. Coinciding with the suggested growth of these freshwater lenses is saltwater seepage due to the displacement caused by the infiltrating fresh water (figure 8e). Overall, this seepage has the highest relative velocities throughout the system (figure 8f).

Concerning the hydraulic head (figure 8f, appendix G4), on average the water table is shallow, which is to be expected in a deltaic area like the Ayeyarwady delta. The 88th percentile is still underneath 2 meters SWL. Especially the south-east, below Pyapon, and the south-west of the Ayeyarwady delta, underneath long island, show a potentiometric surface almost equal to sea level, suggesting a high susceptibility to salt water intrusion. Most of the deeper SWLs start around 150 - 200 km inwards for the Bago and Ayeyarwady Delta, respectively. Unconformities are visible underneath Mein-ma-hla-kyun island, the area south of Myaungmya and the spur on which Yangon City is located, all of which are characterized by being relatively elevated areas amidst low-lying delta terrain.

The delta's fresh groundwater volume evolution (as a percentage of the total volume of all actively modelled cells) preceding these results is presented in figure 9. Starting 129,705 BP with a 'fresh-to-

salt' scenario, during a transgression with an initial sea level of +10 meters, toe development reduced the fresh groundwater volume from 2.8% to equilibrium value 1.9%. During the first regression, a freshening of the groundwater system took place in an exponential decreasingly increasing fashion but did not reach equilibrium before the end of the period. Advancing seas during the second transgression decreased the fresh groundwater reserves through the rapid salinification of the model-layers underneath the Andaman Sea. Interestingly, after reaching a minimum fresh groundwater volume, reserves slowly started to increase again in an irregular (linear) manner. Having not reached equilibrium during the last regression, this contradiction is a consequence of the "flushing" of residual pockets of "paleo"-saltwater left from stands of high sea level. The three-consecutive transgression/regression cycles show similar patterns with two notable changes in their development. Firstly, the relative increase and decrease in fresh groundwater volume are much smaller due to the bathymetric slope development of the research area. The relative size of the landmass being exposed becomes smaller for lower sea levels, even though the change in sea level is relatively large (appendix G5a). Secondly, at the start of the 4th transgression a stable equilibrium presented itself almost immediately, indicating that trapped saline groundwater pockets had been removed entirely. This is confirmed by the subsequent regression during which a freshwater equilibrium is reached. The impact of the 5th transgression is biggest from 10,000 BP (- 65 m to + 4m), inundating a vast area of land, causing the sharp drop in the freshwater volume (appendix G5b). The Holocene clay layer, activated 7000 BP, did not result in significant retardation of any volume changes. The -2m event finally increased the fresh groundwater volume again, which remained similar until the present-day 10.6%.

To evaluate the added value of the paleo-reconstruction relative to the amount of effort it requires, its results were compared to a model run of (almost) equal length (130,000 years), considering only a "static" present-day sea level, starting in a fresh-to-salt scenario. Consisting of 13 consecutive runfiles and a total of 131 SPs, it took approximately 2 hours and 15 minutes per 10,000 years. A complete run thus takes a little over a day to compute and is therefore slightly quicker than the paleo-run. The salinity distribution results per model layer are compared for both the paleo-reconstructive computations (appendix G6a) and the static RSL run (appendix G6b). Both progressions show signs of fingering and saltwater toe development, with salt intrusions quickest to become substantial along the terrain with the lowest hydraulic heads near the south-eastern shore of the Ayeyarwady Delta. The most notable difference is the overall extent of saline groundwater present through the centre and west of the Delta. Furthermore, besides the extended spatial distribution, in the paleo scenario higher salinity values are also experienced shallower. While the paleo-system did not have the time to reach equilibrium yet, when comparing present-day volumes of fresh groundwater, the impact of the last 6425 of sea level fluctuations have been significant, suggesting a 33% overestimation of the fresh groundwater reserves in the static RSL scenario (figure 9).

It would be convenient if a paleo-reconstruction would not have to go back 130,000 years. Therefore, a second, much shorter, paleo-reconstruction run was started from the moment that sea level exceeded current sea level 6425 years BP using a fresh-to-salt scenario (with concentrations as described in appendix C1). Although a salt water wedge still needs to develop using such a scenario, it has become clear from the narrative above that an almost entirely fresh groundwater system had developed (appendix G7). Considering sea level has been below present-day sea level from 119,843 BP until 6,425 BP, groundwater storage underneath the present-day delta was entirely fresh until the first transgression event reached current sea level. The difference in the initial salinity concentration is small (appendix G8), but causes both runs to have a different starting point. The percentages freshwater volumes of both runs are compared in appendix G9. After the very first SP, they follow an almost identical path. System behaviour regarding changes in fresh water volume result in nearly the same fresh groundwater equilibrium for both the truncated and the full paleo-reconstruction. Nevertheless, having run the full paleo-reconstruction, and it still being the most inclusive, its results were used as the starting point for added the groundwater extraction component.

Exemplary 3D model output

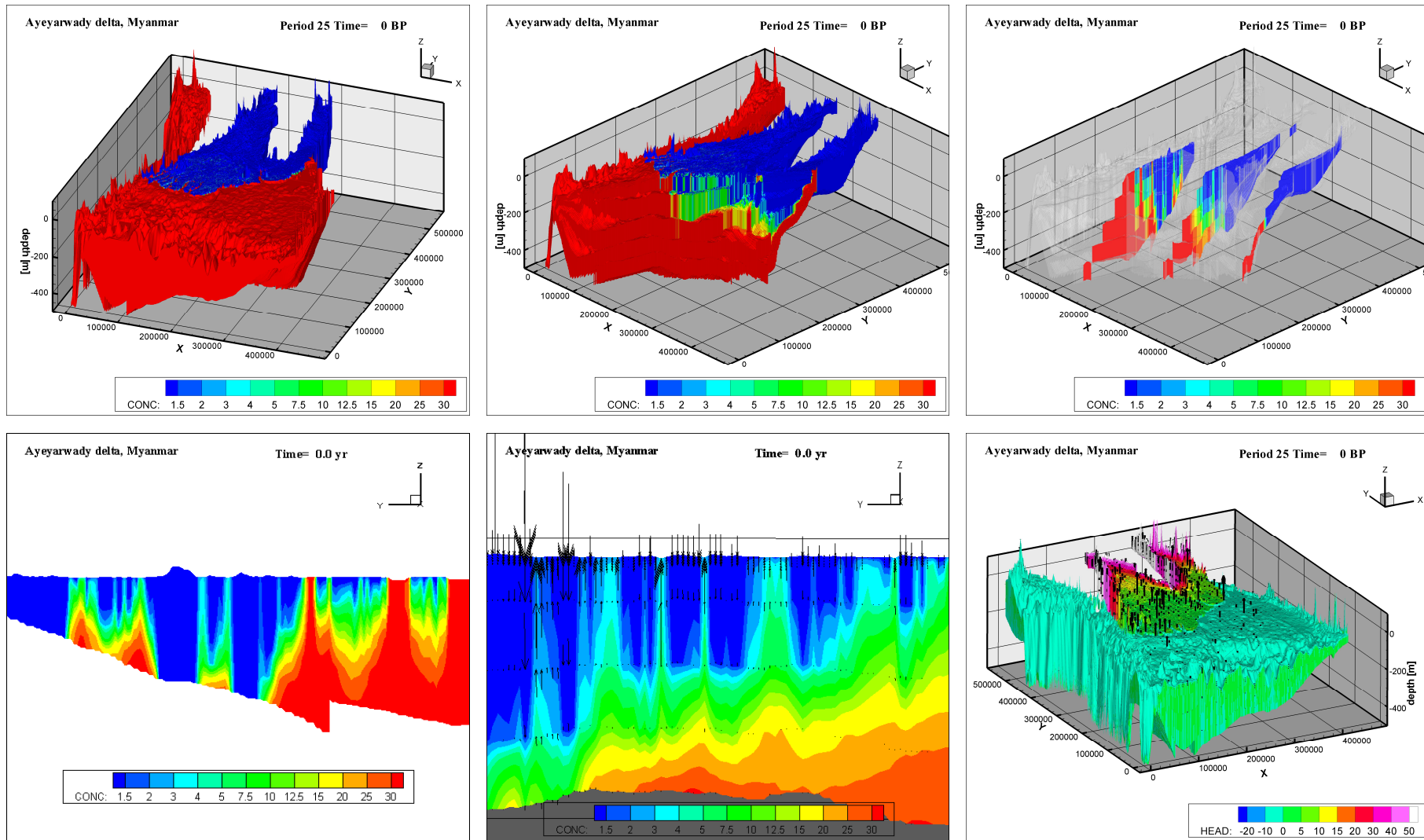


Figure 8a, b, c, d, e, f: 3D salinity concentration overview (a, upper left); 3D salinity concentration tiers (b, upper middle); 2D salinity concentration cross-sections (c, upper right); fresh water fingering touching bedrock at the western edge of the modelled area (d, lower left); 2D velocities cross-section (e, lower middle); 3D velocities delta overview (f, lower left).

Fresh groundwater volume evolution as a result of fluctuations in relative sea level

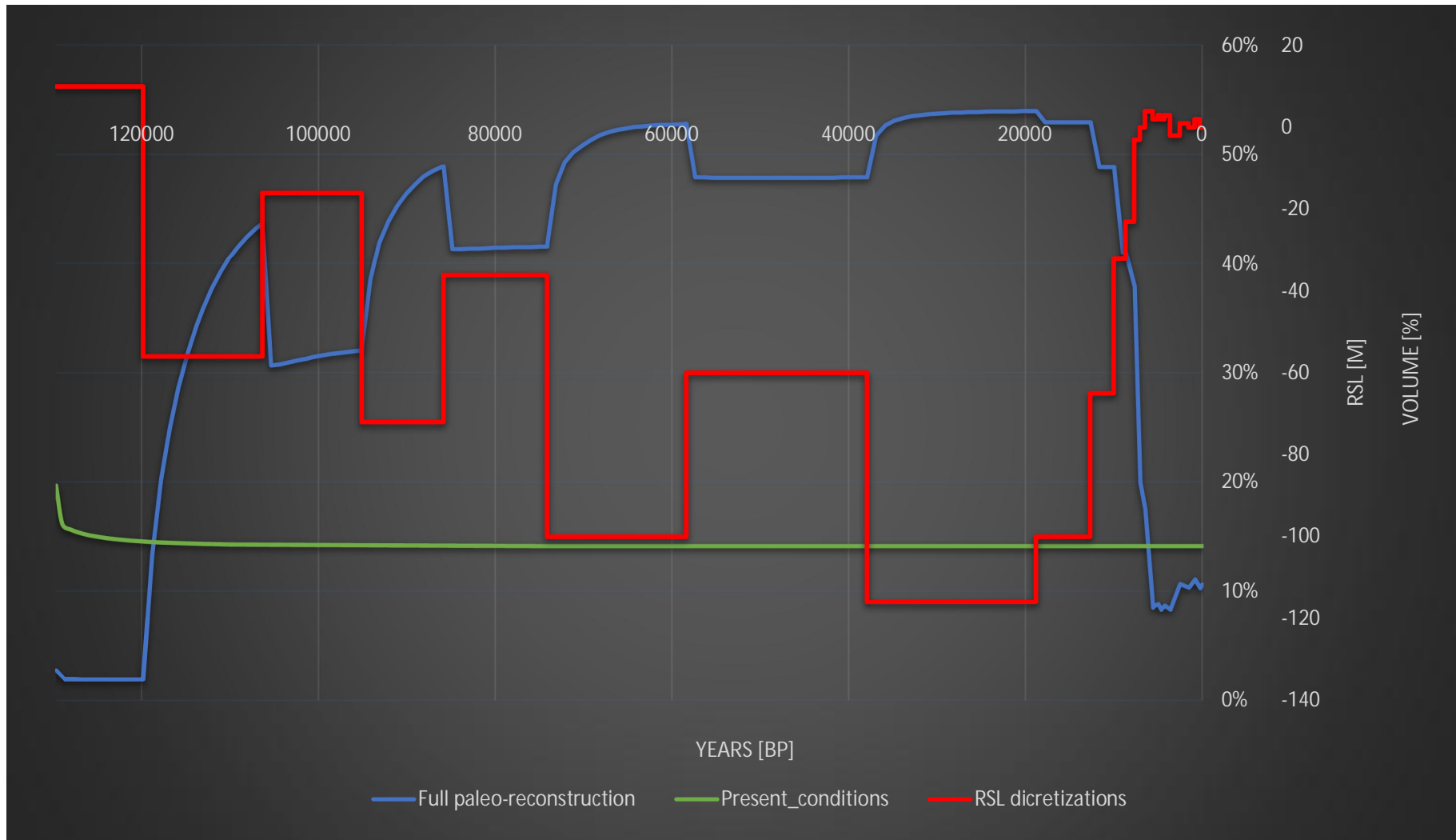


Figure 9: this graph illustrates the change in quantity of fresh groundwater of the entire model as a result of fluctuations in RSL (red) during one full glacial-interglacial cycle (blue), as well as for a fixed present-day RSL (green). The final fresh groundwater volume of 10.6% suggested by the full paleo-reconstruction modelling run is equal to a volume of 2107 km³.

4.3 Extraction component

With a groundwater monitoring system for making continuous measurements of heads and salinities still being under construction, the only available groundwater table measurements (SWLs/PWLs) were those listed in the well-logs used for making the 3D voxel model of the subsurface (figure 2). These measurements, registered during the wells' construction, were ANUDEM Interpolated (Hutchinson et al., 2011) to provide a first estimate (be it a coarse one) of the impact of groundwater extractions on the Ayeyarwady Delta's groundwater table (figure 10 a, b). Excluding the Bago division from analysis, for which no data could be acquired (marked with a black mesh), the SWL interpolation suggests an overall water table within 0 - 6 m from the surface. Further north, the water table becomes less shallow, which is to be expected considering the increase in elevation when moving further inland. The notable exceptions to these observations are centred around Yangon and along the western mountains (figure 10a). The consequent PWL interpolation illustrates an intensification of the proposed water table depressions around Yangon and along the western border (figure 10b). Furthermore, it expands the extraction regime's sphere of influence to include the central Delta. In contrast, the south seems to be relatively unaffected. Although the utmost south does not concur with this general perception, an evaluation of the data points, used to create the interpolation, reveals that a single data point is responsible for this unconformity. These water table measurements suggest a major drawdown to be present underneath Yangon even before additional pumping commenced, indicating a significant groundwater extraction component in and around Yangon preceding the other areas experiencing a drawdown. Drawdown intensity estimates range from 0 – 5 m for the central areas, 5 – 10 m within the areas affected along the western edge and up to 10 – 20 m around Yangon.

These interpolations, being the only measurements available for model validation, were compared to model run 24 and 25 (appendix G3), without and with 20 years of extractions included, respectively (figure 10c, d). Using the same legend as used for the well-log SWL/PWL estimates, at first glance, the modelling results with the added extraction component seem identical to the modelling results without. Also, results show little resemblance to those proposed by the interpolation of the measurements and seem to suggest a deeper water table only at locations with a relatively elevated position within the surrounding landscape. However, further scrutiny reveals that the locations where extractions are most impactful, made visible in figure 11, are much more concurrent when viewed relative to the modelling results instead of relative to the well-log measurements.

Figure 11 confirms the extraction regimes impact on the central Ayeyarwady Delta and also suggests minimal activity in its southern regions. Concerning the latter, given the salinity distribution results presented in section 4.1, the increased groundwater salinity in that particular area could be the cause for this lack of perturbation. Further, also in agreement with the measurement interpolations is the increased activity underneath Myaungmya to the west. Although relatively far to the south, it is apparent from the salinity distribution modelling results (appendix G6a) that this elevated area has remained fresh during periods of high sea level, making it an attractive location for groundwater resource development. Increased activity, and thus a drawdown, would therefore be a logical conclusion. Further to the east, a drawdown is also present around Yangon, but is nowhere near the intensity suggested by the measurements or expected for a location with such a high population density. Because no differentiation was made between villages and cities (with increased freshwater demands), Yangon (and all other larger cities for that matter) are most likely being underestimated in their impact on the groundwater system. Besides these (spatial) similarities, figure 11 differs from the well-log interpolations in its predictions along the western edge of the Ayeyarwady Delta due to the absence of wells probably present in this area. Within the modelling simulations, wells were excluded for that area because of the unambiguous presence of low permeable material in the voxel model. While the addition of an extraction component did not seem to significantly affect the salinity distribution, experiencing only a change from 10.62% to 10.63% during a 20 year period (figure 9), the difference in the magnitude with the drawdown presented by the measurement interpolation is substantial and therefore taken into consideration during the evaluation of the scenario results.

Well-log measurements compared to modelling results

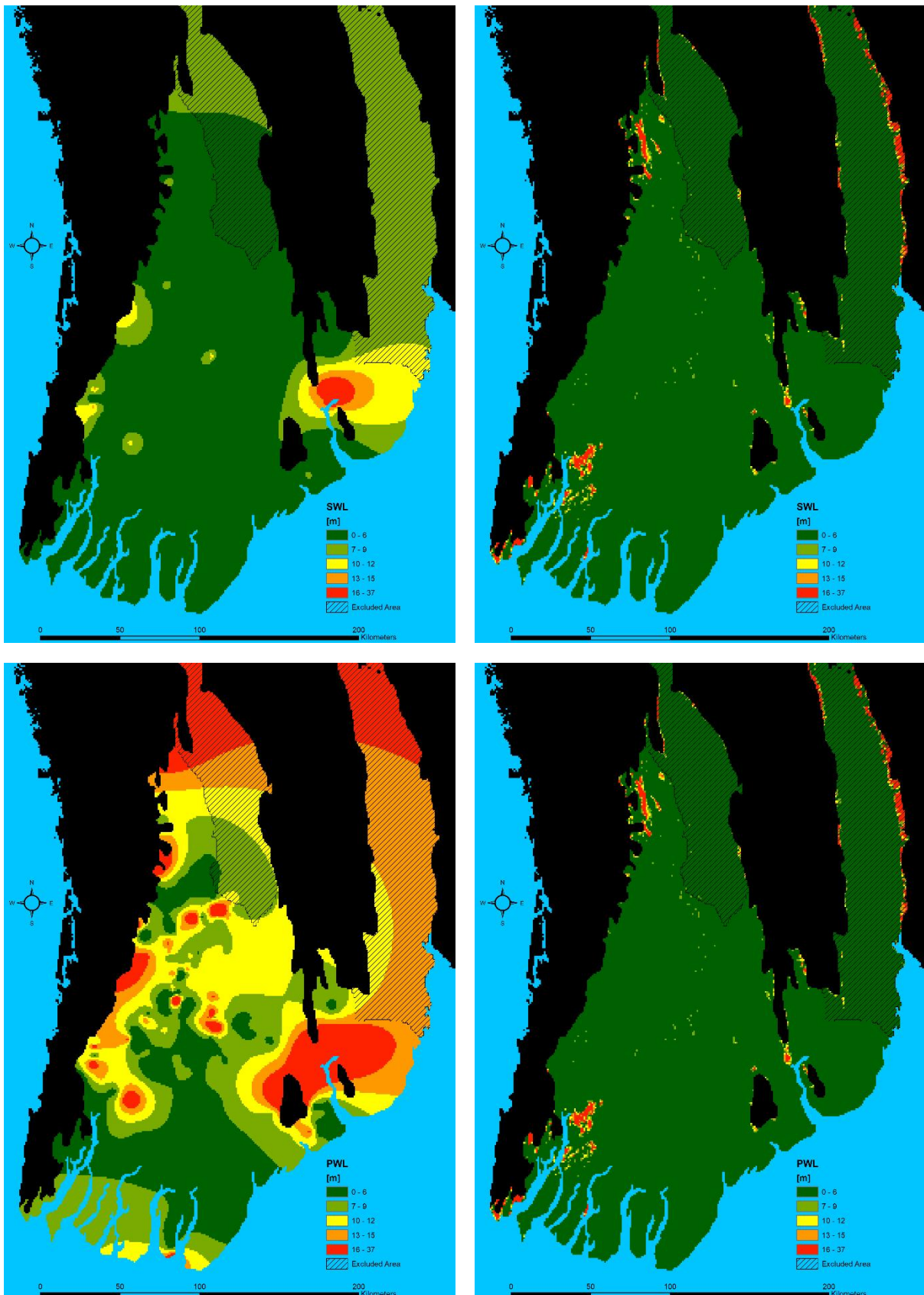


Figure 10a, b, c, d: well-log SWL (a, upper left) and PWL (b, lower left) interpolation. Modelled SWL (c, upper right), PWL (d, lower right). Heads are relative to mean sea level.

Extraction component: hydraulic head difference between 20 BP & present

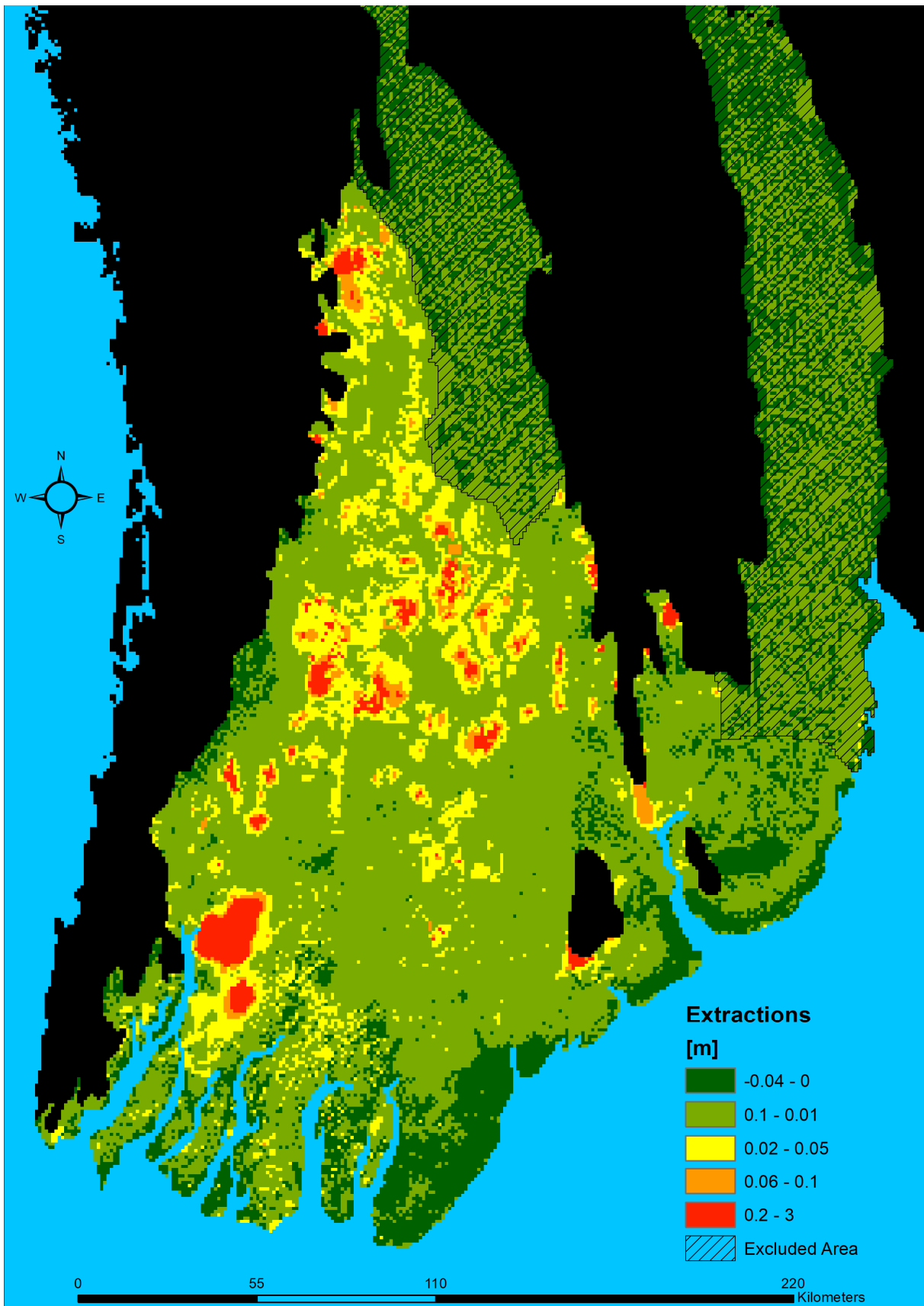


Figure 11: the effect of the groundwater extraction component on the groundwater table throughout the Ayeyarwady Delta (SP 24 minus SP 25). Negative values indicate an increase and positive values indicate a decrease in hydraulic head.

4.4 Scenarios

Using the modelling results of the 129,705-year long paleo-reconstruction as a starting point, the scenarios' results, exploring the impact of increasing groundwater extractions, a drying climate and RSLR on the groundwater system of the Ayeyarwady Delta (as described in section 3.2.4), are presented in figure 12. All eleven scenarios and a "business as usual" scenario ("0Base", referred to as the baseline scenario), were created using the same legend. The legend distinguishes between mm, cm, dm and meter changes in head, decrease or increase, and is used to compare their impact relative to each other and determine for which change the system is most susceptible. Using the FD-method, each 30-year scenario, calculated from 2020 to 2050, could be computed in roughly two minutes, making the model a valuable tool to obtain preliminary results when exploring the impact of parameter changes.

When extrapolating present-day conditions 30 years into the future (baseline scenario), a general diffuse image of an alternating increase and decrease of hydraulic head is presented. When compared to the initial salinity distribution, it becomes evident that a decrease in head, within the millimetre range (up to but not including one centimetre), is expected for the areas affected by saltwater intrusion in the southern part of the delta. The increase in head, also within the millimetre range, can be seen to start in the central delta, continuing land inwards, and for the areas in the direct vicinity of the coastline. However, these changes are small compared to those that occur in the southwestern part of the Ayeyarwady delta, where a decrease in head, mostly limited to areas of higher elevation, and an increase in head, limited to the boundaries of the area's peninsulas and islands, are expected. Invoking a one-meter RSLR (1S1 scenario) is expected to increase the hydraulic head along the entire coastline. This increase in head ranges from a couple of centimetres into the high decimetres, with change diminishing with increased distance from shore. On average, its effects reach 10 kilometres inland, including the position of Yangon, and is largest in the southwestern part of the Ayeyarwady Delta. The 2S2 scenario, an exaggeration of the 1S1 scenario, extends the ocean's influence an additional 5km inland. It also slightly increases the intensity of the increase in head, sporadically exceeding the meter mark. Furthermore, any decrease in hydraulic head projected to occur in the baseline scenario is almost entirely nullified by the rising of the sea.

The 3R scenario eclipses the slight increase and reversed any decrease in head present in the baseline scenario. Although the effect of the 20% decrease in recharge is strongest (within the decimetre range) for locations with a high hydraulic head relative to the surrounding areas, the reduction is omnipresent in the centimetre range. The one outlier that presents itself lies in the far north of the Ayeyarwady Delta, suggesting reductions of up to 3 meters.

The increased groundwater extraction in scenario 4E magnifies the changes discussed in section 4.2 and is in addition to the changes proposed by the baseline scenario. The decrease in head is concentrated around areas suspected of using groundwater for irrigational purposes (primarily the central delta), Yangon and the higher elevations in the southwest of the Ayeyarwady delta. These drops in water table, for the most part, stay within the cm range, bar the elevated area around Myaungmya, which seems more significantly affected (within the decimetre scale). Although domestic extractions are wide-spread and of considerable magnitude when combined, their diffuse nature seems to distribute their impact in such a way that the potentiometric surface is not much affected.

Both the decrease in recharge and the groundwater extraction cause a decrease in the hydraulic head. Their combined effect, represented by scenario 5RE, suggests a near linear addition of the extraction drawdown to the overall decline of the water table caused by diminishing recharge. Within this relation, the effect of the reduction in recharge is approximately one order of magnitude dominant.

Merging the effects of RSLR with the reduction in recharge in the 6S1R and 9S2R scenarios shows that RSLR is the leading process in the southwest, where its effects are largest. However, the distance over which RSLR causes an increase in hydraulic head is being reduced from 10 to 5 km inland. To the southeast and east the RSLR's effects become less prominent, whereas the lowering of the water table suggested near Yangon in the 3R scenario is, for the most part, merely reduced in its intensity, instead

of experiencing an overall increase in hydraulic head as suggested by the scenarios enforcing RSLR alone. Furthermore, the 9S2R scenario, a more intense version of the 6S1R scenario, shows less growth with respect to each other than is visible between the 1S1 and the 2S2 scenario and reduces the overall intensity of the increase in head as a consequence of the RSLR.

Scenario 7S1E and 10S2E combine the effects of RSLR with the groundwater extraction component. For the most part these components interact near Yangon and Myaungmya. The drawdown caused by the groundwater extractions is cancelled out in Yangon for both scenarios, while the areal extent and intensity of the drawdown near Myaungmya are significantly reduced.

The effects of a rise in sea level are still predominant in scenario 8S1RE and 11S2RE and reach a similar extent as for the combined RSLR and recharge results. The inclusion of the extraction component then slightly dampens the intensity of the drawdown in groundwater extraction areas.

The timeframe for which these scenarios are computed is relatively short with respect to the operational times needed for solute transport to effectuate deviations within the salinity distribution. Spatially, change would be minimal and hard to distinguish. To provide an indication on the propagation of saltwater intrusion figure 13 presents the impact on the total fresh groundwater volume following each scenario.

The most striking is the separation of all scenarios into three groups of four scenarios each for which the leading factor is RSLR. The four scenarios without an inducement of increased sea level show a very minor decrease in overall salinity during the 30-year projection. All other scenarios portray an increase in overall salinity, whereas the plus one-meter RSLR scenarios are exceeded by the scenarios experiencing two meters increase in RSL.

Within each scenario quartet, there are minor variations. While the 0Base and 4E scenario illustrate an increase in the percentage of fresh groundwater, the 3R and 5RE scenario lessen this projection. In continuation, for the +1 and +2 RSLR scenarios, the 6S1R and 8S1RE and the 9S2R and 11S2RE scenarios are more saline than the 1S1 and 7S1E and the 2S2 and 10S2E scenarios. The reduced recharge component thus suggests being responsible for a (minor) increase in saltwater intrusion. An increased relative pressure exerted by the sea as a result of the decrease in inland hydraulic head could enforce a stronger saline seepage, providing a plausible explanation.

When comparing the fresh groundwater volume for the 1S1 and 7S1E the 2S2 and 10S2E scenario, the addition of the extraction component does not seem to lead to increased saltwater intrusion. Although their end results are identical, their progression differs. The decrease in fresh groundwater for scenarios with an extraction component are following a progression of a linear nature, while those without an extraction component are decreasingly decreasing. This difference might be originating from the additional SP calculated for scenarios with an extraction component. Regardless of the reason, it suggests that an increase in the extraction intensity does not necessarily lead to an increase in salinization.

As can be distilled from the above, regarding the hydraulic head, the reduction in recharge and the increase in relative sea level are of a similar magnitude, while the extraction component is one order of magnitude smaller for the areas where extractions are most represented. The process of RSLR is most significant in the southwest of the Ayeyarwady Delta, while recharge reductions are dominant land inwards and more successfully equipoise an increase in hydraulic head as a consequence of RSLR to the southeast and the east, including Yangon.

Regarding saltwater intrusion, within these results, RSLR is identified as the largest contributor to salinization, with a reduction in recharge playing a minor contributing role. No proof of salinization as a result of groundwater pumping could be proved. However, areas with a high density of groundwater pumps suspected of being used for irrigation coincide with RSLR affected areas to the southwest (around Myaungmya) and around Yangon. Keeping in mind that extractions are likely still underestimated (section 4.2), an interaction threshold could be preventing the connection.

Ayeyarwady Delta groundwater scenario results for 2050

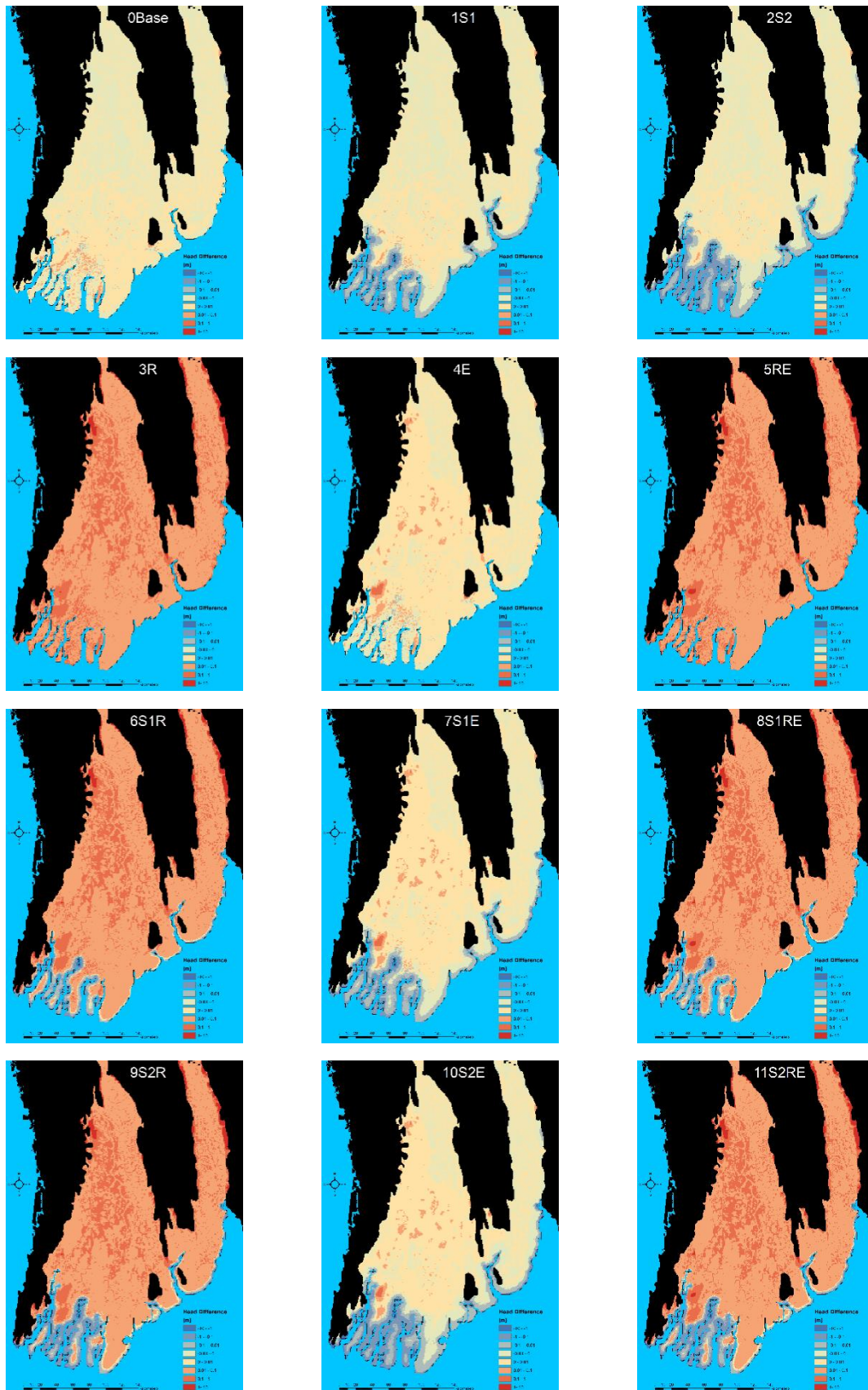


Figure 12: changes expected in the hydraulic head of the 1st model layer for each scenario calculated by subtracting the 30 AP scenario results from the 0 BP paleo-reconstruction result. Therefore, values are inverted, a negative head difference suggests an increase in the water table (blue) and vice versa (red).

Scenario fresh groundwater volume changes

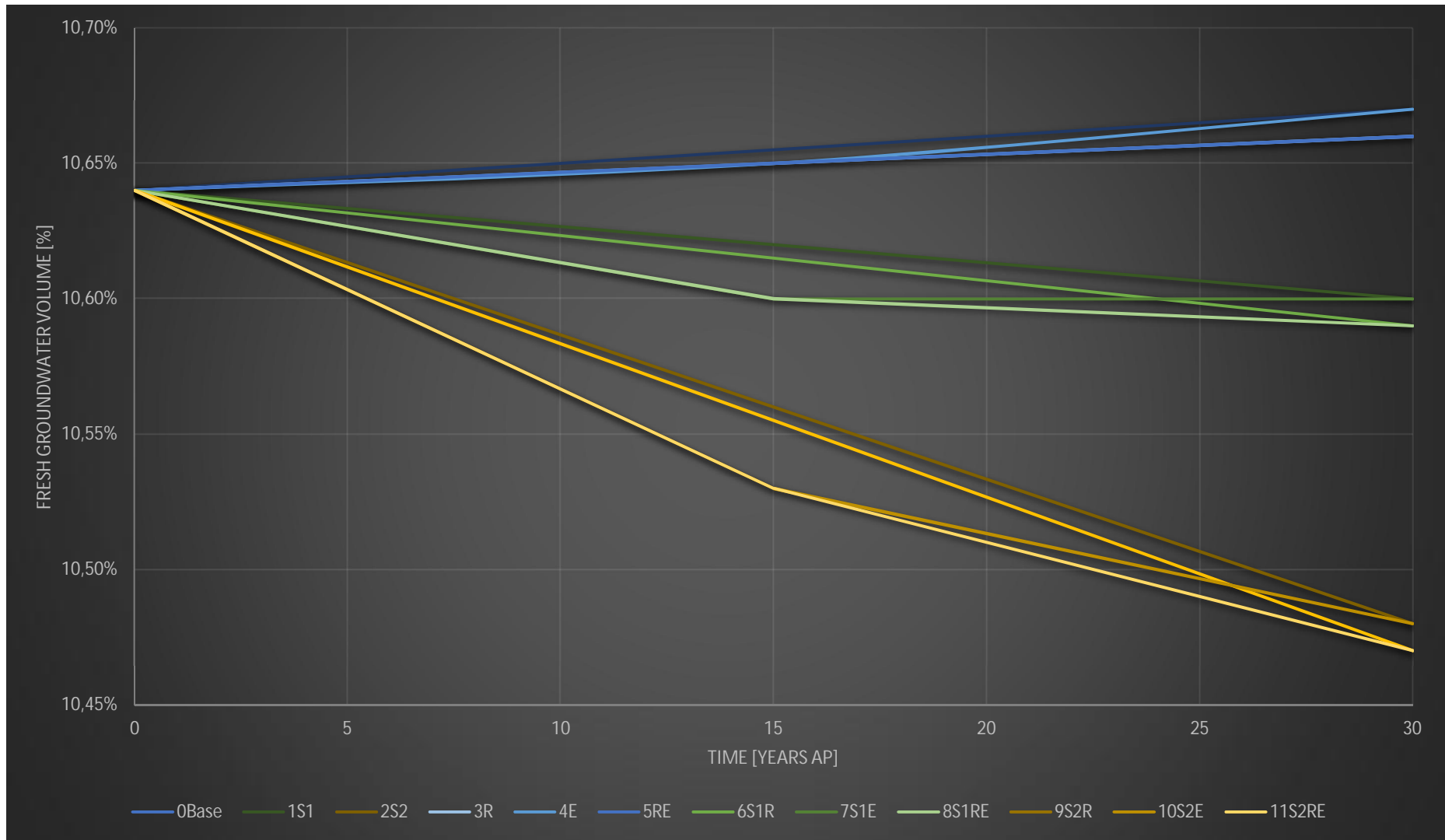


Figure 13: the percentual change of fresh groundwater with respect to all actively modelled cells for each computed scenario (0.01% equals a volume of 1.982 km³ ≈ 2 km³).

5. Discussion

The quality of the results produced by any model are directly affiliated with the quality of its input data. Therefore, pivotal in model development is the gathering and verification of required information. Fortunately, forthcoming individuals, willing to part from predominant reticence to work within a mutually beneficial collaboration, provided essential documentation on the local hydrogeology. Subsequent scouting within the research area then laid the foundation for the assumptions needed within the data scarce environment.

Below, a discussion follows, providing a critical view on the experience working with the input data, the assumptions made and the modelling results. While area specific comparative materials of equal scope are virtually non-existing, a limited literature comparison is made to provide perspective.

Geological model

Regarding the hydrogeology, the 3D voxel model's layer structure resembles that of the assumed structure of the Ayeyarwady Delta's subsurface presented in literature (Viossanges et al., 2017). Although the SOBA report describes three general formation types: the Peguian, Alluvial and Ayeyarwady Formation (Fm), the latter two are by far the most common throughout the Ayeyarwady Delta. The Alluvial Fm, with a thickness ranging from 30 to 50 meters thick, is represented by the first five model layers, which have a combined constant thickness of 25 meters. The second five model layers of variable thickness to a maximum depth of approximately 800 meters then represent the underlying Ayeyarwady Fm, which is thought to exist of mostly sand with interbedded clay layers. The supposed diffuse transition zone between the two formations would therefore be within the sixth model layer. Considering the scale of the groundwater model presented here, this coarseness is thought to be warranted within the limits of providing a first estimate. Nevertheless, a more accurate similarity in absolute terms is desirable. A multitude of the constant vertical level layers with a thickness of 5 meters each, down to 50 meters would be more appropriate for representing the Alluvial Fm. Unfortunately, realizing such a layer sequence, whilst maintaining a logical depth resolution progression, was precluded by the thinning of the proposed regolith thickness near mountainous regions and on sea floor expanses. While the limited artificial thickening of the unconsolidated material through the deepening of the proposed depth to bedrock had a limited interrelation with the actively modelled area (Appendix D7), insufficient evidence exists to suggest a methodical approach to further expend upon the regolith thickness estimates provided by Zamrsky et al. (2017). However, a more extensive thickening is suspected to provide a more accurate depiction of the actual thickness of the sedimentary basin when considering proposed depths to bedrock for the Ayeyarwady Fm by both Viossanges et al. (2017) and the MOGE. In line with this suspicion, a number of wells used in the interpolation of the 3D voxel model where outside of the actively modelled area (+/- 8% of the total amount of wells), assumed to be unconsolidated (Appendix H1), while other wells' depth estimates had to be truncated to not exceed the depth to bedrock (+/- 6% of the total amount of wells (Appendix D4)). Although Zamrsky et al. (2017) their regolith thickness estimates and Hartmann & Moosdorf (2012) their GLiM-dataset provide first estimates for three dimensional model boundaries, these findings suggest additional criteria are needed to define the boundaries of the Ayeyarwady Delta's unconsolidated basin to facilitate the approximately 12% of wells (combined) that had to be altered or excluded during the geohydrological voxel modelling process.

Paleo-reconstruction

Regarding the data used for the paleo-modelling, no reconstruction could be found specific to Myanmar on the regional progression of relative sea level rise. Whilst the composite RSLR-curve provided by Loveson & Nigam (2019) is within the same oceanic region for which change in RSLR should be similar (Pirazzoli, 1996), the RSLR-curve from Grant et al. (2012), with which it was combined to be of sufficient length to model to desired 129705 years into the past, is not. Combining both, the discrepancy between them have been made clear in appendix H2. The relative progression of both curves shows an earlier rise in RSLR by Grant et al. (2012), overtaken by Loveson & Nigam (2019)

roughly 7500 BP. The two most important differences are Loveson & Nigam (2019) their transgressions from, approximately, 6800 – 3800 years BP, absent in Grant et al. (2012) and the increased intensity of its transgressions over the last +/- 2300 years according to Loveson & Nigam (2019), both of which are important in the establishment of the initial salinity distribution. With the period 14500 BP represented by the more appropriate Loveson & Nigam (2019) curve, the use of Grant et al. (2012) their curve was limited to the historic period before 14500 BP. Although the use of the RSLR-curve from Grant et al. (2012) before 14500 is questionable for the Ayeyarwady Delta, the general global tendency of RSLR during the last glacial/interglacial is still represented within its development and the coarseness of the discretizations created.

The paleo-reconstruction results exhibit a dynamic equilibrium development time that is reached more readily for transgression than for regression, which is in accordance with results presented by Mulder (2018). Preliminary examination of the modelling results distinguishes four interlinked processes affecting the Ayeyarwady Delta's freshwater volume progression and its ensuing equilibrium. In order of decreasing rapidity and influence, on a delta scale: vertical saltwater intrusion (transgression inundation), horizontal saltwater intrusion (toe development), density-inverted fingering (freshwater lens development) and the elimination of residual saltwater compartments (christened "paleo-flushing"). Further research would be required to investigate their evolutionary interrelations under different hydrogeological settings using a higher frequency SP interval to improve the understanding of and the predictive possibilities for the concluding salinity distribution. In this particular hydrogeological setting, paleo-flushing removed practically all residual saltwater after roughly 70,000 years. However, it is very well possible that this is a consequence of an oversimplification of the geology and the use of potentially less than pertinent estimates for the hydraulic conductivity. Nevertheless, the shallow paleo-modelling result (especially model layer 6) resembles estimates made of the groundwater salinity front by the IWUMD presented in the SOBA report (Viossanges et al., 2017). The paleo-modelling results differentiate themselves by suggesting a scattered occurrence of saline groundwater pockets further inland, as a consequence of past transgression infiltrations, as well as suggesting an extended salinity front at greater depth. Additionally, the eastern part of the Delta is proposed to be less extensively affected by saltwater intrusion than is suggested by Halcrow & Partners (1983), thereby creating a more realistic scenario considering the extensive use of fresh groundwater in Yangon. Unfortunately, the more recent IWUMD estimations did not include the far east of the Delta, making any further comparison for the Yangon area an impossibility.

Groundwater extraction

Regarding the groundwater extraction component, due to the lack of regulation, information about the Ayeyarwady Delta's pumping regime is very limited. Other than the documentation within the well-logs, no official data was (made) available, neither on the present-day number of wells, nor their location, nor their extraction rate. Despite this inconvenience, to include a more realistic view on the scale of the groundwater extractions than presented by the well-logs alone, assumptions for the groundwater extraction component were formulated on the basis of data gathered in the field (appendix B). However, progressive estimates still seem to underestimate the impact of pumping activities (section 4.2). The influence exerted by pumping in the results is most observed for agricultural areas where extractions are concentrated. On the other hand, domestic use seems to hardly create an impact on the groundwater table. Although there is no data available specific to the research area, a comparison with literature can be made derived from national estimates. Approximately 9% of the country's yearly total water consumption of 33 km³ is of groundwater origin, equalling roughly 3 km³ of fresh groundwater. On average, domestic use in the delta accounts for 50% of the total volume extracted (Thein, 2020), which is in agreement with the SOBA report (Viossanges et al., 2017). When this 50% is taken as the national average for domestic extractions, then the total national volume of domestically used groundwater would amount to roughly 1.5 km³. In turn, this then suggests an equal residual part of 1.5 km³ is used for agricultural purposes, which corresponds

with the estimated groundwater used for irrigation according to (FAO, 2011). Translating these national figures to concern only the Ayeyarwady Delta is of course assumptious, but defensible when serving only the purpose of providing ballpark estimates. Domestically, discriminating on the basis of population, with roughly a quarter of the country's residence (section 2.1) living in the Ayeyarwady Delta, total groundwater use would amount to approximately 0.375 km^3 . While the number of wells over which this divided is unknown, Hulsman et al. (2013) estimated over 400,000 wells to be installed throughout Myanmar, most of which for domestic purposes. Agriculturally, the Ayeyarwady Delta and the Central Dry-Zone make up the vast majority of irrigated land. Dividing extractions between both regions equally then results in a fresh groundwater consumption of approximately 0.75 km^3 . With 4% of a total irrigated area (1,841,000 ha) supplied by tube wells and one tube well allowing supplementary irrigation on 4 ha, around 18,410 tube wells are thought to be responsible for the production of 0.75 km^3 of fresh groundwater intended for irrigation (FAO, 2011). Comparing these estimates from literature with the modelling input estimates (appendix H3a, b), the number of wells intended for agricultural purposes turn out to be within the same order of magnitude, be it slightly underrepresented, 14,044 wells modelled versus 18,410 wells deduced from the Aquastat data (FAO, 2011). Domestic wells are more numerous presented in the groundwater model. Whereas the country-wide estimates are around 400,000 wells, using the methodology presented in section 3.1.3.1, 349,110 wells are thought to be present for the Ayeyarwady Delta alone (!). The domestic extraction rate during modelling was set at 100 L per household per day. Compared to literature estimates of 135 L per person per day, calculated by dividing the estimated 0.375 km^3 of fresh groundwater extracted for domestic purposes over 50% of the Ayeyarwady Delta's population (FAO, 2011; Viossanges et al., 2017). Consequently, dividing the 7,510,000 people over the 349,110 modelled wells results in a (rounded) estimate of 5 people per household. Multiplying the number of people by their average extraction rate of 135 L per day, considering 4 households per well, domestic extractions are then suggested to be around 2700 L per well per day instead of the now implemented 400L per well per day, thus suggestive of a factor 7 underestimation of the domestic extractions. Agriculturally speaking, dividing the estimated total volume extracted yearly by the number of suggested wells, each well is expected to extract approx. 146 m^3 per well per day. When compared to the fieldwork conclusions, agricultural extraction rates are possibly underestimated by a factor 4. The current ratio implemented in the groundwater model is 26% domestic groundwater extractions versus 74% agriculture groundwater, which differs significantly from the expected 50:50 volumetric ratio suggested by literature. Furthermore, it must be noted that the values suggested by FAO, (2011) are two decades old. As noted in section 2, considerable development has taken place, especially with respect to groundwater resources. Since then, Myanmar's population increased by roughly 16% (Worldometer.info, 2020) and agricultural exploits have risen from 1,841,000 ha in 2000 to 2,722,000 ha in 2006 and can be expected to have increase further accordingly. The magnitude of the underestimation might be larger still in the domestic sector. The current methodology used does not (yet) differentiate between villages and cities. The need for additional criteria as such, to more accurately model the stress urban areas exert on the groundwater system, is most apparent when observing the modelling results for Yangon in figure 10 and 11. Groundwater level has declined significantly in Yangon over the last 25 years (Thein, 2019a). Currently, the 4.5 million plus Yangon citizens (Worldometer.info, 2020), of which on average roughly 50% relies on groundwater, use approximately $566 * 10^3 \text{ m}^3$ per day divided over the estimated 100,000+ tube-wells throughout the city (Thein, 2019a). These estimates imply that Yangon alone comprises an extraction component four times larger than what has currently been modelled for the entire Ayeyarwady Delta. Even when the suspected underestimation described above is compensated for, the Yangon component would still make up 60% of what is suggested that should be modelled. Considering the above, it is possible that an increase in extractions will also influence the salinity distribution. Currently, the scenario results don't suggest a relation between saltwater intrusion and groundwater extraction. However, a pumping induced cone of ascension could displace the fresh/salt groundwater boundary significantly, potentially decreasing fresh groundwater resource availability.

6. Conclusion

Through paleo-reconstructive modelling, the present state of the Ayeyarwady Delta's groundwater regime and the initial salinity distribution was approximated and consequently used to model scenarios that provide insight in the Delta's relative sensitivity to future changes in recharge, sea level rise and groundwater extractions.

Throughout the Ayeyarwady Delta's groundwater development four governing processes could be distinguished, ordered in terms of relative rapidity: transgressional infiltration, lateral encroachment, density-inverted fingering and "paleo-flushing". Although being a sluggish process, results indicate that during the lower than present sea level, from 119843 BP until 7000 BP, paleo-flushing has been responsible for the removal of practically all residual saline groundwater pockets that had formed during preceding periods of transgression. Subsequent modelling of the groundwater evolution, starting with a fresh-to-salt scenario at the start of the first transgression exceeding present-day sea level provided a nearly identical outcome to that of the 129705-year computation. These results suggest that, for regions with a historical RSL progression similar to that of the Ayeyarwady Delta, paleo-reconstructive modelling is sufficiently accurate in predicting the initial salinity distribution when modelled from the moment the first transgression exceeds present-day sea level, in this case starting 6425 years BP. Although paleo-reconstructive modelling is labour-intensive, neglecting to include the effects of RSLR in modelling delta groundwater development, modelling only present-day conditions, resulted in an overestimation of the fresh groundwater supply by roughly 33% ($\approx 695 \text{ km}^3$) and can therefore be considered injudicious.

Within the foreseeable future, a decrease in recharge and an increase in SL due to climate change and an increase in groundwater extraction due to population growth and increased agricultural development are expected. Relative to each other, SLR is identified as the largest contributor to groundwater salinization. While projections suggest the entire coastal region to be affected up to 15 km inward, the impact of RSLR on the peninsulas and islands in the southwest of the Ayeyarwady Delta is significantly more extensive. Meanwhile, recharge reductions are dominant land inwards, but play only a minor contributing role to salinization when compared to RSLR. Regarding groundwater extractions, well-log SWL/PWL measurements suggest drawdowns up to 20 meters and beyond due to groundwater extraction all throughout the middle and upper Ayeyarwady Delta and surrounding the cities of Myaungmya and Yangon. Although groundwater extraction modelling results were spatially comparable, extraction intensity was most likely underestimated (by a factor 7 and 4, regarding domestic and agricultural extractions, respectively) when compared to literature estimates. Currently, groundwater pumping could not be associated with increased salinization. However, an interaction threshold due to the underestimation of extraction intensity could be preventing the connection. Meanwhile, awaiting conclusive research, prudence is required.

Considering an estimated 50% of the population is depended on groundwater and fresh groundwater availability is expected to decrease, sustainable management is needed to safeguard resource availability. To fill knowledge gaps, data collection and especially the availability thereof needs to be improved. Appurtenant would be to restrict the currently unregulated use of groundwater through appropriate legislation. Meanwhile, from a precautionary principle point of view, conservative use of water resources is advisable. Localized anthropogenic impact has been largest to benefit agricultural development (with the notable exception of Yangon). Especially rice production during dry season is water intensive. Given the Ayeyarwady Delta's closed system nature, the top clay layer allows for limited recharge and results in high evaporation rates throughout periods of irrigation. Therefore, it would be recommendable to move away from double cropping paddy rice using groundwater and stimulate the cultivation of drought resistant crops instead. Other applicable methods to increase freshwater availability include water loss reduction through increased irrigation efficiency and education as well as increased water retention through e.g. Aquifer Storage and Recovery schemes.

7. Recommendations

A groundwater model is never definitively completed. Being an attempt to create a simplified version of reality, potential improvements always keep presenting themselves to benefit model accuracy. However, increased model complexity tends to lead to longer calculation times. A balance exists between model complexity and performance which should be considered when reading the following overview of potential model improvements.

A primary focus should be the addition of the geology inherent to the Bago region. Being a separate administrative district, also acquiring information necessary to supplement the voxel model's interpolation for the Bago region proved infeasible. However, its inclusion is important to provide accurate boundary conditions for the Ayeyarwady and Yangon Region.

To further benefit the voxel model, lithological complexity can be returned to the system through the uncoupling of the aquifer and aquitard categories into their individual parts (shale, silt, slate, aggregate, sandstone, clay, mud, gravel, different speciation of sand etcetera). Also, better conformity with the estimated thickness of the Alluvial FM would increase model representability. However, the current number of model layers is restricted by the maximum thickness of the thinnest sections of the delta. A way to work around this issue would be to incorporate bedrock as a layer with inert characteristics. In other words, create a mould of the bedrock to facilitate layer continuity.

Furthermore, the number of well-logs used for the geological model's interpolation could be increased to provide an improved overview of the spatial variability of the Ayeyarwady Delta's lithology. The DRD still has complementary well-logs for all other districts than Maubin. The DWIR has bore-logs near sluice gates and the MOGE could provide insight into the deep subsurface. In addition, since most wells are private, tube-well drilling companies might also be able to contribute significantly.

Another pressing limitation is the lack of hydraulic head and EC/TDS measurements needed for model calibration and validation. The Yangon Technical University (YTU) and Yangon University (YU) are in possession of numerous master theses containing relevant information. However, these documents are all hard copy and usually do not exceed township or city level. Furthermore, the two main water quality testing facilities are situated in Yangon and Naypyidaw. They should have relevant information.

Regarding the paleo-reconstruction, the reaction times of saltwater intrusions were relatively quick with respect to the timesteps designed for modelling 129705 years. Therefore, it is suggested to increase the SP resolution for the later stages of Delta development (from 6,425 BP) to increase insight in saltwater intrusion progression and study the processes mentioned in section 4.1 in more detail.

Priority should also be given to more accurately representing the groundwater extraction component as set out in the discussion. Secondary improvements could then include: separate characteristics for cities, a historically accurate evolution of the groundwater extractions in the Ayeyarwady Delta, the use of yearly satellite EVI processing to include the effects of crop rotation and an additional term responsible for the termination of wells that are in contact with salt water.

Although water quality assessment has been limited to salinity, fieldwork points out that both iron and, especially, arsenic concentrations are also important factors throughout the Ayeyarwady Delta. With concentrations high enough to be a potential public health risk, these pollutants need to be taken into consideration when assessing fresh groundwater availability (appendix B).

Other (complimentary) research objectives in which this groundwater model could play a role include the creation of a sub-model for Yangon or in Aquifer Storage and Recovery (ASR) feasibility studies, as well as studies investigating land subsidence (Minderhoud et al., 2017), storms surges and tidal waves (in light of appendix I1), seasonal cycles, extended periods of drought, reduced recharge due to urbanisation, just to name a few.

References

Andreadis, K. A., Schumann, G. J.-P., Pavelsky, T., 2013, a simple global river bankfull width and depth database, *Water Resour*, 49, 7164–7168, doi:10.1002/wrcr.20440

Bing Maps, 2020, Microsoft Corporation Earthstar Geographics SIO ©

Brakenridge, G.R., Syvitski, J.P.M., Overeem, I., Higgins, S.A., Kettner, A.J., Stewart-Moore, J.A., Westerhoff, R., 2013, Global mapping of storm surges and the assessment of coastal vulnerability, *Nat. Hazards* 66, 1295-1312, doi: 10.1007/s11069-01200317-z

Burma act IV, 1930, the underground water act, Myanmar

Church, J.A., Clark, P.U., Cazenave, A., Gregory, J.M., Jevrejeva, S., Levermann A., Merrifield, M.A., Milne, G.A., Nerem, R.S., Nunn, P.D., Payne, A.J., Pfeffer, W.T., Stammer, D., Unnikrishnan, A.S., 2013, *Sea Level Change in Climate Change 2013: The Physical Science Basis, Contribution of Working Group I to the Fifth Assessment Report of the Intergovernmental Panel on Climate Change*, Cambridge University Press, Cambridge, United Kingdom and New York, NY, USA

Delsman, J. R., Hu-a-ng, K. R. M., Vos, P. C., de Louw, P. G. B., Oude Essink, G. H. P., Stuyfzand, P. J., and Bierkens, M. F. P., 2013, Paleo-modeling of coastal saltwater intrusion during the Holocene: an application to the Netherlands

Delsman, J.R., Van Baaren, E.S., Siemon, B., Dabekaussen, W., Karaoulis, M.C., Pauw, P.S., Vermaas, T., Bootsma, H., De Louw, P.G.B., Gunnink, J.L., Dubelaar, W., Menkovic, A., Steuer, A., Meyer, U., Revil, A., Oude Essink, G.H.P., 2018, Large-scale, probabilistic salinity mapping using airborne electromagnetics for groundwater management in Zeeland, the Netherlands, *Environ. Res. Lett.* 13, 13, <https://doi.org/10.1088/1748-9326/aad19e>

Drabbe, J., Badon Ghijben, W., 1889, Nota in verband met de voorgenomen putboring nabij Amsterdam, *Tijdschr. Van K. Inst. van Ingenieurs* 5, 8–22

Drury, L., 2017, *Hydrogeology of the Dry Zone, Central Myanmar*, Australian Water Partnership, Canberra

Faneca Sanchez, M., Bashar, K., Janssen, G.M.C.M., Vogels, M., Snel, J., Zhou, Y., Stuurman, R. and Oude Essink, G.H.P., 2015, SWIBANGLA: Managing saltwater intrusion impacts in coastal groundwater systems of Bangladesh, p.153

FAO, 2011, *AQUASTAT Country Profile Myanmar*, Food and Agriculture Organization of the United Nations (FAO), Rome, Italy

Grant, K. M., Rohling, E. J., Bar-Matthews, M., Ayalon, A., Medina-Elizalde, M., Bronk Ramsey, C., Satow, C., Roberts, A. P., 2012, Rapid coupling between ice volume and polar temperature over the past 150,000 years, *Nature*, Volume 491, 744 – 747, doi:10.1038/nature11593

Halcrow & Partners, 1983, *Irrawaddy Delta Hydrological Investigations and Delta Survey*, Ministry of Agriculture & Forests (Burma), Irrigation Department, Volume 1, Methods, 149.459 A.1

Hall, J. K., 2006, *GEBCO Centennial Special Issue, Charting the secret world of the ocean floor: The GEBCO Project 1903–2003*, *Mar. Geophys. Res.*, 27(1), 1–5, doi:10.1007/s11001-006-8181-4

Hartmann, J. & Moosdorf, N., 2012, The new global lithological map database GLiM: A representation of rock properties at the Earth surface, *Geochem. Geophys. Geosyst.*, 13, Q12004, doi:10.1029/2012GC004370

Herzberg, B., 1901, Die Wasserversorgung einiger Nordseebäder, *J. für Gasbeleuchtung und Wasserversorgung* 44, 815–819

Htun, W. W., 2015, Groundwater issues in Myanmar, CCOP-KIGAM-UNESCO-DGR Workshop on Sustainable Groundwater Management, Bangkok, Thailand

Huizer, S., Karaoulis, M.C., Oude Essink, G.H.P., Bierkens, M.F.P., 2017, Monitoring and simulation of salinity changes in response to tide and storm surges in a sandy coastal aquifer system, *Water Resour. Res.* 53, 6487–6509, <https://doi.org/10.1002/2016WR020339>

Hulsman, H., Rutten, M., Nauta, T., Kreijns, M., Hasman, R., Attema, Y., Commandeur, A., Rathore, P., 2013, Data Inventory to Support the Development of an Integrated Water Resources Management Strategy for Myanmar, Deltares, 1208681-000-ZKS-0012

Huntington, T. G., 2006, Evidence for intensification of the global water cycle: review and synthesis, *Journal of Hydrology*, 319, pag 83-95

Hutchinson, M.F., Xu, T. and Stein, J.A. 2011, Recent Progress in the ANUDEM Elevation Gridding Procedure, *Geomorphometry 2011*, edited by T. Hengel, I.S. Evans, J.P. Wilson and M. Gould, pp. 19–22, Redlands, California, USA

IWMI (International Water Management Institute), 2014, Mapping Agriculture Water Management, Crop Cycle and Natural Land Cover in Salween and Ayeyarwady Basins. Unpublished Internal Report. IWMI

Jenson, S. K. & J. O. Domingue, 1988, Extracting Topographic Structure from Digital Elevation Data for Geographic Information System Analysis, *Photogrammetric Engineering and Remote Sensing*, 54 (11), pag. 1593–1600

Langevin, C.D., Thorne, D.T.J., Dausman, A.M., Sukop, M.C., Guo, W., 2008, SEAWAT Version 4: A Computer Program for Simulation of Multi-Species Solute and Heat Transport, U.S. Geological Survey Techniques and Methods Book 6

Larsen, F., Tran, L.V., Van Hoang, H., Tran, L.T., Christiansen, A.V. and Pham, N.Q., 2017, Groundwater salinity influenced by Holocene seawater trapped in incised valleys in the Red River delta plain, *Nature Geoscience*, 10(5), pp. 376-381, <https://doi.org/10.1038/ngeo2938>

Loveson, V. J. and Nigam, R., 2019, Reconstruction of late Pleistocene and Holocene sea level curve for the East Coast of India, *Journal geological society of India*, Vol. 93, May 2019, pp. 507-514

Mark, D. M., 1988, "Network Models in Geomorphology", *Modelling Geomorphological Systems*, ed. M. G. Anderson, New York: John Wiley, pag. 73–97

MIMU (Myanmar Information Management Unit), 2019, "Village Points Ayeyarwady Region PCode v9.0.1", Myanmar

Minderhoud, P.S. J., Erkens, G., Pham, V. H., Bui, V. T., Erban, L., Kooi, H., Stouthamer, E., 2017, Impacts of 25 years of groundwater extraction on subsidence in the Mekong delta, Vietnam, *Environmental research letters*, 12, 064006

Mulder, T., 2018, Constructing 3D variable-density groundwater flow models for six deltas using global data sets, Utrecht University

OSM (OpenStreetMap), 2020, openstreetmap.org, opendatacommons.org, creativecommons.org
Oude Essink, G. H. P., van Baaren, E. S., de Louw, P. G. B., 2010, Effects of climate change on coastal groundwater systems: A modelling study in the Netherlands, *Water Resources Research*, Vol. 46, W00F04, doi:10.1029/2009WR008719

PAGES (Past Interglacials Working Group), 2016, Interglacials of the last 800,000 years, *Rev. Geophys.* 54, 162–219, doi:10.1002/2015RG000482

Pirazzoli, P.A., 1996, Sea-level changes: the last 20 000 years, Wiley Coastal Morphology and Research Series, ISBN: 978-0-471-96913-6

Post, V.E.A., Houben, G.J., Van Engelen, J., 2018, What is the Ghijben-Herzberg principle and who formulated it?

Smith, A.J., Turner, J. V., 2001, Density-dependent surface water-groundwater interaction and nutrient discharge in the Swan-Canning Estuary, *Hydrol. Process.* 15, 2595–2616, <https://doi.org/10.1002/hyp.303>

Thein, M., 2019a, Overexploitation of groundwater and consequence in greater Yangon, World Water Day, Nay Pyi Taw

Thein, M., 2019b, Water Resources Myanmar, manuscript submitted for publication, Yangon

Thein, M., 2020, Climate change with sea level rise threat to groundwater in coastal region and Ayeyarwady Delta, Myanmar

UNDP, 2019, Human Development Report, Beyond income, beyond averages, beyond today: Inequalities in human development in the 21st century, New York

Viossanges, M., Johnston, R., Drury, L., 2017, Groundwater Resources of the Ayeyarwady Basin. Ayeyarwady State of the Basin Assessment (SOBA) Report 2a, National Water Resources Committee (NWRC), Myanmar

Waelbroeck, C., Labeyrie, L. Michel, E., Duplessy, J.C., McManus, J.F., Lambeck, K., Balbon, E., Labracherie, M., 2002, Sea-level and deep-water temperature changes derived from benthic foraminifera isotopic records, *Quaternary Science Reviews* 21, pag. 295–305

Watanabe, S., Hajima, T., Sudo, K., Nagashima, T., Takemura, T., Okajima, H., Ise, T., 2011, MIROC-ESM 2010: Model description and basic results of CMIP5-20c3m experiments, *Geoscientific Model Development*, 4(4), 845

Weerasekera, W. L., 2017, 3D Variable-density Groundwater Modelling of the Red River Delta, Vietnam, UNESCO-IHE

Worldometers.info, 2020, Elaboration of data by United Nations, Department of Economic and Social Affairs, Population Division, Dover, Delaware, U.S.A

World Bank, 2015, Agriculture, forestry, and fishing, value added (% of GDP), World Bank national accounts data and OECD National Accounts data files, Code: NV.AGR.TOTL.ZS

World Bank, 2017, GDP per capita (constant 2010 US\$), World Bank national accounts data and OECD National Accounts data files, Code: NY.GDP.PCAP.KD

Vallejos, A., Sola, F., Yechieli, Y., Pulido-Bosch, A., 2018, Influence of the paleogeographic evolution on the groundwater salinity in a coastal aquifer, Cabo de Gata aquifer, SE Spain. *J. Hydrol.* 557, 55–66. <https://doi.org/10.1016/j.jhydrol.2017.12.027>

Van Engelen, J., Verkaik, J., King, J., Nofal, E.R., Bierkens, M.F.P., Oude Essink, G.H.P., 2019, A three-dimensional paleo-reconstruction of the groundwater salinity distribution in the Nile Delta Aquifer, *Hydrol. Earth Syst. Sci.* 23, 5175–5198, <https://doi.org/10.5194/hess-2019-151>

Van Pham, H., Van Geer, F.C., Bui Tran, V., Dubelaar, W., Oude Essink, G.H.P., 2019, Paleo-hydrogeological reconstruction of the fresh-saline groundwater distribution in the Vietnamese Mekong Delta since the late Pleistocene. *J. Hydrol. Reg. Stud.* 23. <https://doi.org/10.1016/j.ejrh.2019.100594>

Verkaik, J. & Janssen, G., 2019, iMOD-WQ Manual svn340, Deltares, Delft, The Netherlands

Van Weert, F., J. Van der Gun, and J. Reckman, 2008, World - wide overview of saline and brackish groundwater at shallow and intermediate depths, Rep. GP 2004 - 1, 87 pp., Int. Groundwater Resour. Assess. Cent., Utrecht, Netherlands

Vermeulen, P. T. M., Hendriksen, G., Snepvangers, J. J. J. C., Berendrecht, W. L., Lourens, A., Tambach, T., ... & Minnema, B. (2006). iMOD Interactive Modelling Environment, TNO Software

Vermote, E., Justice, C., Claverie, M., Franch, B., 2016, Preliminary analysis of the performance of the Landsat 8/OLI land surface reflectance product, *Remote Sensing of Environment*, 185, pag 46-56. Landsat 8 OLI/TIRS Digital Object Identifier (DOI):/10.5066/F71835S6

Worland, S.C., Hornberger, G.M., Goodbred, S.L., 2015, source transport, and evolution of saline groundwater in a shallow Holocene aquifer on the tidal deltaplain of southwest Bangladesh, *Water Resour. Res.* 15. <https://doi.org/10.1002/2014WR016262>

Xiao, H., Wang, D., Medeiros, S.C., Bilskie, M. V., Hagen, S.C., Hall, C.R., 2019. Exploration of the effects of storm surge on the extent of saltwater intrusion into the surficial aquifer in coastal east-central Florida (USA), *Sci. Total Environ.* 648, 1002–1017, <https://doi.org/10.1016/J.SCITOTENV.2018.08.199>

Yang, J., Graf, T., Herold, M., Ptak, T., 2013. Modelling the effects of tides and storm surges on coastal aquifers using a coupled surface-subsurface approach, *J. Contam. Hydrol.* 149, 61–75, <https://doi.org/10.1016/j.jconhyd.2013.03.002>

Yang, J., Graf, T., Ptak, T., 2015, Impact of climate change on freshwater resources in a heterogeneous coastal aquifer of Bremerhaven, Germany: A three-dimensional modelling study, *J. Contam., Hydrol.* 177-178, 107-121, doi: 10.1016/j.jconhyd.2015.03.014

Yang, J., Zhang, H., Yu, X., Graf, T., Michael, H.A., 2018, Impact of hydrogeological factors on groundwater salinization due to ocean-surge inundation, *Adv. Water Resour.* 111, 423–434, <https://doi.org/10.1016/j.advwatres.2017.11.017>

Zamrsky, D., Oude Essink, G. H. P., Bierkens, M. F., 2017, Estimating the thickness of unconsolidated coastal aquifers along the global coastline

Zheng, C., Wang, P.P., 1999. MT3DMS: A Modular Three-Dimensional Multispecies Transport Model for simulation of advection, dispersion and chemical reactions of contaminants in groundwater systems, Strategic Environmental Research and Development Program - Contract Report SERDP-99-1

Zin, T., 2017, Pilot project of groundwater monitoring in Myanmar, Ministry of Agriculture, livestock and Irrigation, Irrigation and Water Utilization Management Department, Groundwater Division

Appendices

Appendix A: geographic positioning	page.
- A: Myanmar's relative position	63
Appendix B: field work	
- B1a: Ayeyarwady Delta groundwater extraction survey	64
- B1b: Ayeyarwady Delta groundwater extraction survey – close-up	65
- B1c: groundwater extraction survey well characteristics	66
- B2: groundwater extraction survey transcript	67
Appendix C: modelling characteristics	
- C1: base model	78
- C2: iMOD-WQ	79
- C3: additional model modifications	80
Appendix D: geo(hydro)logy	
- D1a: Department of Rural Development well-log	83
- D1b: Yangon City Development Committee well-log	84
- D1c: Irrigation and Water Utilization Management Department well-log	85
- D2: wells used for the hydrogeological model	86
- D3a: example well codes	86
- D3b: Yangon City Development Committee coding key	86
- D3c: Irrigation and Water Utilization Management Department coding key	87
- D3d: Department of Rural Development coding key	87
- D4: wells exceeding depth to bedrock	87
- D5a: well positions	88
- D5b: lithological sequences	88
- D6a: example .IPF-file	89
- D6b: example .TXT-file	89
- D7: artificially lowered areas	90
- D8a: delta cross-sections, variable vertical levels	91
- D8b: delta cross-sections, constant vertical levels	91
- D9: voxel model batch-file	92
Appendix E: paleo-reconstruction	
- E1: relative sea level rise discretization (130,000 years)	93
- E2a: relative sea level rise discretization (14,500 years)	94
- E2b: relative sea level rise discretization (6,800 Years)	94
- E3: stress-periods (130,000 years)	95
Appendix F: groundwater extraction	
- F1: Ayeyarwady Delta surface water map	96
- F2: domestic well exclusions process	97
- F3a: satellite image IDs	97
- F3b: dry season vs wet season satellite images	97
- F4a: dry season satellite image	98
- F4b: EVI for dry season image	98
- F5: NDVI and EVI workflow	99

Appendix G: results

- G1: iMOD-WQ example runfile	100
- G2: transgression/regression cycles	103
- G3: paleo-reconstruction calculation times	104
- G4: Ayeyarwady Delta hydraulic head	105
- G5a: landmass exposed with respect to RSL	106
- G5b: percentual change in landmass exposure regarding RSLR	106
- G6a: Initial salinity distribution (paleo-reconstruction: 129,705 years)	107
- G6b: initial salinity distribution (present-day sea level: 130,000 years)	108
- G7: groundwater “freshening”	109
- G8: Initial salinity distribution (paleo-reconstruction: 6,425 years BP)	110
- G9: Fresh groundwater volume differences between the full and the partial paleo-reconstructive modelling run	111

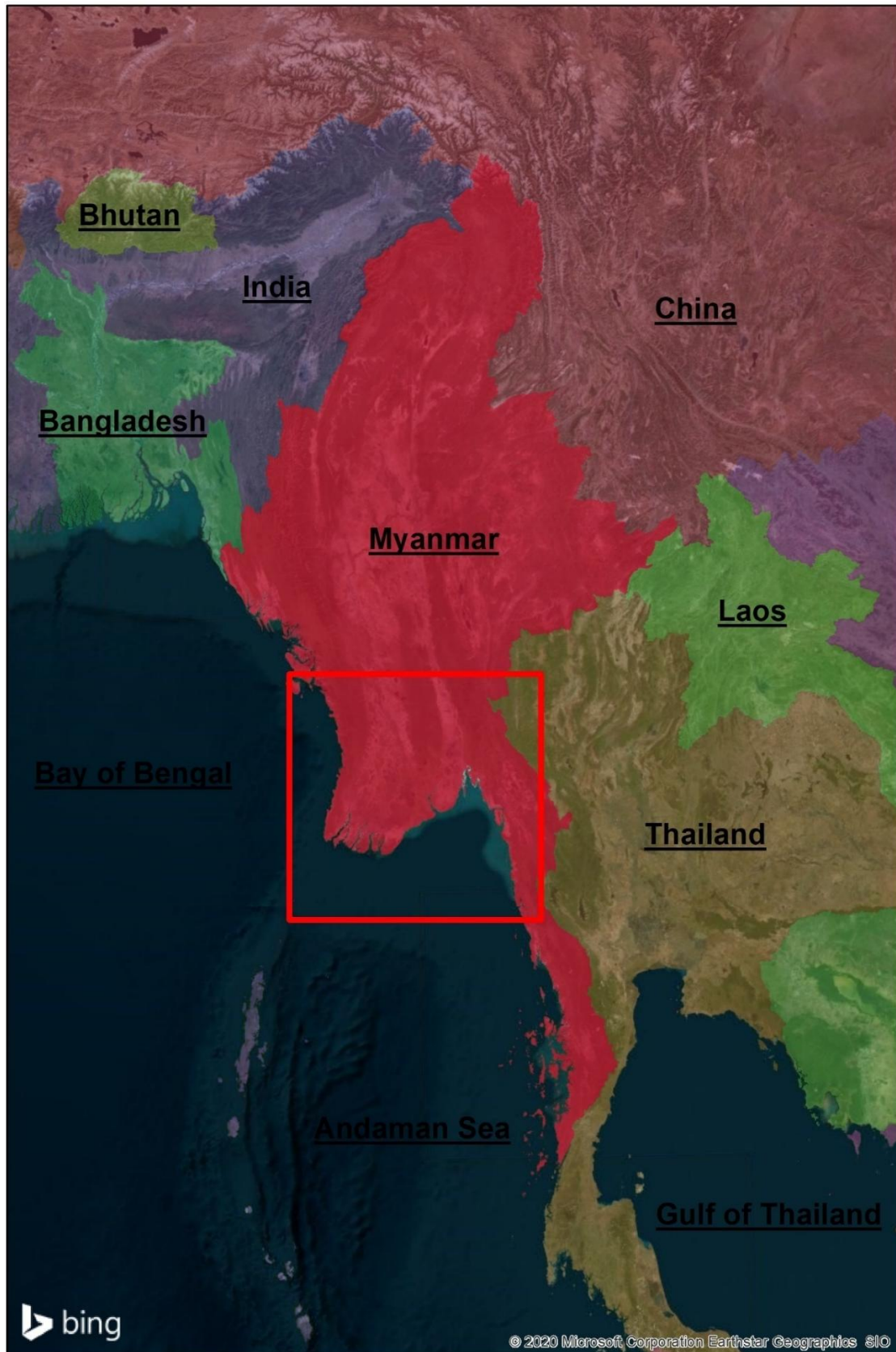
Appendix H: discussion

- H1: wells located in the model’s inactive area	112
- H2: RSLR-curve discrepancies	112
- H3a: agricultural well extractions	113
- H3b: domestic well extractions	113

Appendix I: recommendations

- I1: change in landmass exposure regarding RSLR – zoomed	113
-----------------------------------------------------------	-----

A: Myanmar's relative position



The relative position of Myanmar compared to the neighbouring countries of Thailand and Laos to the East, China to the North and India and Bangladesh to the West. Furthermore, Myanmar is bordered by the Andaman Sea to the South and the Bay of Bengal to the West. The red square defines the research window.

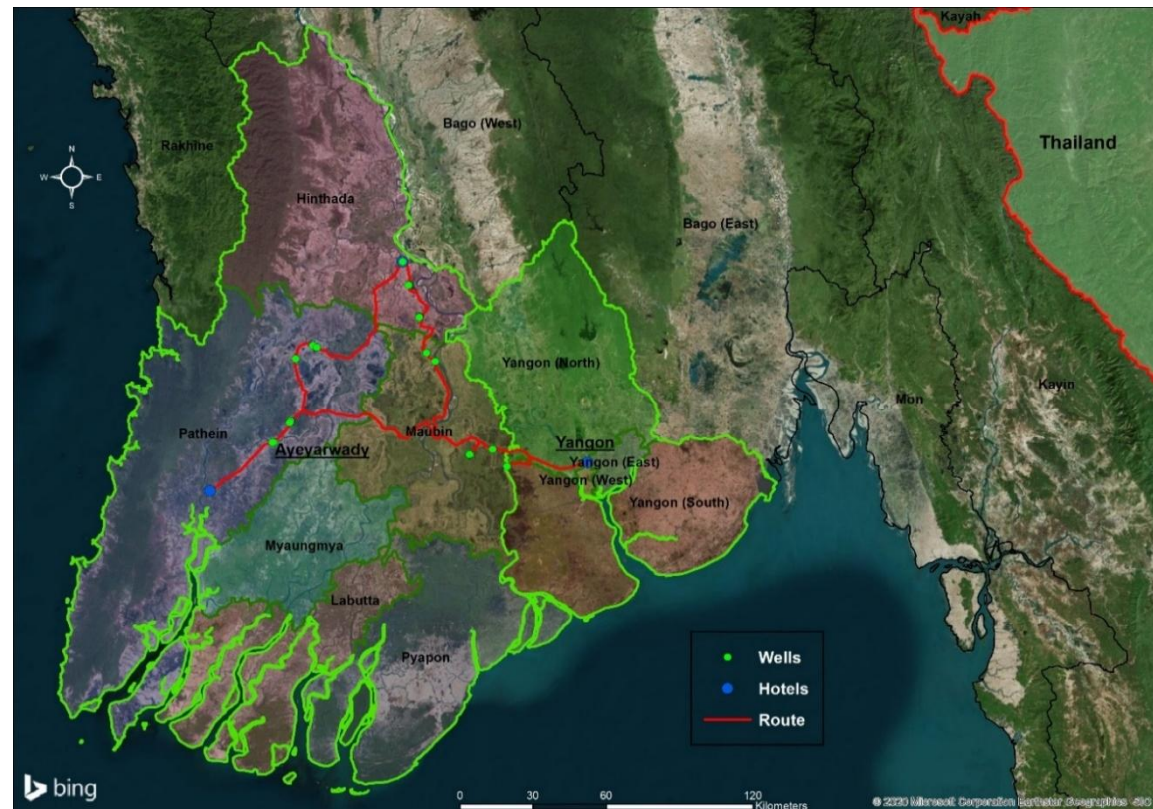
B1a: Ayeyarwady Delta groundwater extraction survey

12 – 14 February 2020

The reader of the following transcript is urged to bear in mind the following. The information provided by local communities could, in most cases, not be verified. Although, in general, quite comprehensive in their descriptions, the information provided could have been incomplete. Questions and answers were translated from English to Burmese and vice versa. While being confident in the skills of the interpreter, translations, at times, were at liberty of the translator. It is known that the spatial extent and temporal nature of this survey is limited to only a part of the research area during the dry season. Regardless, it is believed that the information presented below provides first-hand insight in the reality of groundwater extraction practices throughout the Ayeyarwady Delta.

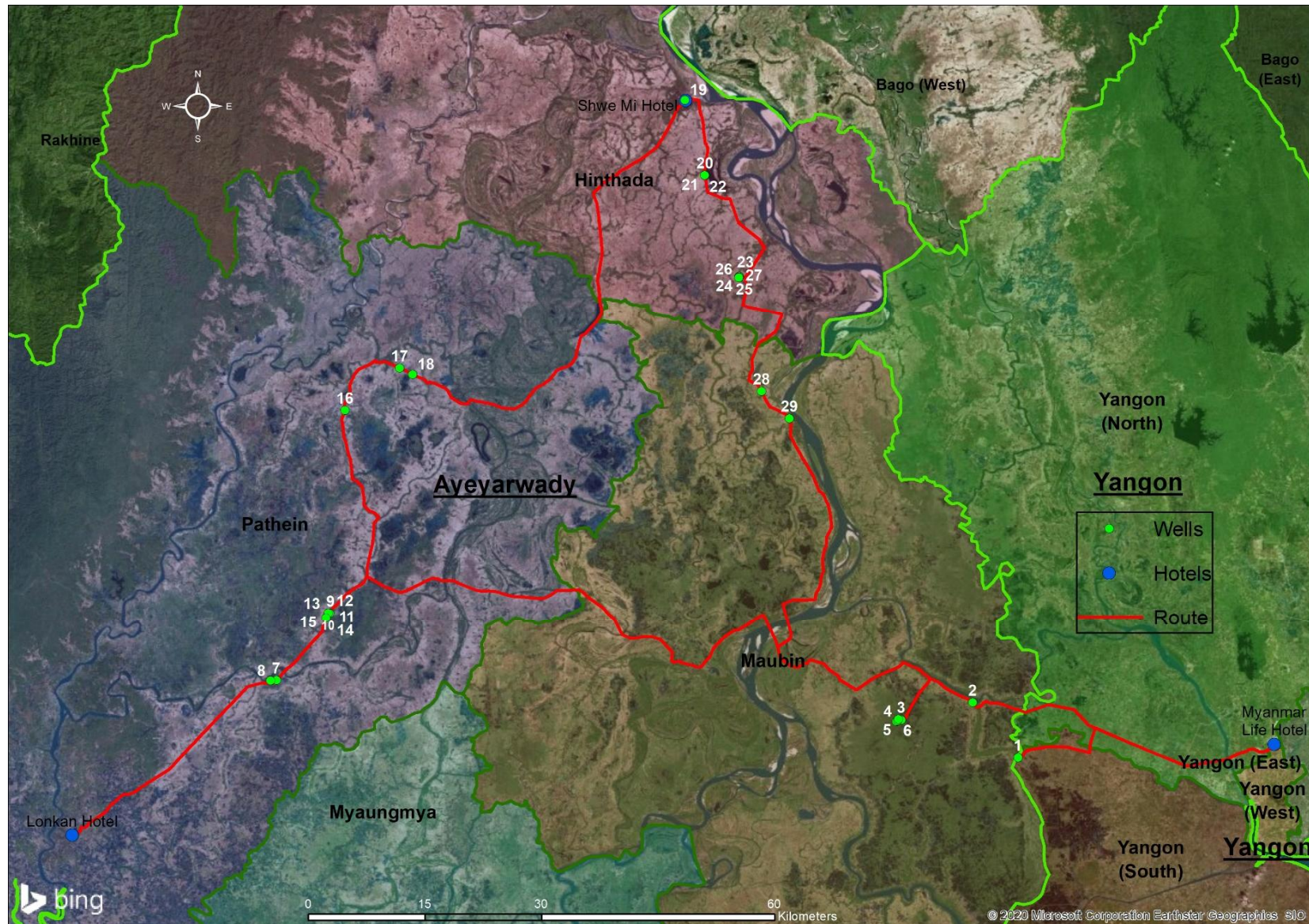
What follows below is a transcript, including photographs, of observations made and conversations held with the local owners and/or users of each groundwater well visited during this survey.

An expression of gratitude is in place with respect to Mr Chan Myeako for translations, Mr “Ted” for chauffeuring and, especially, Mr Jan de Bruin for making this survey possible.



An approximation of the survey route relative to the Ayeyarwady Division (left) and the Yangon Region (right).

B1b: Ayeyarwady Delta groundwater extraction survey – close-up



A close-up of Appendix B1a showing individual wells visited and their corresponding well ID. Further details on well characteristics are provided in Appendix B1c.

B1c: groundwater extraction survey well characteristics

Well ID	X	Y	Owner	Well Type	Purpose	Location	Period	Age [years]	Depth [feet]	Estimated extraction rate [L/hour]
1	95.84473	16.88137	DRD	Tube-well	Domestic	Monastery	All year	3	600	150
2	95.79196	16.94515	Private	Tube-well	Irrigation	Plantation	Dry season	0.33	60	33
3	95.70974	16.92518	Japan	Tube-well	Domestic	High school	Abandoned	11	180	N/A
4	95.70416	16.92323	Private	Tube-well	Domestic	Monastery	All year	18	250	N/A
5	95.70516	16.92427	DRD?	Tube-well	Domestic	Beside a house	N/A	N/A	280	N/A
6	95.70624	16.92599	DRD	Tube-well	Domestic	Communal well	N/A	N/A	N/A	N/A
7	94.98657	16.97103	Private	Tube-well	Domestic	Restaurant	All year	15	40	188
8	94.97978	16.97046	Private	Tube-well	Industrial	Drinking water facility	All year	2	650	250
9	95.04674	17.04934	Private	Tube-well	Domestic	Primary school	Abandoned	20	200	N/A
10	95.04671	17.04936	Private	Tube-well	Domestic	Primary school	All year	5	400	11
11	95.04788	17.04937	Private	Dug well	Domestic	Monastery	All year	60	20	N/A
12	95.04782	17.04929	IWUMD	Tube-well	Domestic	Monastery	All year	7	212	N/A
13	95.04803	17.04956	IWUMD	Tube-well	Domestic	Monastery	All year	7	180	N/A
14	95.04449	17.04441	Private	Tube-well	Domestic	In front of a house	All year	N/A	230	N/A
15	95.04399	17.04361	DRD	Tube-well	Domestic	Communal well	All year	3	480	214
16	95.06570	17.28334	Private	Tube-well	Irrigation	In the rice fields	Dry season	6	200	1184
17	95.12924	17.33201	Private	Dug well	Domestic	Communal well	Abandoned	40	20	N/A
18	95.14401	17.32460	Private	Dug well	Domestic	Communal well	Abandoned	N/A	20	N/A
19	95.45929	17.64262	Private	Dug well	Domestic	Shwe Mi hotel	All year	100	20	N/A
20	95.48216	17.55583	Private	Dug well	Domestic	Police station	Abandoned	50	20	N/A
21	95.48221	17.55562	Private	Tube-well	Domestic	Police station	All year	N/A	50	N/A
22	95.48190	17.55589	Private	Tube-well	Domestic	Police station	All year	N/A	50	N/A
23	95.52171	17.43838	Private	Tube-well	Domestic	In front of house	All year	3	125	1250
24	95.52195	17.43843	IWUMD	Tube-well	Domestic	Communal well	All year	2	530	250
25	95.52190	17.43884	Private	Dug well	Domestic	Communal well	Abandoned	40	20	N/A
26	95.52148	17.43803	Private	Dug well	Domestic	Edge of agricultural field	Abandoned	N/A	20	N/A
27	95.52141	17.43742	Private	Tube-well	Irrigation	Plantation	Dry season	N/A	125	N/A
28	95.54792	17.30518	Private	Dug well	Domestic	Alongside the road	Abandoned	N/A	20	N/A
29	95.58023	17.27391	Private	Tube-well	Industrial	Gold Delta Co.Ltd Rice Mill	all year	2	220	833

The well characteristics for each well visited during the groundwater extraction survey. The estimated average depth of the dug wells is 20 feet, but probably varies per location.

B2: Groundwater extraction survey transcript

Day 1: Yangon to Patheingyi

Well 1: N16.88137, E95.84473

In the construction year 2016/2017, the DRD installed a groundwater tube-well intended to be used for domestic purposes, e.g. washing of clothes, watering of gardens etcetera. The well is located inside and operated by the Khattiya Ywa Thit village monastery (figure 1a, b).



Figure 1a, b: the DRD groundwater well complex, consisting of: the well, the pump house, a water tower and a settling tank (a, left). The pump house contains a diesel fuelled pump (b, right).

During construction, the DRD drilled to a depth of 600 feet to find a suitable aquifer from which to take fresh water. According to the villagers, the optimal depth decided upon was 280 feet. This information corresponded with the well-log present in the pumphouse.

The pump, with a capacity of 1800 GPH, is not used continuously. It takes roughly 30 minutes to fill the water tower, which is only refilled again when (almost) empty. The overall extraction is unknown. However, a rough, visually deduced, estimation made by looking at the water tower results in the following calculation:

$$3 * 4 m = 12.000 L = 3000 Gallons / 1800 GPH \approx 30 minutes$$

This seems to correspond with the information provided. If refilled once a day, that would mean an overall extraction of 150 L/hour throughout the year.

The fresh water that the well produces is not (and never was) suitable for drinking, because of the water's unclear aesthetics and its rusty smell. Instead, the village has several ponds of which one is kept especially clean and used as a source of drinking water (figure 2a, b).



Figure 2a, b: a fresh water pond meant for domestic use. The pond is full of lotus flowers, believed to purify the water (a, left). One of the village elders (shown in the picture) gave a tour around the village, explaining the village's water consumption habits (b, right).

Water is pumped up from the pond and stored overnight to let any suspended material settle to the bottom, after which it is stored into clay pots until it is consumed. Throughout the years and the seasons, this drinking water pond has never been dry (figure 3a, b).



Figure 33a, b: Clay pots are filled with pond water for domestic use. Usually, a similar, separate pot with a lid used for drinking water (a, left). Smaller clay pots are then filled to provide drinking water for thirsty by passers (b, right)

According to the villagers, the construction of the DRD-well and accessories had cost 19 million Kyat. They do not really understand why it was constructed, since they never had experienced any water shortages. They would have preferred proper fencing around their precious drinking water pond to keep the animals out. They even suspect the well to be connected underground, taking water from the drinking water pond. However, they did note that other villages nearby have experienced a lack of fresh water and a well like theirs is considered to be a possible solution.

The agricultural fields (mainly paddy rice) surrounding the village use creek water for irrigation. Everywhere along the creek pumps are present with hoses attached to get the water out of the creek and onto the plot in need of irrigation (figure 4 a, b).



Figure 4: a pump and hose installed next to a creek. The creek water everywhere is milky with suspended clay particles (a, left). The rice paddy next to creek is being irrigated with creek water (b, right).

Well 2: N16.94514, E95.79196

Used for a relatively small plantation, this private tube-well reaches a depth of 60 feet and has an average extraction rate of 600 gallons per day (figure 5a). The well's use was, for the most part, limited to 4 months of complimentary irrigation during the dry season. During the rainy season additional irrigation was not necessary. Spread over a calendrical year this implies a consumption of $((2400L * (4 * 30)) / 365) / 24 \text{ hours} \simeq 33L/\text{hour}$.

The farmer said that a lot of farms and houses use wells similar to his. They are dug by hand for 800 kyat per feet and they are not registered with the government. While his well provides fresh (drinkable) groundwater with $0 \mu\text{g}/\text{L}$ of arsenic, it does have a rusty smell and the water it produces needs time to let any suspended materials settle out. In contrast, the neighbours well, roughly 100 meters further, had to be shut down due to its high arsenic content of over $80 \mu\text{g}/\text{L}$.

The well is used in combination with an irrigation system (figure 5b) and has been active for 4 months. During that time no changes were experienced in either the groundwater quality or quantity.



Figure 5a, b: the tube-well with improvised water tower (a, left), which was built to create the pressure needed for the irrigation system (b, right).

Well 3: N16.92518, E95.70974

In 2009, Japan donated a, 180 feet deep, tube-well to the high school in Thazin Yay Kyaw (figure 6a). However, the water from the well had a rusty smell to it and the filtration system and pump provided were too expensive to maintain and operate. Therefore, the well was abandoned (figure 6b, c). Instead, rainwater is collected and made suitable for drinking with the aid of drinking water tablets. Located on a river-peninsula, creek water is abundant and nearby. Whenever rainwater reservoirs are depleted, treated creek water is used (figure 7a, b).



Figure 6a, b, c: actual tube well (a, left). Japanese filtration system (b, middle). Pump (c, right).



Figure 7a, b: settling tank donated by Japan (a, left). Rain water collector (b, right).

Well 4: N16.92323, E95.70416

The Thazin Yay Kyaw monastery is equipped with a, 250 feet deep, private tube-well, which provides potable water. It was donated and in use for roughly 18 years.

Pumped groundwater goes in a settling tank overnight, after which it is filtered and ready for consumption. Again, the well is complementary to collected rainwater for drinking.

In the dry season they experience more difficulty pumping than during the rainy season. The water quality was never officially tested.

Well 5 and 6: N16.92427, E95.70516; N16.92599, E95.70624

The search for a DRD-well coinciding with this village tract and name led to a tube-well near the creek next to the monastery, probably less than 100 meters from well number 4. This presumed DRD-well, 280 feet deep, had no sign present (figure 8a). When asked, the sign for this well was said to be placed at another location. The well was not used for consumption. The water has a rusty smell to it and is only used for domestic purposes other than drinking.

Although the tube-well's location is close to the coordinates of the DRD-well, it remains questionable who constructed it, especially when considering the structure across the river, resembling the previous DRD-well at the monastery (figure 8b). Unfortunately, a visit to verify the structure across the river to be the DRD-well from the well-logs did not fit into the schedule.

When leaving, a boat was noticed with empty 20L drinking water bottles (figure 8c). It is remarkable that when asked the villagers did not mention the use of such bottles.



Figure 8a, b, c: the well said to be constructed by the DRD (a, left). The suspected DRD-well at the other side of the river (b, middle). The boat with the empty 20L drinking water bottles (c, right).

Day 2: Pathein – Hinthada

Well 7: N16.97100, E94.98671.

The private tube-well is used for domestic purposes and operating the restaurant in Daga village (figure 9a). A different source is used only for drinking, being 20L bottles of drinking water. The well is roughly 15 years old and provides fresh water with an, initially, rusty smell. The estimated depth is approx. 40 feet. Before pumping the water up to the water tower (3000L), they give the water time to let any suspended materials settle out. They have always had water and experienced no difference between the rainy season and dry season in water quality and quantity. It was constructed by a private company and the well is unregistered. Water is pumped up 2 to 3 times a day on the restaurant's behalf. However, pumping does not commence whenever the water tower is completely empty. To get an estimate of the magnitude of the water consumption, a simple calculation suggests $((3000/2) * 3)/24 \approx 188\text{L/hour}$. According to the restaurant owner (figure 9b), the drilling company responsible for constructing the well did a water quality check. No salinity is experienced.

She said that almost every house in Daga village has a similar well, but she did not know anything about the water quality at other locations. Upon departure, she gave directions to her son in law, who operates the drinking water processing plant on the other side of town.



Figure 9a, b: the restaurant's water tower, indicating the location of the groundwater well (a, left). The restaurant owner (b, right).

Well 8: N16.97046, E94.97978

The drinking water production facility in Daga village has a private tube-well installed (figure 10a). However, in contrast to the other private tube-wells so far, this tube-well is registered, because of the corporate nature of the enterprise.

The company provides 20L bottles for a price of 300 Kyat when picked-up or 500 Kyat when delivered. Sometimes they use a compressor to 'clean' the well. The well is approximately 650 feet deep and only operational during working hours. They produce, on average, 300 bottles of 20L every day ($300 * 20 = 6000L / 24 \approx 250L/hour$) and claim the groundwater is drinkable straight from the well. Regardless, it is further purified to be sold as potable water.

First, water is pumped to a settling tank, which is only used for temporary storage (figure 10b). Secondly, the raw water has a pH of 6.3 which is converted to a pH of 7 when the water from the settling tank goes through the water filters (figure 11a). Finally, it goes to the first 3000L storage cylinder and onwards to the second cylinder of 3000L after an UV-treatment to remove any remaining biological contamination (figure 11b).

The well is 2 years into production and the water quality had been thoroughly checked in the water quality control lab in Yangon (or Naypyidaw) before starting the operation. They experienced no difference between the rainy and the dry season in both water quality and quantity.

The company owner explained that he was lucky with the well. Compared to others in the Daga village that have tube-wells, his water quality is far superior. Thanks to his tube-well he can supply multiple village-tracts surrounding his village with drinking water.



Figure 10a, b: the drinking water plant's private tube well (a, left). The storage (settling) tank (b, right).



Figure 11a, b: the water filters (a, left). The storage cylinders prior to and after UV treatment (b, right).

Well 9/10: N17.04934, E95.04674; N17.04936, E95.04671

Two tube-wells are located on the primary school's premise. The first, 200 feet deep, was installed 20 years ago and was manually operated. Its use was limited to the dry season. However, it has been decommissioned since the installation of a second well, 5 years ago. The new well, 400 feet deep, was tested for arsenic contamination by the township government and is primarily used as a source of drinking water. Water is allowed to settle for 1 day, after which it is filtered twice. The 900 L storage tank is filled twice a week, which translates to an extraction rate of roughly $((900 \times 2) / 7 / 24 \approx) 11$ L/hour. No change in quality and quantity were experienced since the well went into production.

The well is only used when the school is in operation and was constructed using the school budget.

Well 11/12/13: N17.04937, E95.04788; N17.04929, E95.04782; N17.04956, E95.04803

There are three wells located on the Latpanchaung monastery grounds. One dug well over 60 years old and two IWUMD tube-wells constructed 7 years ago. The water is mainly used for the monastery, however, during periods of drought, also for villagers when they are in need.

The abbot gave a tour around the monastery. He has been the head monk there for 20 years and said that they used to clean the dug well every 2 years. However, it has not been used anymore since the construction of the IWUMD tube-wells. Interestingly, the dug well shows an estimated 5-meter change in static water level between the seasons (figure 12a, b).

The well only fell dry during the drought of 2013. It is during that time that the monastery requested the construction of the IWUMD tube-wells. The abbot said that in 1988 the military government wanted farmers to also produce a crop during the dry season. Initially, by rerouting surface waters and increasing the number of dug wells, and later by constructing tube-wells. He suspects the increase in groundwater used for irrigation to have caused for the well to dry up during the 2013 drought. To this day, they use groundwater during the dry season for double cropping.



Figure 12a, b: the dug well at the Latpanchaung monastery (a, left). The monastery's abbot (b, right).

The IWUMD, placed two tube-wells. The initial tube-well is around 212 feet deep and uses a diesel-fuelled pump (figure 13a). Therefore, its operation is considered expensive. Thus, another well, referred to as the “Bangladeshi well”, was installed to reduce costs. This well, with an approximated depth of 180 feet, is manually operated (figure 13b). Water quality for both wells was analysed in Naypyidaw for, amongst other things, arsenic concentrations.

As a concluding remark to the tour, the abbot pointed out the importance of educating the people to not put their latrine and groundwater well close together due to the potential contamination hazard.



Figure 13a, b: automatically operated tube-well (a, left). The manual “Bangladeshi” well (b, right).

Well 14: N17.04454, E95.04468

Searching for the IWUMD-well in Latpanchaung village, another privately owned manually operated tube-well was encountered, 230 feet deep. To commence pumping, air has to be removed out of the piping system by filling it with water (figure 14a).

The water smells of iron (figure 14b). No other specifics on the well could be provided.



Figure 14a, b: the exhaust is turned upside down to fill the tube with water (a, left). The water smelled of iron (b, right).

Well 15: N17.04361, E95.04399

Installed in Latpanchaung village 3 years ago upon request, with a depth of 480 feet, this DRD-well is considered to provide excellent drinking water (figure 15a, b, c). Since its construction the water quality has always been potable, and it does not smell of iron. People from all over the village-tract come to this well to get their drinking water. It takes roughly three hours to fill the reservoir, which is estimated around 12 m³. It is filled 3 times a week, thus $((12000 \times 3) / 7) / 24 \approx 214$ L/hour is being extracted year-round. It was estimated that there are 30 wells throughout Latpanchaung village alone and over 100 wells within the boundaries of the Latpanchaung village-tract. 60 years ago, dug wells were the main source for domestically used water. People used to walk great distances to satisfy their daily requirements. This changed when the tube-wells started appearing around 20 years ago. Because of their relative convenience, almost all dug wells now serve a subordinated function. Their use, if any, is limited to watering gardens in their immediate vicinity. Only the poorest of people that do not have access to a communal well or nearby surface waters still use them when further away and for drinking.



Figure 15a, b, c: the DRD tube-well's reservoir (a, left). Translator Chan explaining the spatial variability of the hydrogeology and thus water quality (b, middle). An invitation for a cup of tea was accepted (c, right).

Well 16: private tube-well; rice fields; N17.28334, E95.06570

Alongside the road, on numerous occasions, paddy rice fields were spotted without any surface waterbodies in the vicinity that could be used for irrigating them. Therefore, a farmer was approached to ask about the specifics of the irrigation system used to water the rice paddies. He told us he has been working the same 6 acres for 6 years, growing two crops of rice in a year. Winter rice (dry season) and monsoon rice (rainy season).

He uses groundwater during the dry season and, only when the rains are late, in the rainy season. His well is approximately 200 feet deep and provides good quality water, which he claims to be drinkable (figure 16a). Since the well's construction 6 years ago, he has never run out of water. However, according to him, some other farmers nearby have had to increase their well's depth to reach the water table. His pumps are on every other day to water the paddy using a network of irrigation ditches (figure 16b). The pump runs an estimated 12 hours per session and, during that time, use 4 gallons of fuel. The pipe is 3 inches in diameter, and he estimates he uses 104 gallons of fuel during the 120 days it takes to grow the winter rice. Considering the above, the pump runs 24/7 for one entire month.



Figure 16a, b, c: groundwater pump being used for rice paddy irrigation (a, left). One of the rice fields irrigation channels (b, middle). Measuring the groundwater extraction rate (c, right).

Because the extraction rate was unknown, an improvised measurement was performed using a bamboo container to get a rough estimate (figure 16c). The container was filled with half a litre water bottles until full and was found to contain roughly 4 litres. The time it took to fill the container was around one second, thus the extraction rate should be close to 4L/sec (although somewhat inaccurate). Using the information provided by the farmer, this translates into $(4 * 3600 * 30) / 365 \approx 1184$ L/hour spread over a whole year for a 6-acre plot (not considering complementary use in the rainy season). No quantity or quality issues were mentioned for the time his well has been in operation. At least 3 similar pumps were visible from this point. Well depth supposedly ranges from 60 to 200 feet throughout the area.

Well 17: N17.33199, E95.12935

This dug well did not hold any standing water at the time (figure 17a). Instead, it contained a lot of rubbish. Using a long stick, the depth of the well was estimated to be about 7 meters deep (figure 17b). Underneath the rubble, the well still contained moisture. According to the local inhabitants, they stopped using the well 1 year ago. The well is roughly 40 years old and it was said to contain water during the rainy season. Using their (the villagers) indications, with a total depth of 7 meters, the well

is estimated to have a 5-meter SWL fluctuation between the seasons. Due to the superior nature of the tube-well's water quality, its convenient location and the minimal effort required to operate it, water usage from the dug well is now limited to watering the plants in the immediate vicinity of the well.



Figure 17a, b: the well appears to be dry (a, left). Measuring the well depth with a stick used for drying clothes (b, right).

Well 18: N17.32461, E95.14410

For the next dug well, alongside the road, the distance from the rim to the water level was estimated to be about 6 m (figure 18a). Its location is a short walk away from the previous well (well number 17). A bystander said that, nowadays, it is used only for bathing (figure 18b). According to him, around 20 years ago the groundwater tube-wells started appearing, which is in agreement with earlier testimonies. Only the very poor cannot afford a private tube-well and still use the dug well for their daily water supply. He also suggested a SWL difference of roughly 5 m between the dry and the rainy season.



Figure 18a, b: the well still contained standing water at around the same depth as the previous well (a, left). Next to the dug well there was evidence of it still being used for bathing (b, right).

Day 3: Hinthada, Yangon

Well 19: N17.64262, E95.45929

The hotel has its own dug well, said to be around 100-year old (figure 19a). During the hotel's construction, the well was renovated after being abandoned for an undefined period. Currently, the water from the well is used for irrigating the hotel gardens. Compared to previously visited dug wells, this well had a relatively high-water level, around 2 meters under the rim of the well (figure 19b). This is relative, because the elevation of the well in the landscape was not yet considered at this stage. During conversation, it was mentioned that almost every building in the city has a private well, because there is no general distribution network. Therefore, to satisfy the domestic fresh water demands, people have to rely on their own (ground)water source.

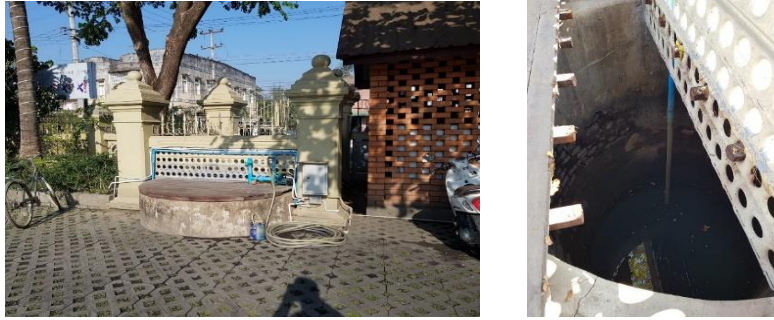


Figure 19a, b: a revived groundwater well of the Shwe Mi hotel (a, left). The SWL was relatively high compared to previously visited dugwells (b, right).

Well 20/21/22: N17.55583, E95.48216; N17.55562, E95.48221; N17.55589, E95.48190

The local police station also has a dug well. After asking permission, they agreed to show their groundwater wells. The dug well was built around 1970. The well's SWL was around 5 meters from the rim (visual estimate), again this does not take into consideration the relative elevation of the well in the landscape. The well was said to have water year-round. Nevertheless, it is currently not being used anymore due to the availability of two new tube-wells (approximate depth, 50 feet). Due to the relative ease of operating the tube-wells and its superior water quality, the dug well is now abandoned. Their construction date was unfortunately not known.

Although the tube-wells provide good quality water, preference is given to bottled water (20L) for drinking. The tube-wells their use is therefore limited to other domestic uses, e.g. cooking, gardening, washing etcetera. Due to the location of the wells in the yard of the police station, no pictures were allowed to be taken.

Well 23/24/25/26/27: N17.43838, E95.52171; N17.43843, E95.52195; N17.43884, E95.52190; N17.43803, E95.52148; N17.43742 E95.52141

The first well visited in Thayat Taung Oakshitkwin village is a private tube-well, 3 years old, 125 feet deep, producing water with an iron smell to it (figure 20a). It is for domestic use (not for drinking) and had cost roughly 150,000 Kyat (100 USD) to develop. Pumping was reported to be easier during the rainy season than during the dry season.

When extracted, the water is let to settle overnight. The next morning, the smell would be gone, but the colour would have become a little rusty. It was said that some villages nearby experience groundwater having a dark yellow colour. Therefore, a homemade filter from the ashes of burned rice peels is being used. After passing through the rice peels, the yellow colour would have disappeared, and the water is thought to be potable.

The owner of the well estimated there to be 1 well for every 4 houses. With Oakshitkwin village having roughly 300 houses, she approximated there to be 75 wells in this one village.

Her tube-well produces, on average, ten 10-litre buckets of water per house per day. This amounts to approximately 1250 L/hour for the entire village or, divided over 75 wells, 17L/hour daily. These wells are located at a variable depth, usually between 200 and 60 feet.



Figure 20a, b: a private tube well used by 4 neighbouring houses (a, left). The IWUMD communal well (b, right).

The second well was installed by the IWUMD in December 2017 (figure 20b). The well was drilled to 600 feet, has a screen-depth of 530 feet and a pipe diameter of 4 inches. The reservoir, containing approximately 6000 litres, has to be filled once every day when empty. No settling time is required to remove suspended materials. Water from the well is either used as drinking water directly or filtered first with a homemade cotton filter before being stored in, the by now familiar, clay pots. Roughly 100 households make use of this communal well and a similar IWUMD-well is located further east in the village-tract (which was too far to also visit). Since its installation, no changes were observed in either water quality or quantity.

It's the right of the village to apply for a communal well, to the benefit of the villagers that are unable to pay for a (joint) private well. Also, when asked, some villagers said that they did not know in advance there was going to be a communal well. Therefore, there are some wells that otherwise would not have been developed. Nevertheless, other villagers said they still would have ordered a private well to be developed in front of their house for the sake of convenience. People who are living relatively far away prefer a local well in their vicinity, regardless of the water quality difference. This change in attitude and the overall availability of water is a far cry from earlier times when people would spend a great amount of time and effort to get their drinking water.

The third well encountered is a dug well of approx. 40 years old and 7 meters deep, with a diameter slightly narrower than the other dug wells visited earlier (figure 21a). It was reported to fall dry around April each year. It was the first well encountered during this field trip which was said to be too salty for some domestic purposes. Therefore, its use is limited to showering and providing drinking water for the village's animals. The palm trees next to the well were occasionally watered with it, but it isn't used for doing the laundry, because of its (relatively) high salt content. The difference between the rainy and dry seasons was again said to be around 5 meters (figure 21b). All the dug wells in the village (7 or 8 wells) were said to have similar characteristics.

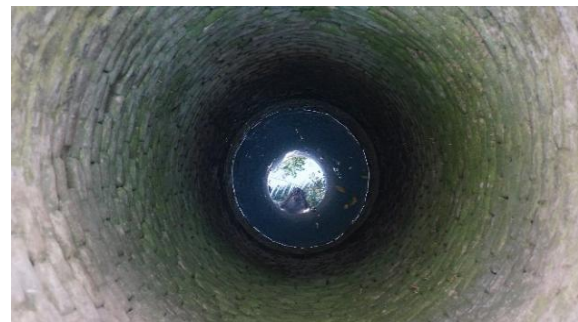


Figure 21a, b: standing next to the first dug well encountered, while the villagers explain its purpose (a, left). The water level is approximately 7 meters below the surface (b, right).

The fourth well, also a dug well, is located on the private plantation of one of the houses of the village (figure 22a, b). Once upon a time, it was probably used to water the plantation. However, no one was around to explain the history of this particular well.



Figure 22a, b: another dug well on a small plantation in the immediate vicinity of the village (a, left). With a rim slightly closer to the ground, this well showed to have similar SWL characteristics as the other dug wells in the village (b, right).

The fifth and final tube-well visited in Oakshitkwin is located at the edge of the village and is destined for irrigation purposes (figure 23a). The farmers we talked to (Figure 23b) said that during the rainy season they grow mostly rainfed paddy rice and only occasionally, when the rains are late, use their groundwater well for irrigation. In the dry season, they use the land for black gram beans that need little water (figure 23c). Only occasional pumping is required to grow the crop, usually no more than 2 or 3 times during the entire dry season. When they do use their well, they water the fields until satisfied with the result. Therefore, they have no estimate on the amount of water being used, because it depended on their subjective decision whether to water the crop and for how long. They never experienced a water shortage from the well nor was the water at any time saline. The well is estimated to be between 100 to 150 feet deep. The agricultural land around the village uses roughly 1 well per 10 acres.



Figure 23a, b, c: the tube-well(s) used for irrigating the crops (a, left). Discussing the use of irrigation waters with the local farmers (b, middle). The black gram bean agricultural plot (c, right).

Well 28: N17.30518, E95.54792

Another abandoned dug well was spotted alongside the road back to Yangon (figure 24a). Unfortunately, nobody was around to answer any questions. The water was roughly 5 meters below the edge of the well (figure 24b). There were no signs of the well still being used.



Figure 24a, b: Interpreter 'Chan Myeako' next to the dug well (a, left). The well's SWL (b, right).

Well 29: N17.27391, E95.58023

With the water tower from this factory clearly visible from the main road (figure 25a, b), a comparison of the (ground)water demands from such a factory with that of domestic and irrigational demands was thought to be most interesting.

Hospitably received by the management of the (now known to be) rice mill plant, it became clear that production had not started yet. Built after a Japanese design, the plant had just entered the final stages of its construction. The main purpose of the water tower, with its distinct green and orange colours, is being a symbol for the company. Until now, the plant's water tower had only been used for the construction phase and currently provides water for domestic purposes.

The tube-well (figure 25c), supplying water to the water tower, was constructed a little over 2 years ago and reaches a depth of 220 feet. The water tower has a secondary reservoir of equal capacity at its base (5000 gallons). However, this reservoir does not have another function than temporary storage.

The tube-well produces clear fresh water without any specific smell to it. With a well diameter of 4 inches, the water tower is supplied by this single well in combination with a pump capable of pumping 1800 GPH. The water tower is filled once a day, but pumping does not commence when the water tower is entirely empty.

So far, no seasonal changes in pumping were experienced. No official water quality analysis had been requested. The future extraction demands are still uncertain and will depend on the production levels. The primary purpose of the water tower will be cooling a 150-ton engine, used in the production process. To assess the order of magnitude of the future groundwater extraction, using an entire reservoir of 5000 gallons would translate to $((5000 \times 4) / 24) = 833\text{L/hour}$.

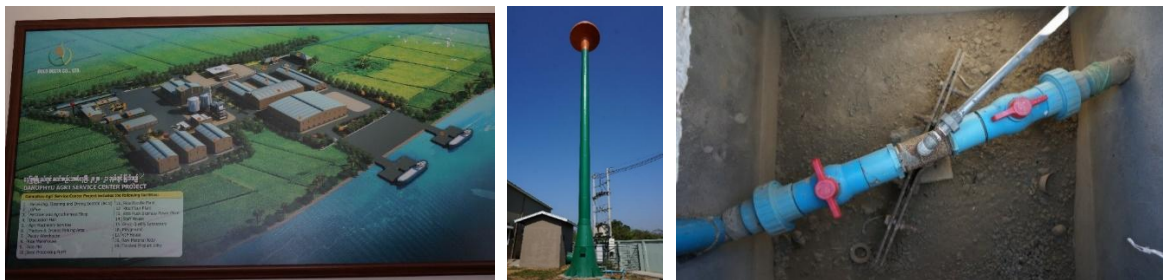


Figure 25a, b, c: an overview of the rice processing plant (a, left). The water tower (b, middle). The tube-well (c, right).

Well 30: not officially part of this survey

Although not having been able to directly compare dug well SWLs during this survey. One dug well was visited by Jan de Bruin twice, once during the dry season and once during the rainy season (figure 26a, b, c).



Figure 26a, b, c: the dug well visited in both the rainy season and the dry season (a, left). The SWL during the rainy season (b, middle). The SWL during the dry season (c, right). Photographs courtesy of Jan de Bruin.

C1: base model

A 3D variable-density groundwater flow and coupled salt transport model for the Ayeyarwady Delta, using local to global datasets, has been previously defined by Mulder (2018) in order to quantify the fresh groundwater gaps and calculate delta equilibrium times. Below, his model is referred to as the base model. Since this study builds upon the base model, a brief overview of the base model's characteristics is hereunder provided. More detailed information can be found in the work of Mulder (2018).

The base model's spatial boundaries are defined using the GEBCO 2014 DEM (Hall, 2006), which provides an earth's surface DEM as well as information on the bathymetry. Being constructed with the intent to simulate flow through the low-lying areas of the delta, and not to assess mountain hydrology, the delta area to be actively modelled is defined according to two criteria. First, all locations where the DEM suggests an elevation of more than 300 m above sea level are excluded. Secondly, only those areas marked as being comprised of unconsolidated sediment (through which flow is possible) according to the GLIM-dataset from Hartmann & Moosdorf (2012), are used to represent the deltaic area. To include the effect of salt water intrusion coming from the seas, parts of the Andaman Sea are also included, resulting in a model 470 km from East to West and 544 km North to South with a 1*1 km cell-size resolution. An illustration of the result is presented in figure 1.

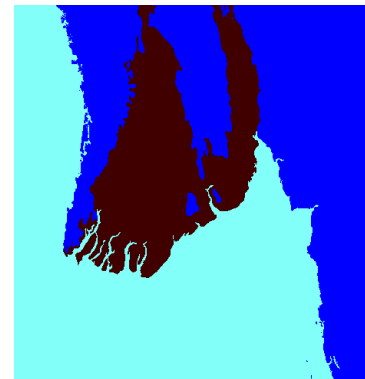


Figure 1: In black, blue and cyan: areas for which changes in hydraulic head and concentrations are being calculated, inactive cells and fixed level cells, respectively.

The DEM is used to represent the top of the system, while the bottom of the system, the assumed depth to bedrock, is represented by regolith thickness estimates from Zamrsky et al. (2017). In between the top and bottom a total of 10 layers, of variable thickness, represent the hydrogeological layering, calculated by dividing the regolith thickness in 10 equal parts. Due to the lack of a global hydrogeological database, hydrogeological scenarios were implemented.

A rivers network is constructed with the aid of the GAIA dataset (Andreadis et al., 2013), containing information on river system widths and depths. This information is used to calculate the rivers' conductance. Consequently, the river head is equal to the DEM's elevation. Furthermore, an extensive drainage network is assumed to be present. Therefore, all active model cells are drained at -0.5 m below the DEM with a conductivity of 1000 m²/day.

Past and present recharge is derived from paleo-precipitation estimates by MIROC-ESM and the GSMaP data set for current precipitation (Watanabe et al., 2011).

The starting heads are made equal to relative sea level (0 m), and general head boundaries are set at the DEM's elevation with a conductance of 0.001 m²/day along the inactive/active cell border and 1000 m²/day where groundwater coming from the North is entering the system.

The base model does not include a groundwater extraction component.

The following starting concentrations are used: 0 g/L TDS inland, 35 g/L TDS at sea, 0.2 g/L TDS for rivers and 0.001 g/L TDS for recharge.

Other model settings include: a porosity of 0.3, anisotropy of 0.4, storage coefficient of 0.0021, horizontal and vertical dispersivity ratio of 0.1, longitudinal dispersivity of 10 m and a diffusion coefficient of 8.64×10^{-5} m²/day.

The finite difference solver, used for the iteration process, converges for a HCLOSE of 0.05 m and RCLOSE of 200 m³/d.

C2: iMOD-WQ

This research project's groundwater modelling computations are performed by Deltares's (iMOD-Water Quality) iMOD-WQ software (Verkaik & Janssen, 2019), previously referred to as iMOD-SEAWAT. The software is used to calculate density-dependent flow and reactive transport and combines the USGS's code for density-dependent flow and transport "Seawat" (Langevin et al., 2008) and the University of Alabama's MT3DMS (Zheng and Wang, 1999) and the Pacific Northwest National Laboratory's RT3D codes for 3D multispecies reactive transport (Verkaik & Janssen, 2019).

A very brief overview of the underlying equations being solved, and the solver used to calculate variable density flow follows below.

Darcy's formula for saturated groundwater flow is expanded into a 3D environment (eq 1):

$$\frac{\partial}{\partial x} * \left(K_{xx} \frac{\partial h}{\partial x} \right) + \frac{\partial}{\partial y} * \left(K_{yy} \frac{\partial h}{\partial y} \right) + \frac{\partial}{\partial z} * \left(K_{zz} \frac{\partial h}{\partial z} \right) - W = S_s \frac{\partial h}{\partial t} \quad (\text{eq. 1})$$

The solute transport equation (eq. 2) is used to calculate solute concentrations:

$$\frac{\partial(nC)}{\partial t} = \nabla * (nD * \nabla C) - \nabla * (qC) - q'_s C_s \quad (\text{eq. 2})$$

Calculated concentrations are then used as input for the equation of state to calculate density differences (eq. 3):

$$\rho_{i,j,k} = \rho_f + \frac{\partial \rho}{\partial C} * C_{i,j,k} \quad (\text{eq. 3})$$

iMOD-WQ ultimately combines eq. 1, 2 and 3 to compute saturated variable density flow in three dimensions (eq. 4):

$$\nabla * \left[\rho K_f \left(\nabla h_f + \frac{\rho - \rho_f}{\rho_f} \nabla z \right) \right] = \rho S_{sf} \frac{\partial h_f}{\partial t} + n \frac{\partial \rho}{\partial C} \frac{\partial C}{\partial t} - \rho_s q'_s \quad (\text{eq. 4})$$

The base model uses the 'Preconditioned Conjugate Gradient' (PCG) package and the 'Generalized Conjugate Gradient' (GCG) package to solve the groundwater flow equation and the transport/reaction terms, respectively. However, these solvers allow for single core processing only. Recent developments have provided the possibility of parallel processing using multiple cores. Therefore, when running the enhanced model, developed during this research project, the new 'Parallel Krylov Solver Flow' (PKSF) and 'Parallel Krylov Solver Transport' (PKST) packages were implemented to speed up computations (Verkaik & Janssen, 2019).

While iMOD-WQ allows for several methods to be used to numerically solve the partial differential equations (FD, MOC, MMOC, HMOC, TVD), computations were limited to the use of the finite difference (FD) method, due to the fact that the FD-method is the quickest and computational times required for performing paleo-reconstructive modelling are already very long.

A more detailed description on the different types of modelling methods available and in-depth explanation of the underlying equations, the reader is referred to (Verkaik & Janssen, 2019).

C3: additional model modifications

A groundwater model is defined by the interactions of its components. Therefore, adjusting one parameter might require the adjustment of another. While hydrogeology, RSLR and groundwater extraction are the focus of this research, it was also a necessity to adjust the parameters discussed below.

Rivers: with the extension of the delta's surface area to facilitate the paleo-reconstruction, the river network had to be extrapolated to fit the altered model boundaries. To recreate extinct river systems, the DEM was made fit for hydrological modelling using a sink fill function (Mark, 1988). Consequently, the flow direction and accumulation (Jenson & Domingue, 1988) were calculated to define both river location and size for the otherwise inundated areas of the DEM.

The extrapolated river network (visually determined) showed a similar density to that of the original for a flow accumulation succession of 5%, 1%, 0.5%, 0.1%, 0.05%, 0.025% (largest to smallest river branches). Preserving the original system, the existing river network was combined with the newly defined categorized calculated estimates (figure 1).

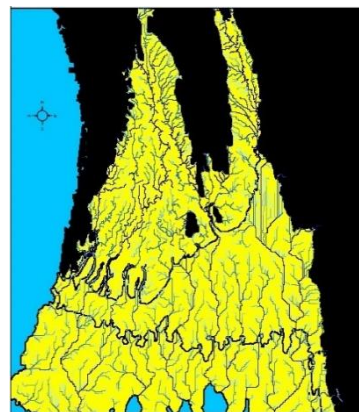


Figure 1: river network extrapolation

iMOD requires a minimum of three river input raster's: river conductance, river level and river depth. Since no values were available to calculate conductance values for historic rivers, values had to be derived from the statistics of the already defined river network. Dividing the base model's river conductance network into 6 quantiles, the median conductance value for each quantile was imposed on the 6 categories comprising the river network extrapolation, being: 3692, 573, 360, 276, 194, 178 m^2/day for the 5%, 1%, 0.5%, 0.1%, 0.05%, 0.025% flow accumulation, respectively. Using the same 6 categories and associated succession, a depth gradient of 1, 2, 3, 4, 5 and 9 m was applied to maintain a distinction between river categories in accordance with base model statistics. Consequently, the river level adopted the bathymetry values suggested by the DEM. The previously defined river depths were then subtracted from these elevation values to obtain the river depths relative to the surface.


DEM: The DEM for the original model boundaries remained unchanged. However, it was combined with the hydrological sound, sink filled, DEM used for the extended paleo-reconstructive boundaries to guarantee a natural runoff gradient that is compliant with the flow accumulation calculations.

Drainage: The Ayeyarwady Delta has a rich and long agricultural history. Being a low-lying area cultivated for generations, with rice as the main crop, it is assumed that an extensive drainage network has developed. Having converted most values to integers, the original uniform drainage 0.5 m below DEM with a conductance of 1000 m^2/day has been lowered to 1 meter below DEM.

Starting heads: Initial starting heads were set equal to sea level. Now, with the aid of SWL measurements provided by well-logs, starting heads were defined by subtracting the median SWL value of 4 meters below the DEM. For every location this subtraction proposed a hydraulic head below sea level, the head was raised to be equal to sea level.

If a parameter is not addressed, neither in this section nor in the main body of text, it can be assumed that the model variable remains unchanged with regards to base model settings described in Appendix C1.

D1a: Department of Rural Development well-log



Department Of Rural Development Well Log

		Soil	Colour			
SWL	Y			0'-20'	မြေ	အဝါ
PWL	Y			20'-80'	မြေ	အပြာ
				80'-90'	နုံးသဲ	အပြာ
				90'-120'	သဲ	အပြာ
				120'-140'	သဲ	ဖြူပြာ
				140'-160'	မြေ	အပြာ
				160'-180'	သဲ	ဖြူဝါ
				180'-190'	သဲကြမ်း	အဝါ
				190'-200'	သဲကျောက်စက္ကဲ	အဝါ
				200'-210'	သဲကျောက်စက္ကဲ	အဝါ
				210'-220'	သဲကျောက်စက္ကဲ	အဝါ
				220'-240'	သဲကျောက်စက္ကဲ	ဖြူဝါ

Well No.		DNU.3 18-19	
Division		ဧရာဝတီတိုင်း	
District		မအူပင်	
Township		ဓနုဖြူမြို့	
Villagerttack		ရေတွင်းကုန်း	
Village		လှည်းဆိပ်	
Drilling Depth		400'	
Casing Length		200'	
Casing Size		4" φ	
Casing Type		PVC pipe	
Screen Size		4" φ	
Screen Type		slotted , PVC	
Screen Opening Size		1mm	
Screen Setting		From	To
		200'	220'
Slump	20'	220'	240'
Water Level		SWL	PWL
		20'	40'
Yields		1500 gph	
Commence Date		6.1.2019	
Completed Date		10.1.2019	
Rig No		adpw - 3	
Remark			
U Chit San Maung Managing Director Ayeyar Daung Phan War Co.,Ltd.			
Than Swe Win (BE - Civil) Assistance Engineer Ayeyar Daung Phan War Co.,Ltd.			

An example DRD well-log providing information on (amongst other things): the well's location, the date of construction, the SWL and the PWL during construction, the extraction depth and the location's lithological sequencing (here in Myanmar language).

D1b: Yangon City Development Committee well-log

ရန်ကုန်မြို့တော်စည်ပင်သာယာရေးကော်မတီ

အင်ဂျင်နီယာဌာန (ရေနှင့်သန့်ရှင်းမှု)

အဝီစိတွင်းများဌာနစု

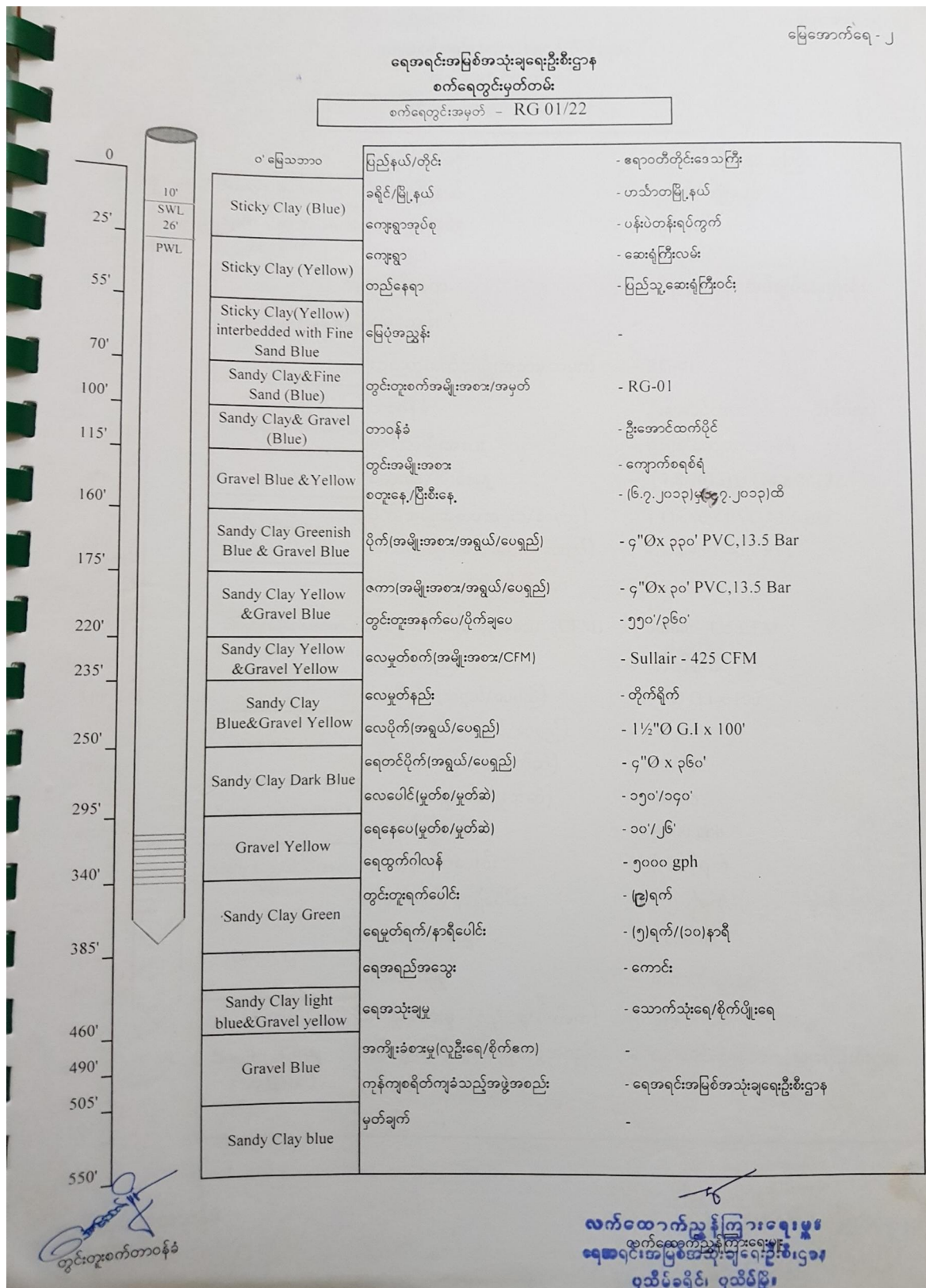
WELL LOG

(အဝီစိတွင်း၏ မြေအောက်၊ မြေလွှာများ)

အနက်(ပေ)	မြေလွှာအမျိုးအစား
၀' - ၃၀'	ဂံမြေနီ
၃၀' - ၄၀'	သဲဝါနု
၄၀' - ၆၅'	သဲဝါကြမ်း
၆၅' - ၇၅'	သဲညိုနု
၇၅' - ၈၇'	သဲဝါနူးမြေ
၈၇' - ၁၁၀'	သဲဝါကြမ်း(ကျောက်ကွဲ)

An example YCDC well-log providing information on (amongst other things): the well's location, the date of construction, the SWL and the PWL during construction, the extraction depth and the location's lithological sequencing (here in Myanmar language).

D1c: Irrigation and Water Utilization Management Department well-log



An example IWUMD well-log providing information on (amongst other things): the well's location, the date of construction, the SWL and the PWL during construction, the extraction depth and the location's lithological sequencing (here in English)..

D2: wells used for the hydrogeological model

Region	District	DRD	IWUMD	YCDC	Total
Ayeyarwady	Maubin	33	15	0	48
	Hinthada	2	22	0	24
	Pathein	3	64	0	67
	Myaungmya	0	11	0	11
	Labutta	0	0	0	0
	Pyapon	0	14	0	14
Yangon	Yangon North	0	1	4	5
	Yangon South	0	17	2	19
	Yangon East	0	2	13	15
	Yangon West	0	0	12	12
Total	Overall	38	146	31	215

The number of wells used for modelling the hydrogeology, grouped per administrative district.

D3a: example well codes

Data Source	Example code	Explanation
IWUMD	F1	F = Hinthada district, 1 = well number 1, which is also the oldest well in the district.
DRD	MaDNP1	Ma = Maubin district, DNP = Danuphyu township (first letter of each Syllable), 1 = well no. 1
YCDC	B0101	B = bore-log, "01" = township (see Appendix D3b), "01" = well no. (Follows coding provided by YCDC well-logs).

The explanation of an example code for one tube-well of each governmental organization.

D3b: Yangon City Development Committee coding key

YCDC-CODE Township		
01 = Sanchaung	12 = Botataung	23 = Kyimyindaing
02 = Ahlone	13 = Dala	24 = Kyaukdata
03 = Kamayut	14 = Pazundaung	25 = Dawbon
04 = Bahan	15 = Tamwe	26 = Shwepyitha
05 = Thingangyun	16 = South Okkalapa	27 = Seikkyi Kanaungto
06 = Mayangon	17 = Mingaladon	28 = Hlaingtahaya
07 = Dagon	18 = N/A	29 = North Dagon
08 = Mingala Taungnyunt	19 = Thaketa	30 = South Dagon
09 = Insein	20 = North Okkalapa	31 = East Dagon
10 = Hlaing	21 = Lanmadaw	32 = Dagon Seikkan
11 = Pabedan	22 = Latha	33 = N/A

*No well logs were received for township 18 and 33, Seikkan and Yankin, respectively.

YCDC township coding key.

D3c: Irrigation and Water Utilization Management Department coding key

IWUMD-code			
A = Hinthada	C = Myaungmya	E = Labutta	G = Yangon
B = Maubin	D = Pyapon	F = Pathein	

IWUMD district coding key.

D3d: Department of Rural Development coding key

DRD	Maubin	Pathein	Hinthada
District-Code	Maubin = Ma	Pathein = P	Hinthada = Hi
Township-Code	DNP = DaNuPhyu	KG = KyaungGone	HTD = HinThaDa
	MUB = MaUBin	KGD = KanGyiDaunt	Ma = MyanAung
	ND = NyaungDone	KP = KyonPyaw	
	PTN = PanTanaw		

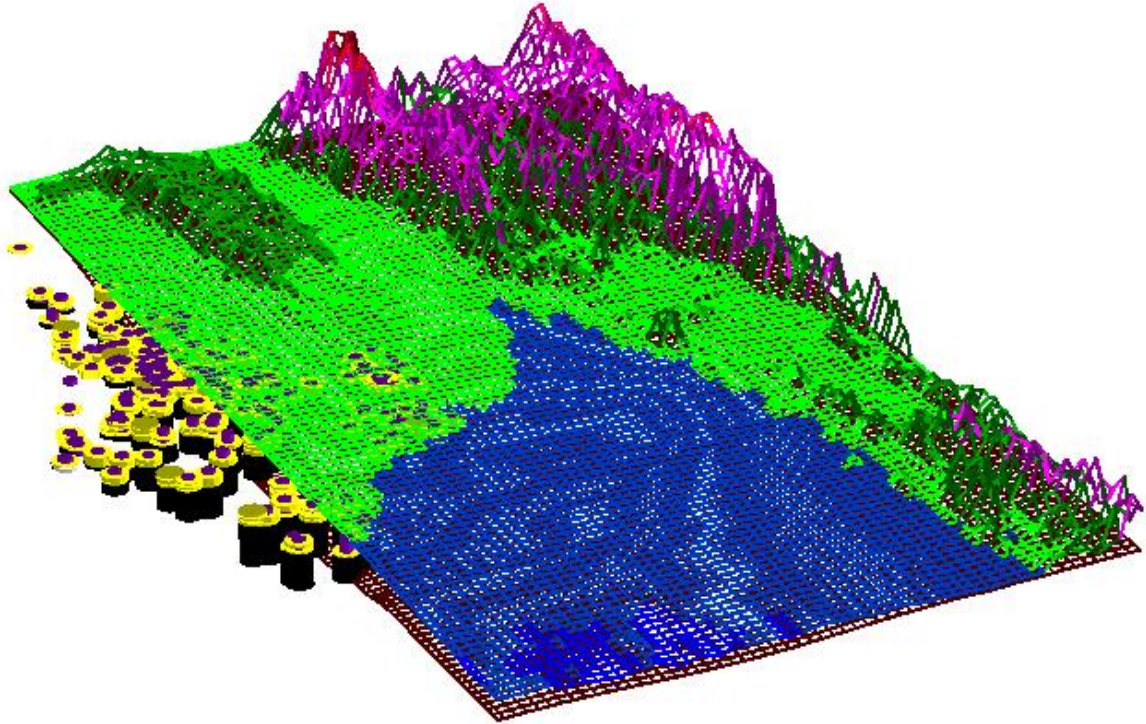
The DRD district and township coding key.

D4: wells exceeding depth to bedrock

YCDC/IWUMD well code	Depth to bedrock	Tube well screen depth
B1705	-101	-138
A21	-46	-160
A24	-156	-168
F49	-159	-176
F51	-140	-174
F56	-144	-180
F67	-142	-177
F68	-124	-168
F70	-61	-172
F71	-121	-178
F72	-121	-178
F73	-152	-170
F74	-86	-169

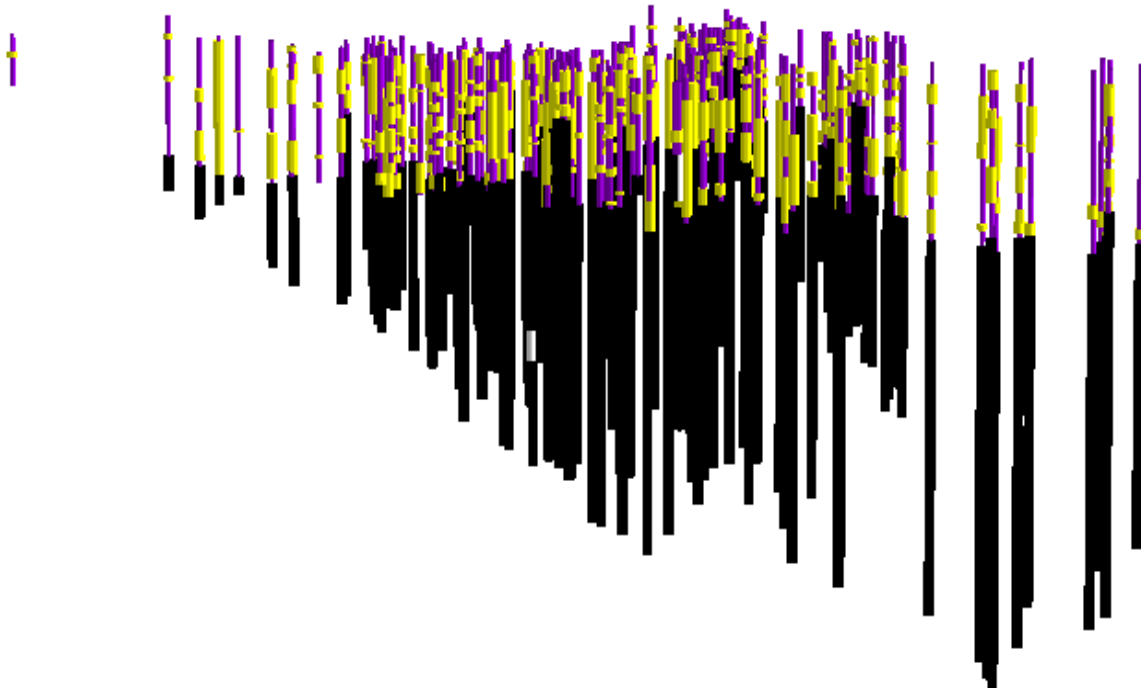
Wells that had to be curtailed to not exceed the depth to bedrock estimates.

D5a: well positions



A 3D visual of the wells' position throughout the Ayeyarwady Delta, looking into the Gulf of Martaban.

D5b: lithological sequences



A 3D representation of the wells' lithological sequences within iMOD viewed from aside. In purple, yellow and black, the aquitards, aquifers and unknown categories. The well log sequences run from the DEM to bedrock.

D6a: example.IPF-file

```
7          #Number of bore-log .TXT files the .IPF is referring to
3          #Number of fields (X, Y and BOREID)
"X-COORDINATE (UTM)" #X-coordinate header
"Y-COORDINATE (UTM)" #Y-coordinate header
BOREID     #BOREID header
3,TXT     #>1 = associated files?, filetype to be read
102056.38,98640.46,B1 #X-coordinate & Y-coordinate, respectively
102945.18,99219.98,B2 #Decimal coordinates indicated with a dot
103422.61,98142.02,B3 #Coordinates separated by a comma
100618.09,98751.56,B4 #No spaces, use comma before indicating BOREID
102701.96,98268.12,B5 #BOREID refers to the name of the .TXT file
101780.13,97937.83,B6 #.TXT files and .IPF need to be in same directory
101608.98,99105.88,B7
```

*Entries that contain spaces should be encapsulated by quotes.

**Don't use tabs for delimitation!

***Files with another extent than .TXT can be given as well.

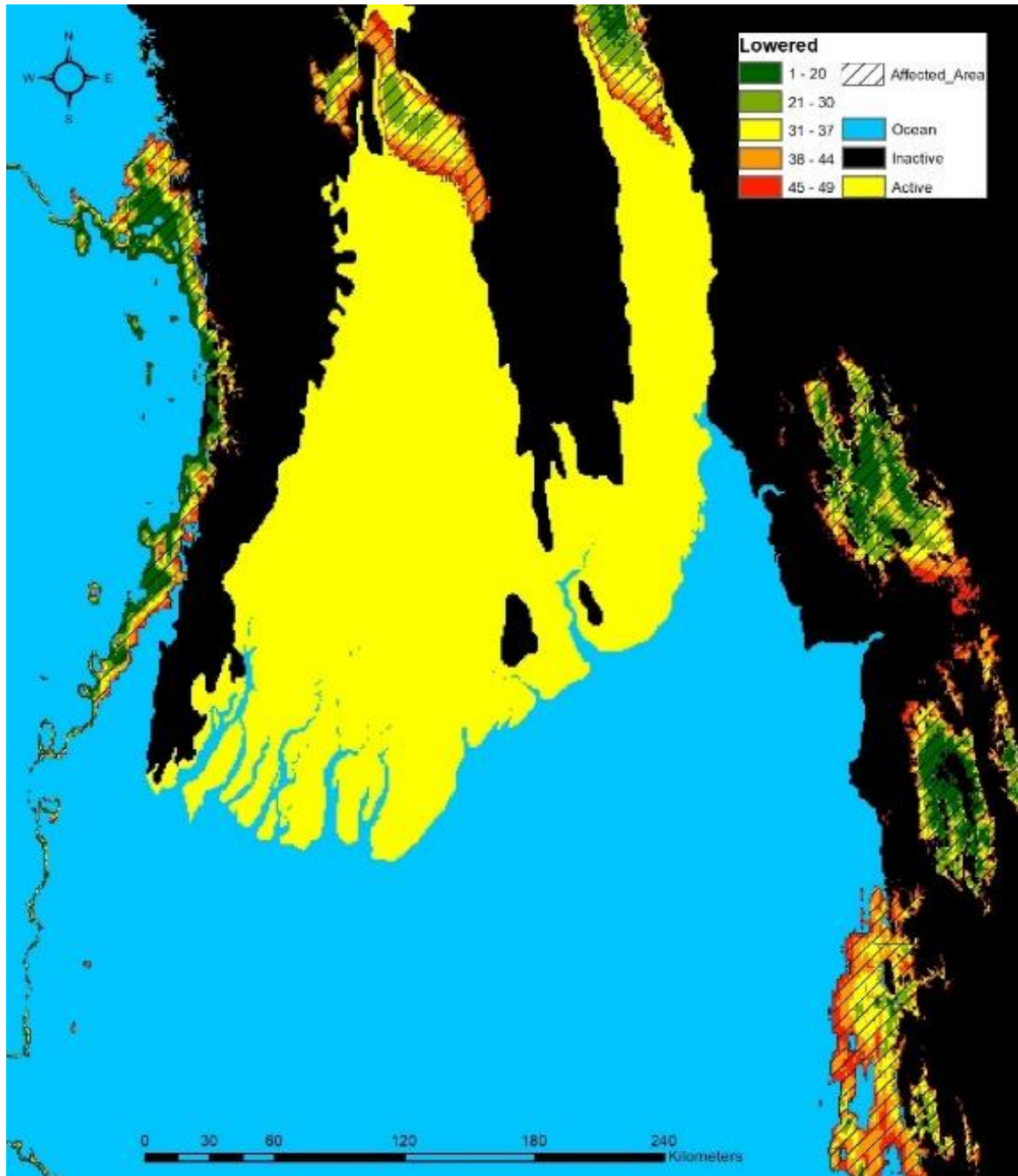
An example .IPF-file for interpreting the wells' their location and referring to the well-logs' ascociated .TXT-file.

D6a: example .TXT-file

```
5          #number of formation types defined by bore-log
2,2       #2 columns, 2 rows (rows expended automatically (line 1))
Z,-999    #indicates the header name displaying depth
LITHOLOGY,-999 #indicates the header name displaying formation type
4.4,"S"   #4.4 m above sea level
-5.0,"C"  #-5.0 meters below sea level
-11.0,"S" #"S" is the written symbol of the formation
-20.0,"LST" #formation continue until the next defined formation
-25.0,"-" #"- " 'not classified', signalling the end of the sequence
```

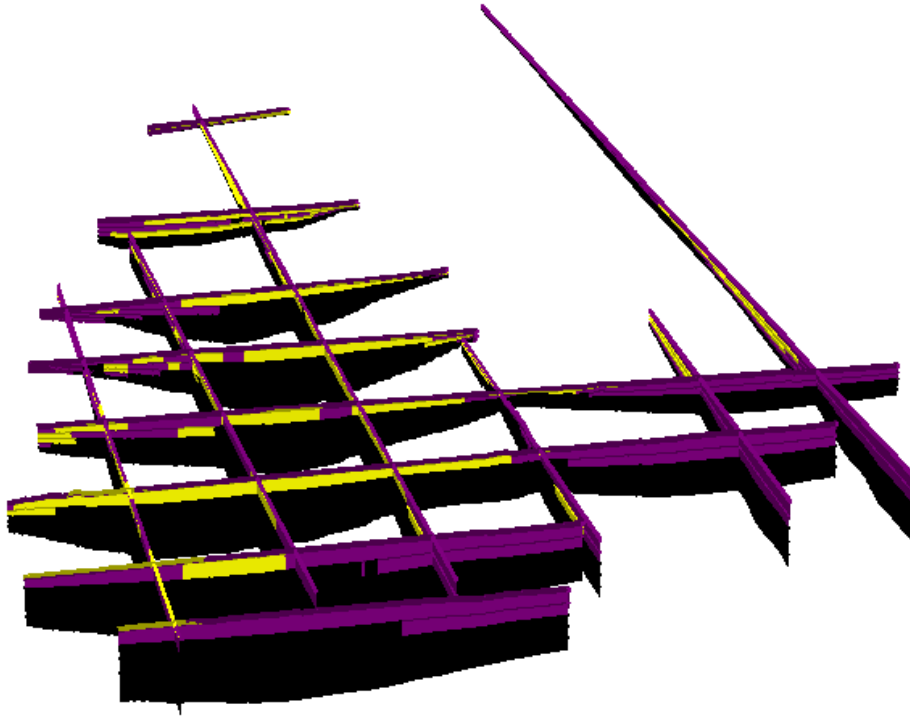
An example .TXT file with the associated well-log's lithology.

D7: artificially lowered areas



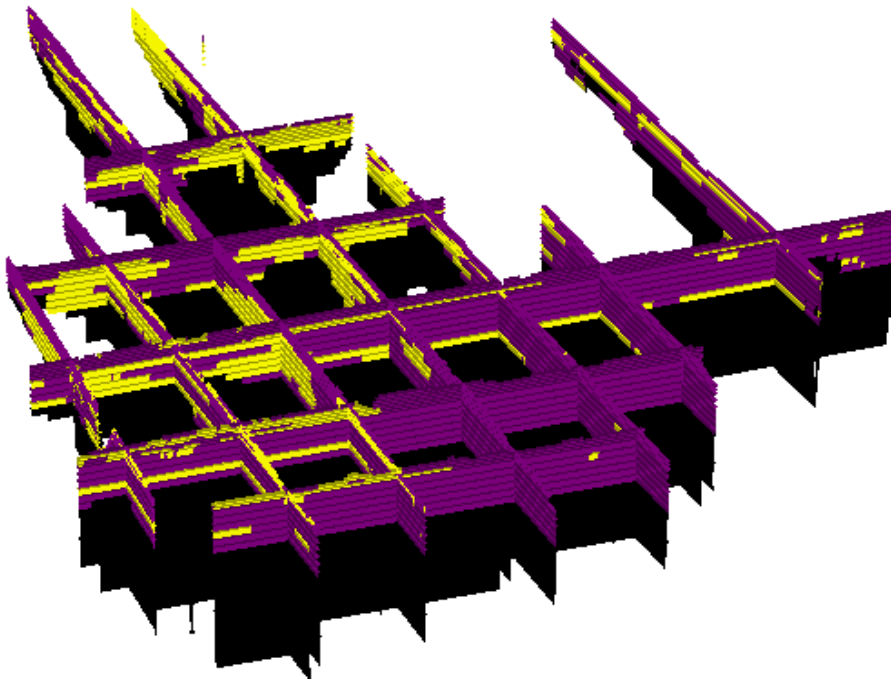
Areas artificially thickened to allow predefined layer interpolation.

D8a: delta cross-sections, variable vertical levels



Cross-sections through the actively modelled area (Appendix D7) of the hydrogeological voxel model with variable vertical levels. In purple, yellow and black, the aquitards, aquifers and unknown categories.

D8b: delta cross-sections, constant vertical levels



Cross-sections through the actively modelled area (Appendix D7) of the hydrogeological voxel model with constant vertical levels. In purple, yellow and black, the aquitards, aquifers and unknown categories.

D9: voxel model batch-file

```

SET cs=1000
SET dir=C:\2_iMOD_Workdirectory_v4_4\Hydrogeological_Model\Voxel_Model\Voxels

SETLOCAL ENABLEDELAYEDEXPANSION

SET N=0
FOR %%A IN ("Z","C") DO (
  SET /A N=N+1
  SET VAR[!N!]=%%A
)

SET M=0
FOR %%A IN (100,1.0E-2) DO (
  SET /A M=M+1
  SET KVR[!M!]=%%A
)

SET P=0
FOR %%A IN (100000.0,
  100000.0) DO (
  SET /A P=P+1
  SET RNG[!P!]=%%A
)

SET /A B=0
FOR /L %%B IN (1,1,!N!) DO (
  ECHO FUNCTION=XYZ2IDF >> XYZ2IDF_%%B.INI
  ECHO IPFFILE=%dir%\All_Well_Logs\All_Tube_Wells.IPF >> XYZ2IDF_%%B.INI
  ECHO WINDOW=0.0,0.0,470000.0,544000.0 >> XYZ2IDF_%%B.INI
  ECHO CS=%%cs% >> XYZ2IDF_%%B.INI
  ECHO IZCOL=1 >> XYZ2IDF_%%B.INI
  ECHO IZCOL=2 >> XYZ2IDF_%%B.INI
  ECHO IZCOL=3 >> XYZ2IDF_%%B.INI
  ECHO ILOG=0 >> XYZ2IDF_%%B.INI
  ECHO ASSF_COLUMN=2 >> XYZ2IDF_%%B.INI
  ECHO GRIDFUNC=OKRIGING >> XYZ2IDF_%%B.INI
  ECHO KTYPE=2 >> XYZ2IDF_%%B.INI
  ECHO IQUADRANT=1 >> XYZ2IDF_%%B.INI
  ECHO RANGE=!RNG[%%B!] >> XYZ2IDF_%%B.INI
  ECHO SILL=100.00 >> XYZ2IDF_%%B.INI
  ECHO NUGGET=0.0 >> XYZ2IDF_%%B.INI
  ECHO INDICATOR=1 >> XYZ2IDF_%%B.INI
  ECHO THRESHOLD1=!VAR[%%B!] >> XYZ2IDF_%%B.INI
  ECHO K_THRESHOLD1=!KVR[%%B!] >> XYZ2IDF_%%B.INI
  ECHO NTHRESHOLD=1 >> XYZ2IDF_%%B.INI
  ECHO ASSF_IDEPH=2 >> XYZ2IDF_%%B.INI
  ECHO NLAY=10 >> XYZ2IDF_%%B.INI

  SET /A N=0
  FOR /L %%C IN (1,1,10) DO (
    SET /A N=N+1
    ECHO INT_!N!=%dir%\Base_L%%C.IDF >> XYZ2IDF_%%B.INI
  )

  ECHO IDFFILE=%dir%\Voxel_Model_Output\GEO_ASSF_IDEPH_2\GEO_%%cs%\GEO3D.IDF >> XYZ2IDF_%%B.INI
  ECHO STDEVIDF=%dir%\Voxel_Model_Output\STDDEV_ASSF_IDEPH_2\STDDEV_%%cs%\GEO3D_VAR.IDF >> XYZ2IDF_%%B.INI

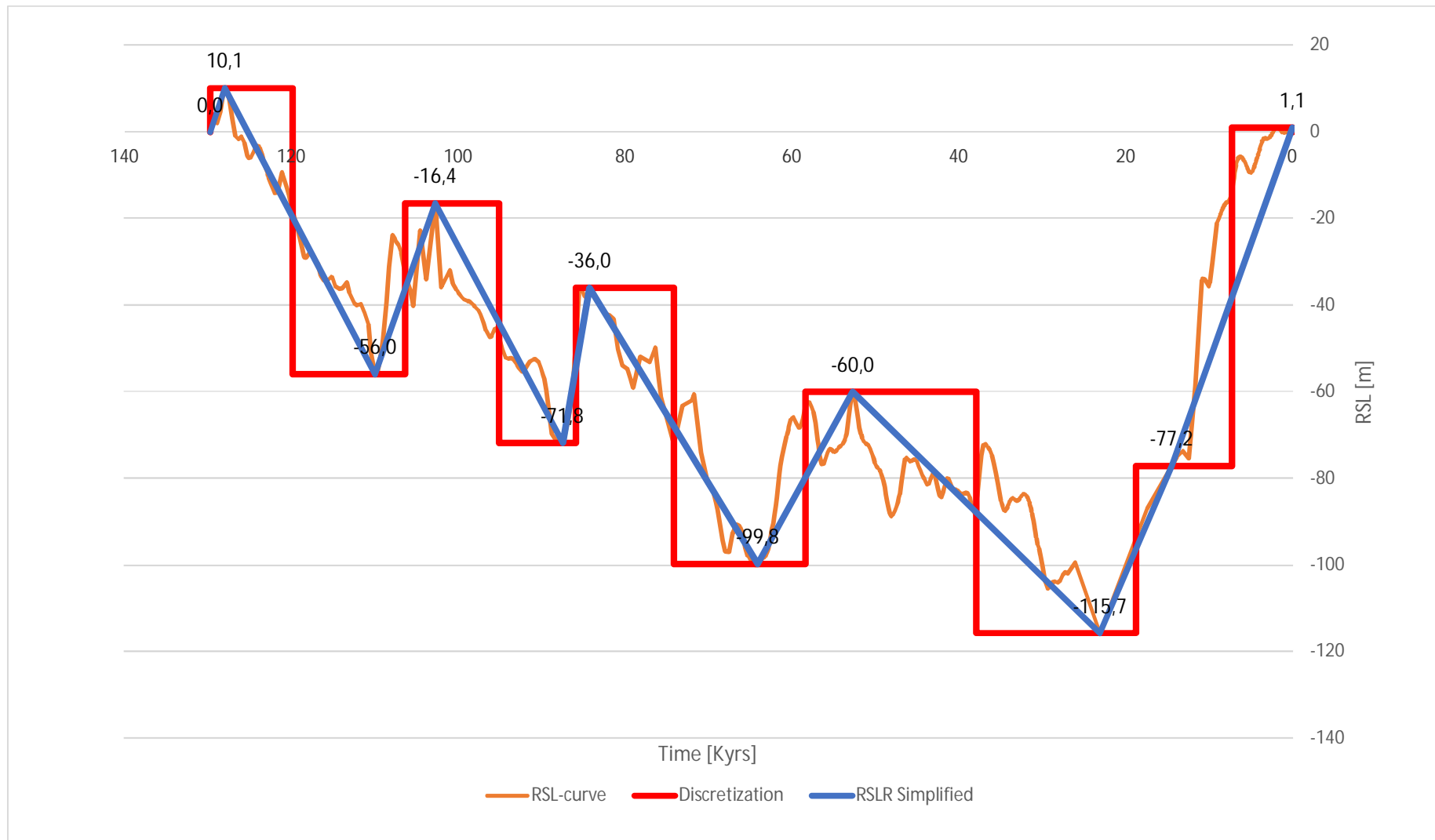
  START C:\2_iMOD_Workdirectory_v4_4\iMODv4_4\iMOD_V4_4_X64R.exe XYZ2IDF_%%B.INI
)

pause

```

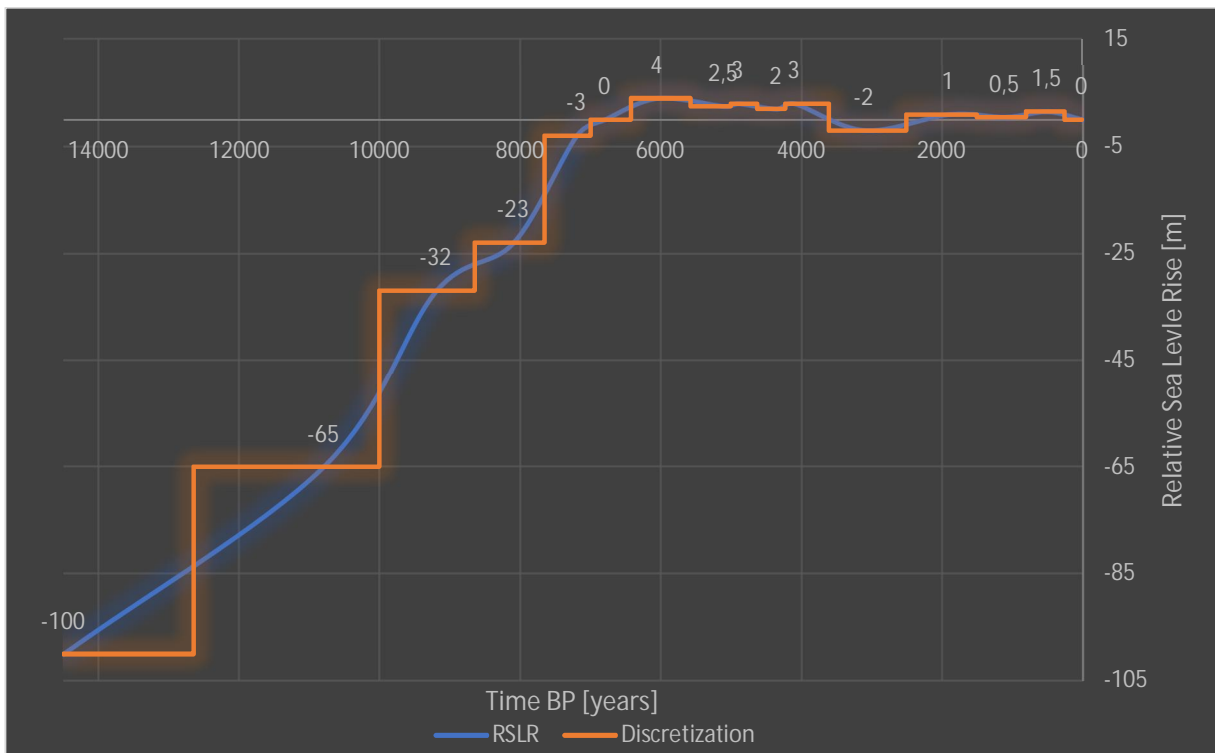
An example XYZtoIDF iMOD batch-file script that can be used to create a 3D hydrogeological model of the subsurface.

E1: relative sea level rise discretization (130,000 years)



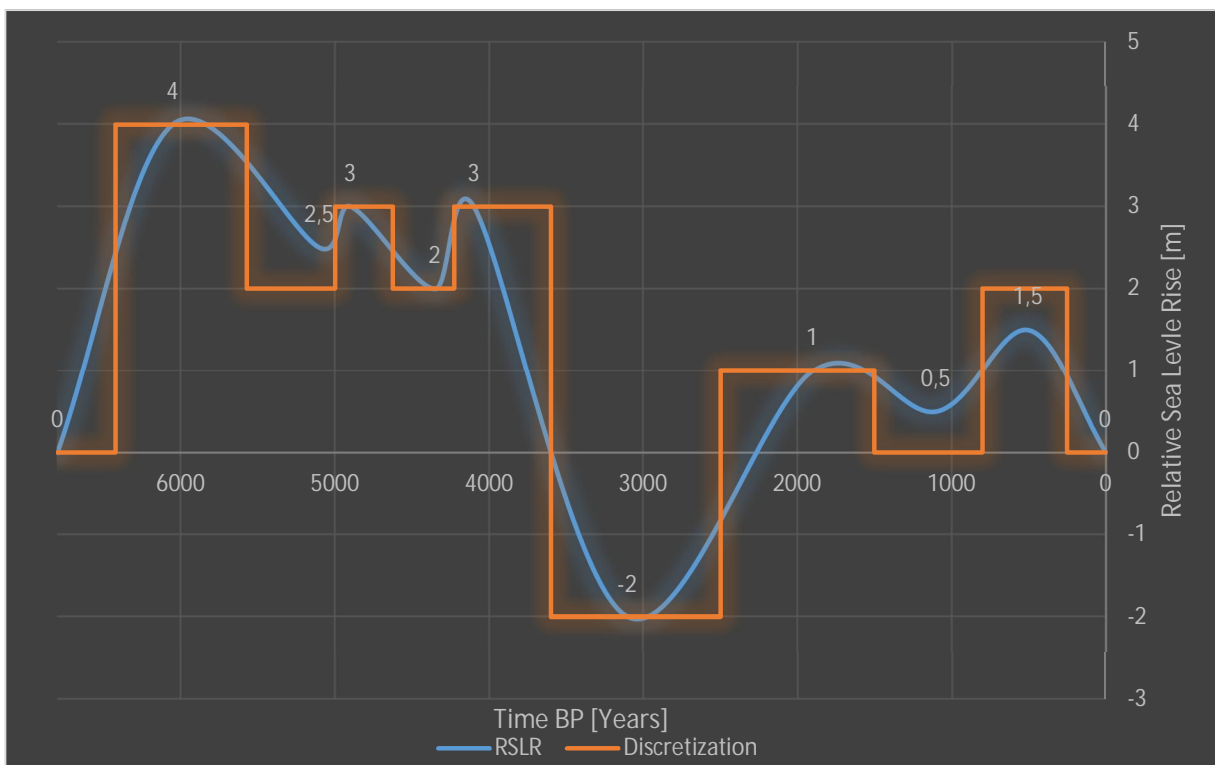
In orange the composite RSLR reconstruction from Grant et al. (2012). In blue the simplification of the RSLR-curve and in red the discretization's that follows from this simplification.

E2a: relative sea level rise discretization (14,500 years)



Relative Sea level Rise discretization derived from Loveson (2019) for the past 14,500 years. In blue the RSLR curve, in orange the derived discretization's.

E2b: relative sea level rise discretization (6,800 Years)



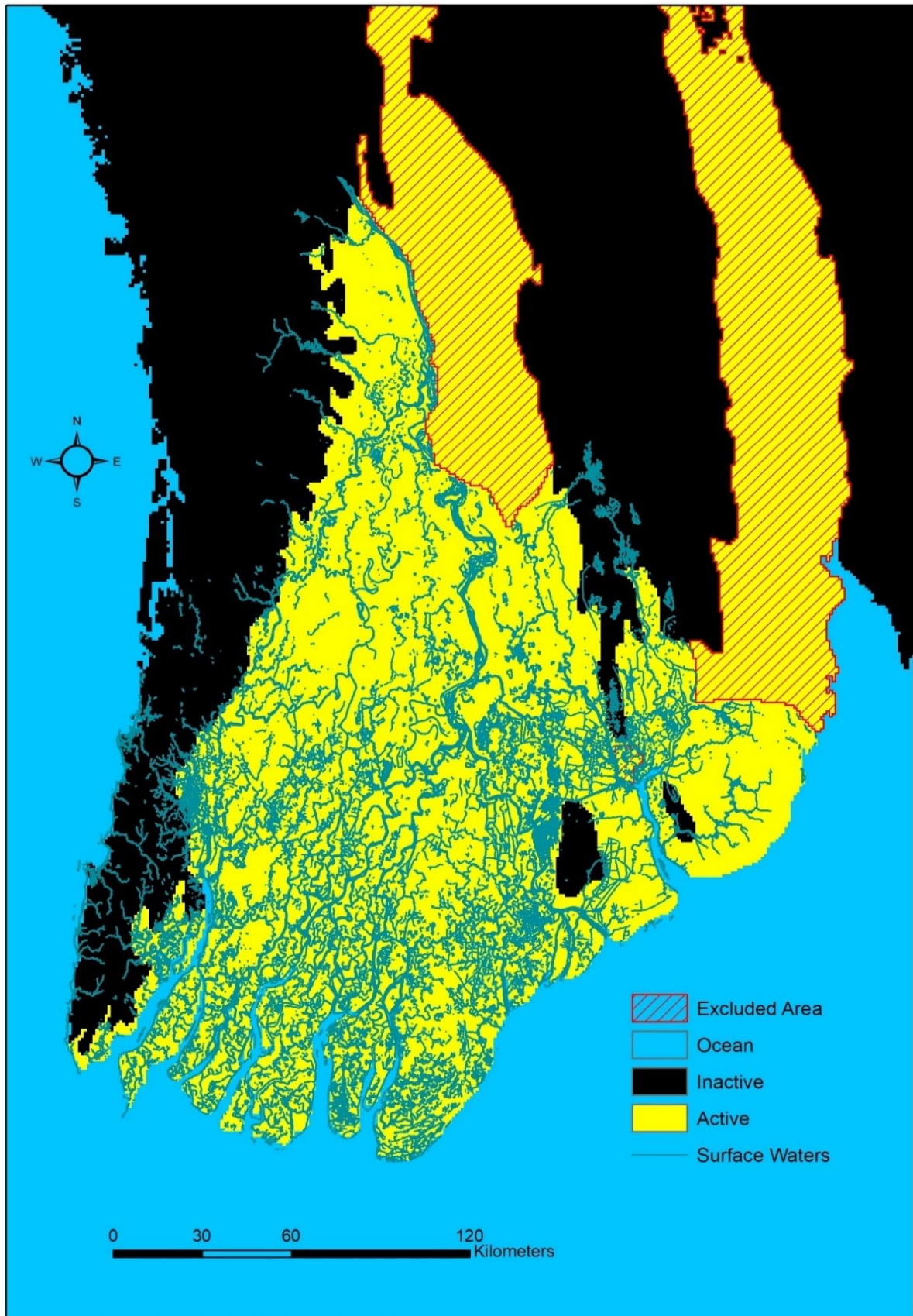
Relative Sea level Rise discretization derived from Loveson & Nigam (2019), zoomed in, showing the past 6800 years. In blue the RSLR-curve, in orange the derived discretization's. Floating values were rounded, up for transgressions and down for regressions.

E3: stress-periods (130,000 years)

Stress-periods	From	Until	Duration	RSL (m)
1	129705	119843	9861	10
2a	119843	106367	6738	-56
2b	119843	106367	6738	-56
3a	106367	95114	5626	-16
3b	106367	95114	5626	-16
4	95114	85863	9251	-72
5a	85863	74160	5852	-36
5b	85863	74160	5852	-36
6a	74160	58390	7885	-100
6b	74160	58390	7885	-100
7a	58390	37897	6831	-60
7b	58390	37897	6831	-60
7c	58390	37897	6831	-60
8a	37897	18793	9552	-116
8b	37897	18793	9552	-116
9	18793	12650	6143	-100
10	12650	10000	2650	-65
11	10000	8650	1350	-32
12	8650	7650	1000	-23
13	7650	7000	650	-3
14	7000	6425	575	0
15	6425	5575	850	4
16	5575	5000	575	2
17	5000	4625	375	3
18	4625	4225	400	2
19	4225	3600	625	3
20	3600	2500	1100	-2
21	2500	1500	1000	1
22	1500	800	700	0
23	800	250	550	2
24	250	0	250	0

The 24 stress periods resulting from the discretization of the combined Grant et al. (2012) and Loveson & Nigam (2019) RSLR-curves for the last (+/-) 130,000 years. Stress periods longer than 10,000 years have been subdivided to stay within the maximum allowed runtime per run-file supported by the iMOD-WQ software.

F1: Ayeyarwady Delta surface water map



The Surface Water map used for calculating a buffer zone in the well definition process. The map was created using the OSM (2020) and the IWMI (2014) land use maps' surface water characteristics.

F2: domestic well exclusions process

Methodological steps	Total number of wells
Initial Open Street Map Buildings	1610807
Within the active modelling boundary	1411797
Outside of surface water buffer zone of 200m	621,947
Multiplied by the correction factor of 0.6	373168
Total number of grouped wells	21361

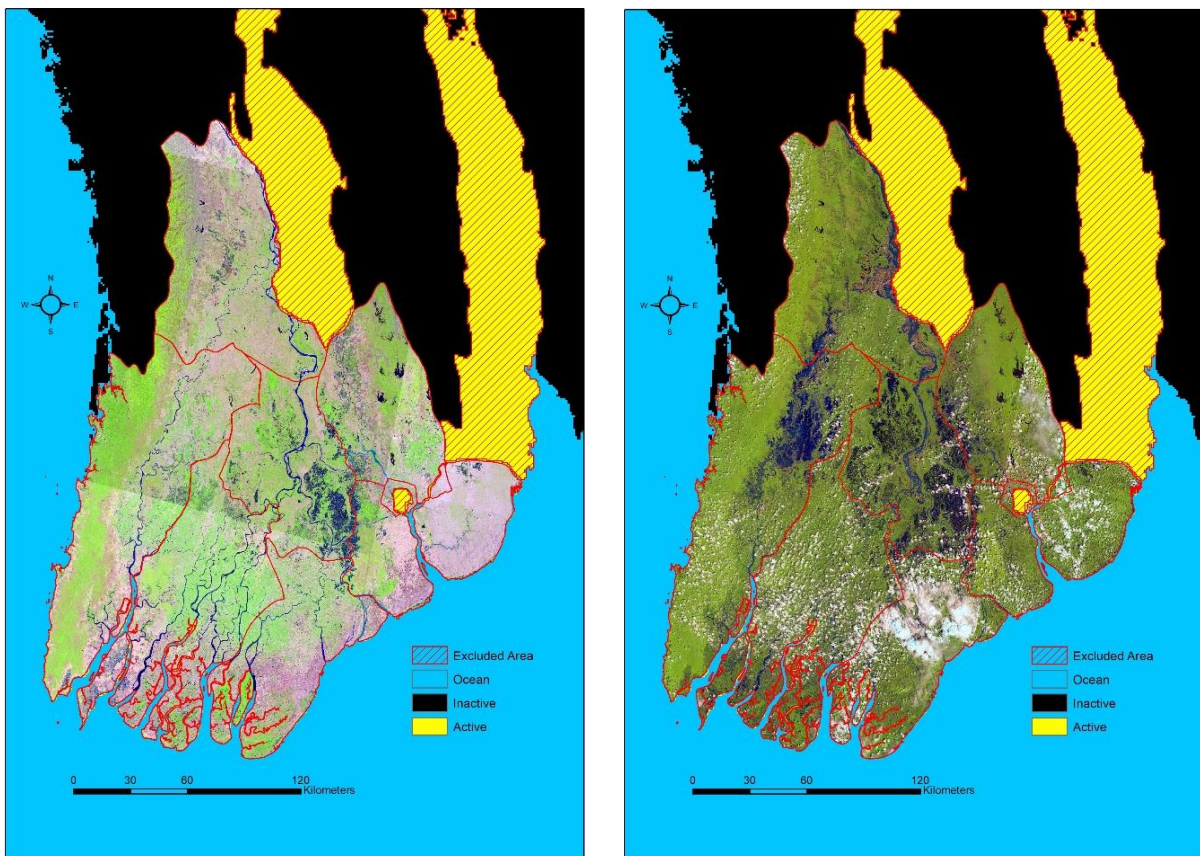
A succession of the number of domestic wells remaining after each step in the well exclusion process.

F3a: satellite image IDs

Dry season scenes Landsat 8 OLI	Rainy season scenes Landsat 8 OLI
LC08_L1TP_132047_20200327_20200409_01_T1	LC08_L1TP_132047_20190917_20190925_01_T1
LC08_L1TP_132048_20200327_20200409_01_T1	LC08_L1TP_132048_20190917_20190925_01_T1
LC08_L1TP_132049_20200311_20200325_01_T1	LC08_L1TP_132049_20190917_20190925_01_T1
LC08_L1TP_133047_20200403_20200410_01_T1	LC08_L1TP_133047_20190924_20191017_01_T1
LC08_L1TP_133048_20200215_20200225_01_T1	LC08_L1TP_133048_20190924_20191017_01_T1
LC08_L1TP_133049_20200403_20200410_01_T1	LC08_L1TP_133049_20190924_20191017_01_T1

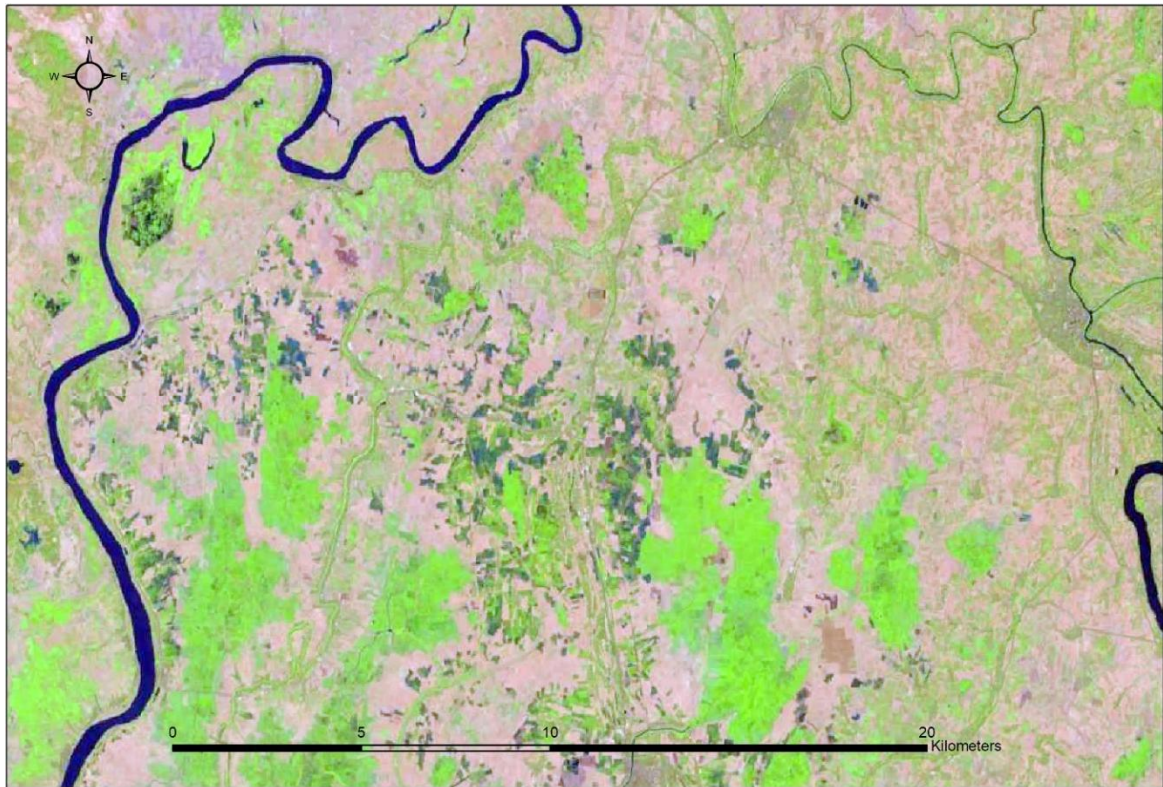
Landsat 8 scene IDs for the Ayeyarwady Delta during both dry season and wet season. Rainy season scenes were selected that were taken one year prior to the dry season scenes, because of their minimal cloud cover. For the same year as the dry season, cloud cover obscured much of the land surface, making a comparison between the seasons less strong.

F3b: dry season vs wet season satellite images



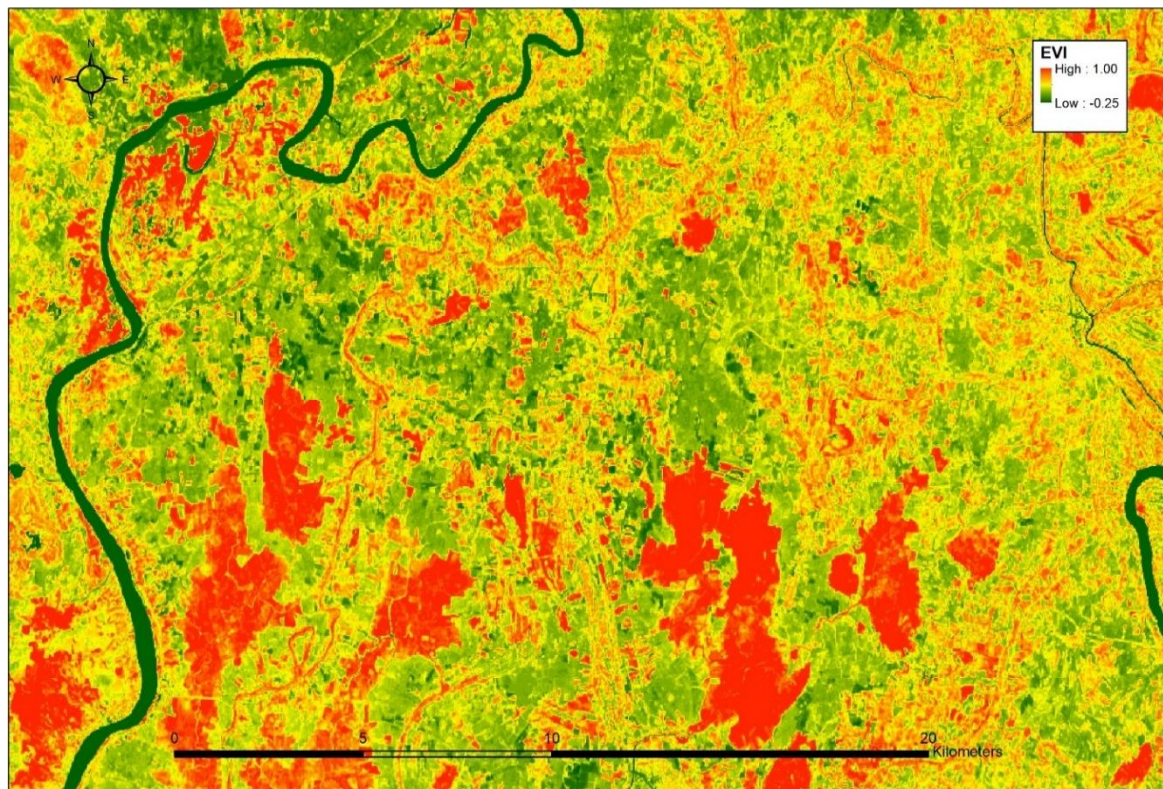
A clear distinction is visible between the vegetated state of the Ayeyarwady Delta during the dry season (left) and the rainy season (right). Not all scenes are shot on the same day. Therefore, the difference in contrast (dry season) and the degree of cloud cover (rainy season) is visible in the otherwise seamless flow of one scene to the next.

F4a: dry season satellite image



Landsat 8 OLI (Vermote et al., 2016) dry season satellite image for an arbitrary location within the research area.

F4b: Enhanced Vegetation Index for dry season image



Calculated EVI for the Appendix F4a satellite image. Vegetated areas are now highlighted in red and selectable.

F5: Normalized Difference Vegetation Index and Enhanced Vegetation Index workflow

Step 1: Earth Explorer

- Landsat imagery → bulk download provides individual bands → “bulk app”.
- Formula NDVI = (Band 5 – Band 4)/(Band5 + Band 4).
- Formula EVI = G *(Band 5 – Band 4)/(Band5 +C1*Band4 - C2*Band2 +L).
- Thus, prep individual bands 2, 4, 5 by removing zero-values (SetNull(raster == 0, raster)).

Step 2: prep imagery

- Digital Number (DN) Spectral radiance conversion to Top Of Atmosphere (TOA) planetary reflectance for Landsat-8 Operational Land Imager scenes in 4 steps.
 - o Within the metadata necessary information: reflectance_mult_band, reflectance_add_band, sun_elevation.

1. General formula for calculating the reflectance value, without sun angle adjustment

$$\rho\lambda' = M \rho * Q_{cal} + A \rho \quad (\text{formula 1})$$

$\rho\lambda'$ = TOA planetary reflectance, without correction for the solar angle

$M \rho$ = the band-specific multiplicative rescaling factor from the metadata (reflectance_mult_band_x)

Q_{cal} = quantized and calibrated standard product pixel value (DN) (the band-raster in GIS)

$A \rho$ = the band-specific additive rescaling factor from metadata (reflectance_add_band_x)

2. General formula for correcting the reflectance value with sun angle

$$\rho\lambda = \rho\lambda' / \cos(\Theta_{SZ}) = \rho\lambda' / \sin(\Theta_{SE}) \quad (\text{formula 2})$$

$\rho\lambda$ = TOA planetary reflectance, with correction for the solar angle

Θ_{SE} = Sun elevation

Θ_{SZ} = local solar zenith angle

Θ_{SZ} radian = $(90^\circ - \Theta_{SE})$

3. Formula 1 and 2 combined

$$\rho\lambda = (M \rho * Q_{cal} + A \rho) / (\cos((90^\circ - \Theta_{SE}) * \pi / 180^\circ)) \quad (\text{formula 3})$$

4. Calculate in raster calculator

- E.g. default Run: $\rho\lambda = (2.0000E-05 * \text{band-raster} + -0.100000) / (\cos((90^\circ - \Theta_{SE}) * \pi / 180^\circ))$

Step 3: mosaic

- Create empty raster dataset (check source specs).
- Then → data management tools, raster, raster dataset, mosaic.

Step 4: calculate EVI & NDVI

- Raster Calculator: $EVI = 2.5 * ((\text{Band 5} - \text{Band 4}) / ((\text{Band 5} + 6 * \text{Band 4}) - (7.5 * \text{Band 2} + 1)))$
- Raster Calculator: $NDVI = \{\text{NIR} - \text{Red}\} / \{\text{NIR} + \text{Red}\}$
Where band 4 is the Red colour, Band 2 is the blue colour and Band 5 is the Near Infra-red colour.

G1: iMOD-WQ example runfile

[GEN]

RUNTYPE = SEAWAT
MODELNAME = Ayeyarwady_01
WRITEHELP = TRUE
RESULT_DIR = \Results\Paleo_results\2a_Ayeyarwady_Voxels_Parallel_0_MIN56
PACKAGES = DIS, BAS6, OC, LPF, GHB, RIV, DRN, RCH, BTN, ADV, DSP, SSM, VDF, PKSF, PKST
COORD_XLL = 0.000000
COORD_YLL = 0.000000

[DIS]

NLAY = 10
NROW = 544
NCOL = 470
NPER = 8
DELC_R? = 1000.
DELR_C? = 1000.
TOP = \DB_Wouter\DIS\BOT\Wouter\Voxel_Model_Ayeyarwady\DEM_Ayeyarwady.IDF
BOTM_L1
= \DB_Wouter\DIS\BOT\Wouter\Voxel_Model_Ayeyarwady\ASSF_IDEPH_2_Methode\CreateLayers\Layers_5x5_5xvar\INT_L1.IDF
BOTM_L2
= \DB_Wouter\DIS\BOT\Wouter\Voxel_Model_Ayeyarwady\ASSF_IDEPH_2_Methode\CreateLayers\Layers_5x5_5xvar\INT_L2.IDF
BOTM_L3
= \DB_Wouter\DIS\BOT\Wouter\Voxel_Model_Ayeyarwady\ASSF_IDEPH_2_Methode\CreateLayers\Layers_5x5_5xvar\INT_L3.IDF
BOTM_L4
= \DB_Wouter\DIS\BOT\Wouter\Voxel_Model_Ayeyarwady\ASSF_IDEPH_2_Methode\CreateLayers\Layers_5x5_5xvar\INT_L4.IDF
BOTM_L5
= \DB_Wouter\DIS\BOT\Wouter\Voxel_Model_Ayeyarwady\ASSF_IDEPH_2_Methode\CreateLayers\Layers_5x5_5xvar\INT_L5.IDF
BOTM_L6
= \DB_Wouter\DIS\BOT\Wouter\Voxel_Model_Ayeyarwady\ASSF_IDEPH_2_Methode\CreateLayers\Layers_5x5_5xvar\INT_L6.IDF
BOTM_L7
= \DB_Wouter\DIS\BOT\Wouter\Voxel_Model_Ayeyarwady\ASSF_IDEPH_2_Methode\CreateLayers\Layers_5x5_5xvar\INT_L7.IDF
BOTM_L8
= \DB_Wouter\DIS\BOT\Wouter\Voxel_Model_Ayeyarwady\ASSF_IDEPH_2_Methode\CreateLayers\Layers_5x5_5xvar\INT_L8.IDF
BOTM_L9
= \DB_Wouter\DIS\BOT\Wouter\Voxel_Model_Ayeyarwady\ASSF_IDEPH_2_Methode\CreateLayers\Layers_5x5_5xvar\INT_L9.IDF
BOTM_L10
= \DB_Wouter\DIS\BOT\Wouter\Voxel_Model_Ayeyarwady\ASSF_IDEPH_2_Methode\CreateLayers\Layers_5x5_5xvar\INT_L10.IDF
LAYCBD_L? = 0
PERLEN_P1 = 0.001
PERLEN_P2 = 365250.0
PERLEN_P3 = 365250.0
PERLEN_P4 = 365250.0
PERLEN_P5 = 365250.0
PERLEN_P6 = 365250.0
PERLEN_P7 = 365250.0
PERLEN_P8 = 269726.0
NSTP_P? = 1.
SSTR_P1 = SS
SSTR_P2 = TR
SSTR_P3 = TR
SSTR_P4 = TR
SSTR_P5 = TR
SSTR_P6 = TR
SSTR_P7 = TR
SSTR_P8 = TR

[BAS6]

IBOUND_L1 = \DB_Wouter\BAS6\IB\Wouter\IB_0_MIN56.IDF
IBOUND_L2:10 = \DB_Wouter\BAS6\IB\Wouter\Active_inactive\IB_0_MIN56.IDF
HNOFLO = -9999.
STRT_L1 = \DB_Wouter\BAS6\Starting_Head\Wouter\Starting_Head_0_MIN56.IDF
STRT_L2 = \Results\Paleo_results\1_ayeyarwady_voxels_parallel_0_10\head\head_11861082_I2.idf
STRT_L3 = \Results\Paleo_results\1_ayeyarwady_voxels_parallel_0_10\head\head_11861082_I3.idf
STRT_L4 = \Results\Paleo_results\1_ayeyarwady_voxels_parallel_0_10\head\head_11861082_I4.idf
STRT_L5 = \Results\Paleo_results\1_ayeyarwady_voxels_parallel_0_10\head\head_11861082_I5.idf
STRT_L6 = \Results\Paleo_results\1_ayeyarwady_voxels_parallel_0_10\head\head_11861082_I6.idf
STRT_L7 = \Results\Paleo_results\1_ayeyarwady_voxels_parallel_0_10\head\head_11861082_I7.idf
STRT_L8 = \Results\Paleo_results\1_ayeyarwady_voxels_parallel_0_10\head\head_11861082_I8.idf

STRT_L9 = .\Results\Paleo_results\1_ayeyarwady_voxels_parallel_0_10\head\head_11861082_I9.idf
STRT_L10 = .\Results\Paleo_results\1_ayeyarwady_voxels_parallel_0_10\head\head_11861082_I10.idf

[OC]

SAVEHEAD_P?_L? = TRUE
SAVECONCLAYER_P?_L? = TRUE
SAVEBUDGET_P?_L? = TRUE
SAVEHEADTEC_P?_L? = TRUE
SAVECONCTEC_P?_L? = TRUE
SAVEVXTEC_P?_L? = TRUE
SAVEVYTEC_P?_L? = TRUE
SAVEVZTEC_P?_L? = TRUE

[LPF]

HDRY =1E+30
NPLPF =0
LAYTYP_L? =0
LAYAVG_L? =0
CHANI_L? =1.0
LAYVKA_L? =1.0
HK_P?_L1:5 =10.0
HK_P?_L6 =.\DB_Wouter\LPF\Wouter\LYR_INT6_K.IDF
HK_P?_L7 =.\DB_Wouter\LPF\Wouter\LYR_INT7_K.IDF
HK_P?_L8 =.\DB_Wouter\LPF\Wouter\LYR_INT8_K.IDF
HK_P?_L9 =.\DB_Wouter\LPF\Wouter\LYR_INT9_K.IDF
HK_P?_L10 =.\DB_Wouter\LPF\Wouter\LYR_INT10_K.IDF
VKA_P?_L? =0.1
SS_P?_L1:10 =0.0021

[GHB]

MXACTB = 2500000
IGHBCB = 0
MGHBSYS = 1
BHEAD_P?_S?_L1 =.\DB_Wouter\GHB\HEAD\Wouter\Layer_1_10\GHB_HEAD_0_MIN56.IDF
COND_P?_S?_L1 =.\DB_Wouter\GHB\COND\Wouter\Layer_1_10\GHB_COND_0_MIN56.IDF
GHBSSMDENS_P?_S?_L1 =1000.0

[RIV]

MXACTR = 2500000
IRIVCB = 0
MRIVSYS = 1
STAGE_P?_S?_L1 =.\DB_Wouter\RIV\LEVEL\Wouter\Layer_1\RIV_LEVEL_L1_0_MIN56.IDF
STAGE_P?_S?_L2 =.\DB_Wouter\RIV\LEVEL\Wouter\Layer_2\RIV_LEVEL_L2_0_MIN56.IDF
COND_P?_S?_L1 =.\DB_Wouter\RIV\COND\Wouter\Layer_1\RIV_COND_L1_0_MIN56.IDF
COND_P?_S?_L2 =.\DB_Wouter\RIV\COND\Wouter\Layer_2\RIV_COND_L2_0_MIN56.IDF
RBOT_P?_S?_L1 =.\DB_Wouter\RIV\DEPTH\Wouter\Layer_1\RIV_DEPTH_L1_0_MIN56.IDF
RBOT_P?_S?_L2 =.\DB_Wouter\RIV\DEPTH\Wouter\Layer_2\RIV_DEPTH_L2_0_MIN56.IDF
RIVSSMDENS_P?_S?_L? =1000.

[DRN]

MXACTD = 2500000
IDRNCB = 0
MDRNSYS = 1
ELEVATION_P?_S?_L1 =.\DB_Wouter\DRN\Wouter\Drainage_Elevation_0_MIN56.IDF
COND_P?_S?_L1 = 5000.0

[RCH]

NRCHOP = 1
IRCHCB = 0
RECH_P? =.\DB_Wouter\RCH\Wouter\Uniform\Recharge_Uniform_1mm_0_MIN56.IDF

[BTN]

DZ_P?_L1:5 =.\DB_Wouter\BTN\DZ\Wouter\DZ_New\DZ_5m.IDF
DZ_P?_L5:10 =.\DB_Wouter\BTN\DZ\Wouter\DZ_New\DZ_Variable.IDF
PRSITY_L1:10 =.3
ICBUND_L1 =.\DB_Wouter\BAS6\IB\Wouter\IB_0_MIN56.IDF
ICBUND_L2:10 =.\DB_Wouter\BAS6\IB\Wouter\Active_inactive\IB_0_MIN56.IDF
SCONC_L1 =.\DB_Wouter\BTN\Starting_Concentration\Wouter\Starting_Concentration_0_MIN56.IDF
SCONC_L2 =.\Results\Paleo_results\1_ayeyarwady_voxels_parallel_0_10\conc\conc_11861082_I2.idf
SCONC_L3 =.\Results\Paleo_results\1_ayeyarwady_voxels_parallel_0_10\conc\conc_11861082_I3.idf
SCONC_L4 =.\Results\Paleo_results\1_ayeyarwady_voxels_parallel_0_10\conc\conc_11861082_I4.idf

SCONC_L5 = \Results\Paleo_results\1_ayeyarwady_voxels_parallel_0_10\conc\conc_11861082_I5.idf
SCONC_L6 = \Results\Paleo_results\1_ayeyarwady_voxels_parallel_0_10\conc\conc_11861082_I6.idf
SCONC_L7 = \Results\Paleo_results\1_ayeyarwady_voxels_parallel_0_10\conc\conc_11861082_I7.idf
SCONC_L8 = \Results\Paleo_results\1_ayeyarwady_voxels_parallel_0_10\conc\conc_11861082_I8.idf
SCONC_L9 = \Results\Paleo_results\1_ayeyarwady_voxels_parallel_0_10\conc\conc_11861082_I9.idf
SCONC_L10 = \Results\Paleo_results\1_ayeyarwady_voxels_parallel_0_10\conc\conc_11861082_I10.idf
CINACT = -9999
NPRS = 0
IFMTCN = -1
CHKMAS = TRUE
NPRMAS = 10
NPROBS = 1
DTO_P? = 1000.
MXSTRN_P? = 10000
TTSMULT_P? = 1.

[ADV]

MIXELM = 0
PERCEL = .75
MXPART = 1000000
ITRACK = 1
WD = 0.5

[DSP]

AL_L? = 10.
TRPT_L? = 0.1
TRPV_L? = 0.1
DMCOEF_L? = 0.0000864

[SSM]

MXSS = 20000000
CRCH_T1_P? = 1.1
CRIV_T1_P? = 1.1
CDRN_T1_P? = 1.1
CGHB_T1_P?_L1 = \DB_Wouter\GHB\CONC\Wouter\Layer_1\GHB_CONC_L1_0_MIN56.IDF

[VDF]

MTDNCONC = 1
MFNADVDF = 2
NSWTCPL = 1
IWTABLE = 0
DENSEMIN = 1000.
DENSEMAX = 1025.
DENSEREF = 1000.
DENSESLP = 0.7143

[PKSF]

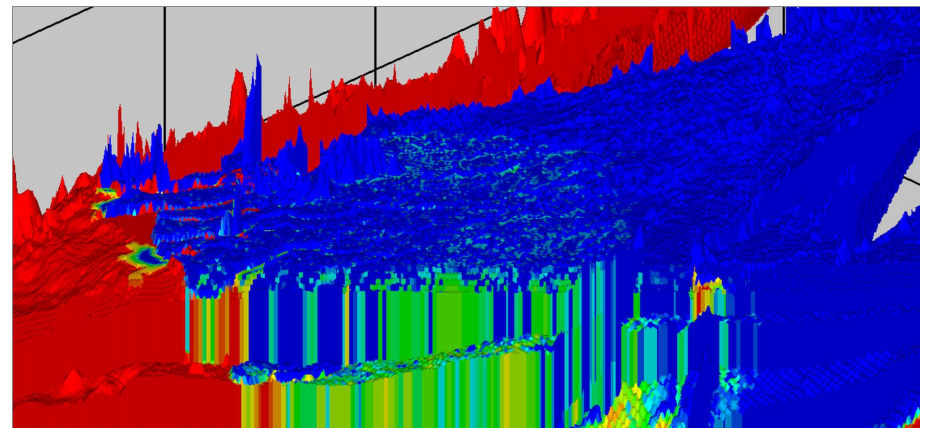
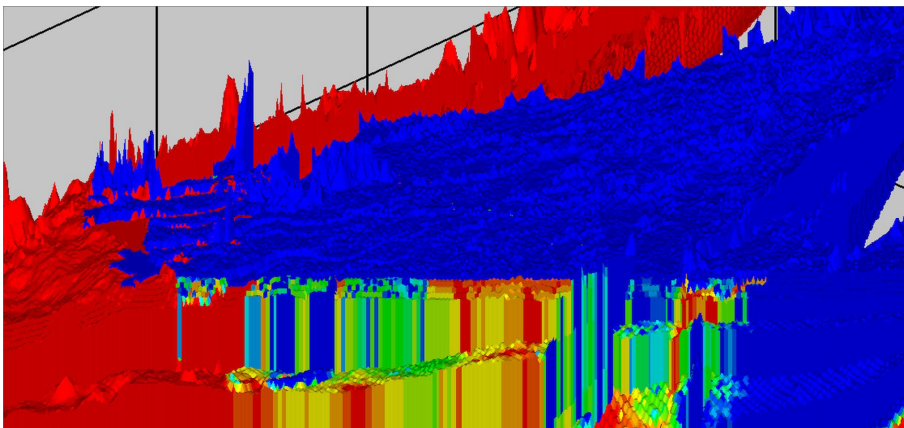
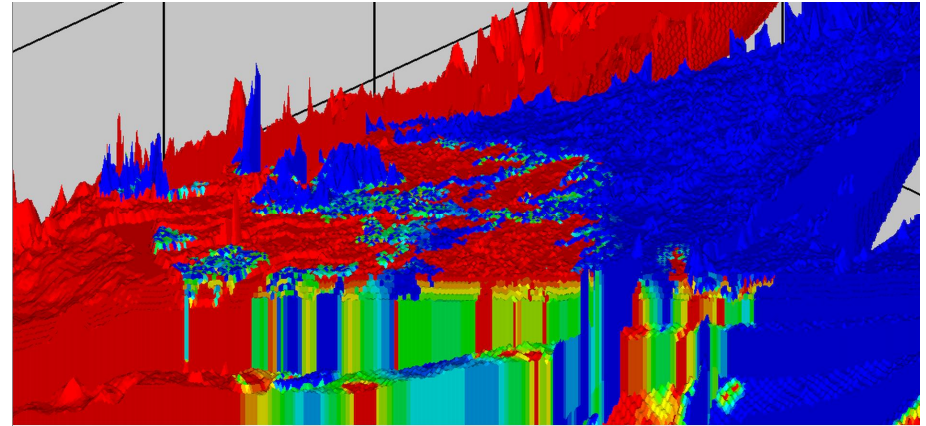
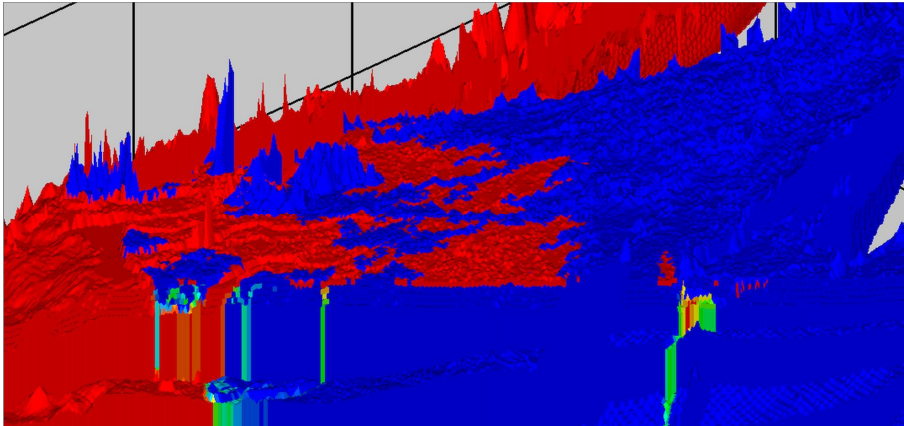
ISOLVER = 1
NPC = 2
NPCDEF = 0
MXITER = 200
INNERIT = 30
RELAX = 0.98
HCLOSEPKS = 0.01
RCLOSEPKS = 10000.0
PARTOPT = 0

[PKST]

ISOLVER = 2
NPC = 2
MXITER = 1000
INNERIT = 30
RELAX = 0.98
CCLOSEPKS = 0.00001
PARTOPT = 0

**More information on packages and their corresponding input parameters can be found in the iMOD-WQ Manual (Verkaik & Janssen, 2019).*

G2: transgression/regression cycles



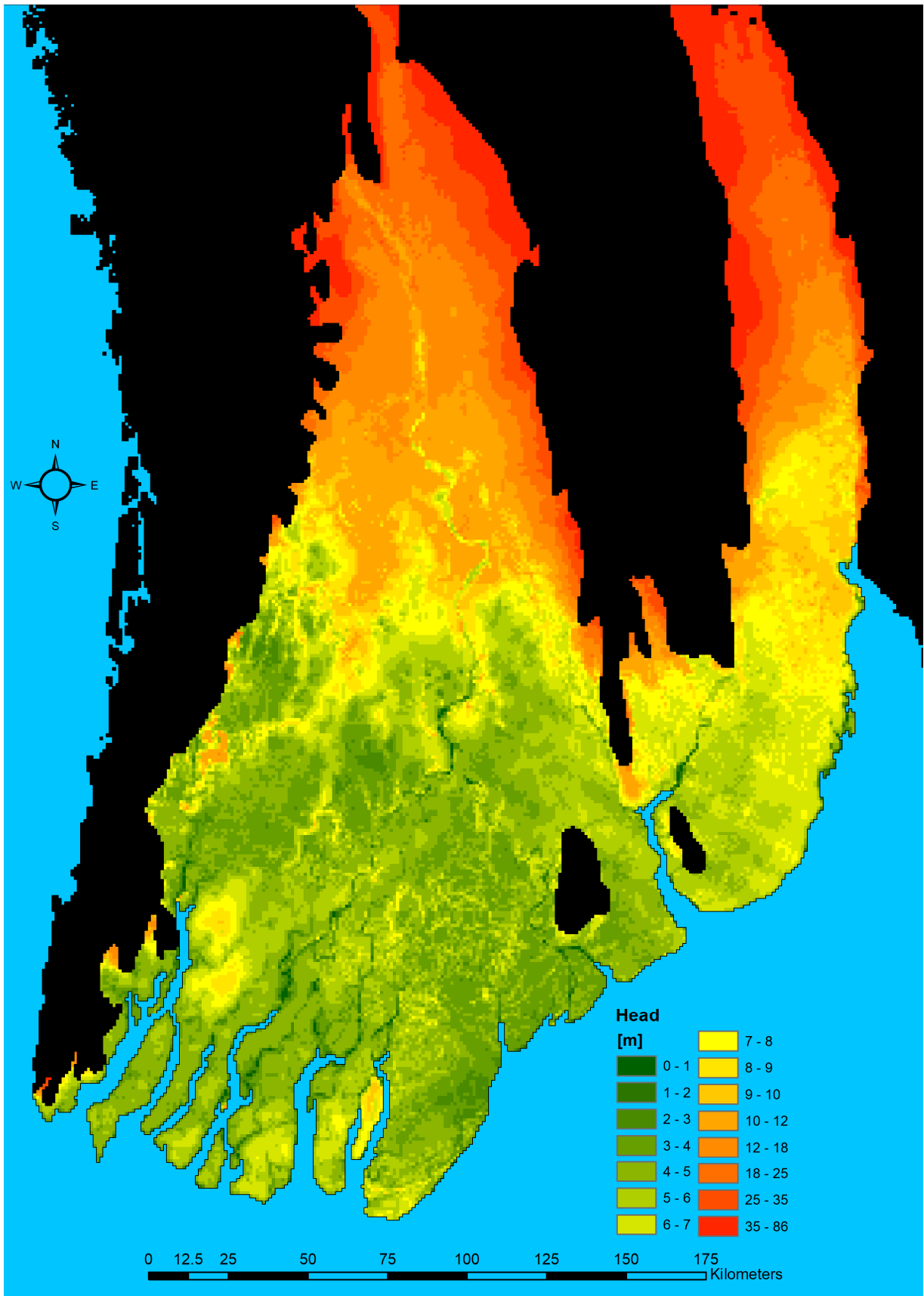
Transgressional seawaters (red) are forced upon the model by imposing a 35 g/L salt concentration on the first model layer (upper left). The initially fresh groundwater (blue), infiltrated during earlier periods of regression, slowly becomes saltier (green, yellow, orange), until reaching its proposed salinity after 850 years (upper right). The salinity of the first model layer is then reduced to 1 g/L, to simulate a receding RSL (lower left). The fresh water supply from above (recharge) manages to flush-out only a part of the salt groundwater after 1100 years of infiltration, leaving behind brackish to salty groundwater in the subsurface at certain locations (lower right).

G3: paleo-reconstruction calculation times

Run No.	RSL	Duration	No. SPs	Time	Time	Time
[-]	[m]	[years]	[-]	[hours]	[minutes]	[seconds]
1	10	9862	11	1	36	14
2a	-56	6738	8	1	59	43
2b	-56	6738	7	1	44	57
3a	-16	5627	7	1	43	11
3b	-16	5627	6	1	37	46
4	-72	9251	11	2	54	16
5a	-36	5852	7	1	51	29
5b	-36	5852	6	1	42	35
6a	-100	7885	9	2	27	56
6b	-100	7885	8	2	24	15
7a	-60	6831	8	2	3	56
7b	-60	6831	7	2	2	20
7c	-60	6831	7	2	1	30
8a	-116	9552	11	2	55	34
8b	-116	9552	10	2	50	29
9	-100	6143	8	1	53	33
10	-65	2650	4		52	21
11	-32	1350	3		28	34
12	-23	1000	2		21	50
13	-3	650	2		14	53
14	0	575	2		13	16
15	4	850	2		18	36
16	2	575	2		13	9
17	3	375	2		8	26
18	2	400	2		8	55
19	3	625	2		12	47
20	-2	1100	3		23	26
21	1	1000	2		20	24
22	0	700	2		14	7
23	2	550	2		11	30
24	0	230	2		5	53
25	0	20	2		1	29
Total		129705	160	23	842	1040
Equal to 37 hours and 17 minutes = roughly one and a half days.						

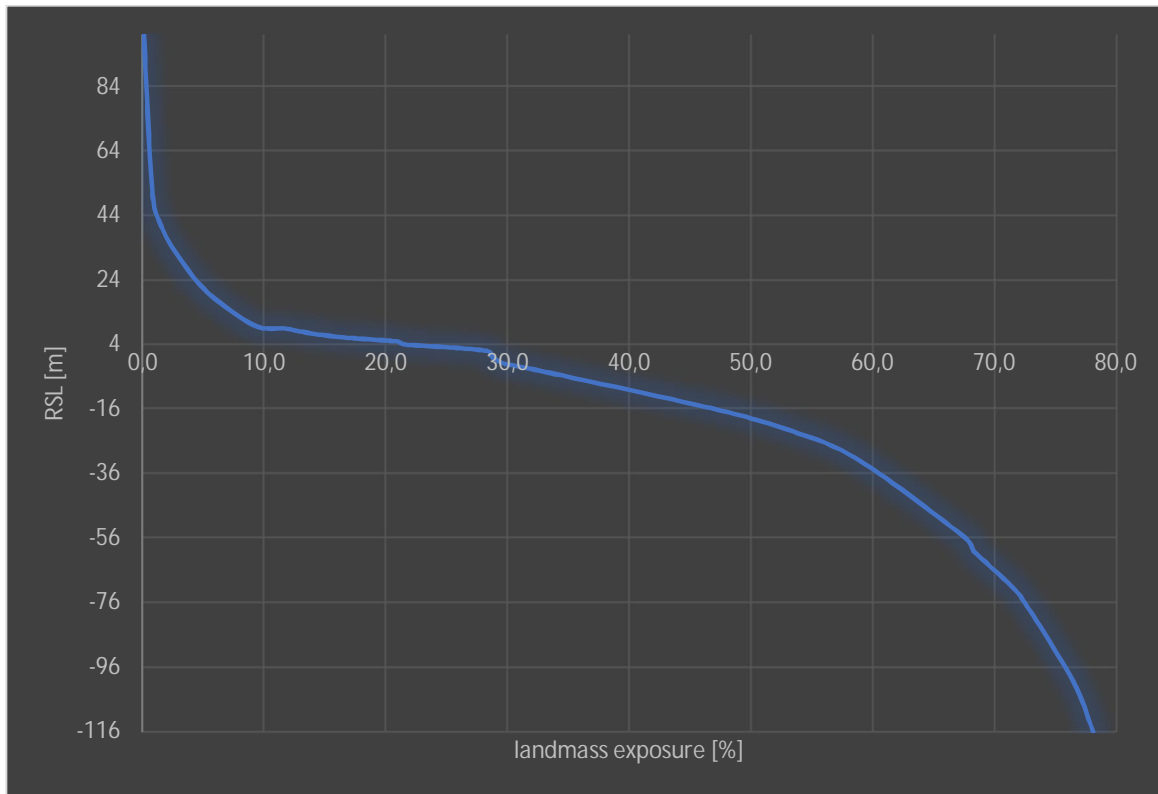
Computational times for each runfile in the paleo-reconstruction, including a summary of the total runtime of the whole paleo-reconstruction.

G4: Ayeyarwady Delta hydraulic head



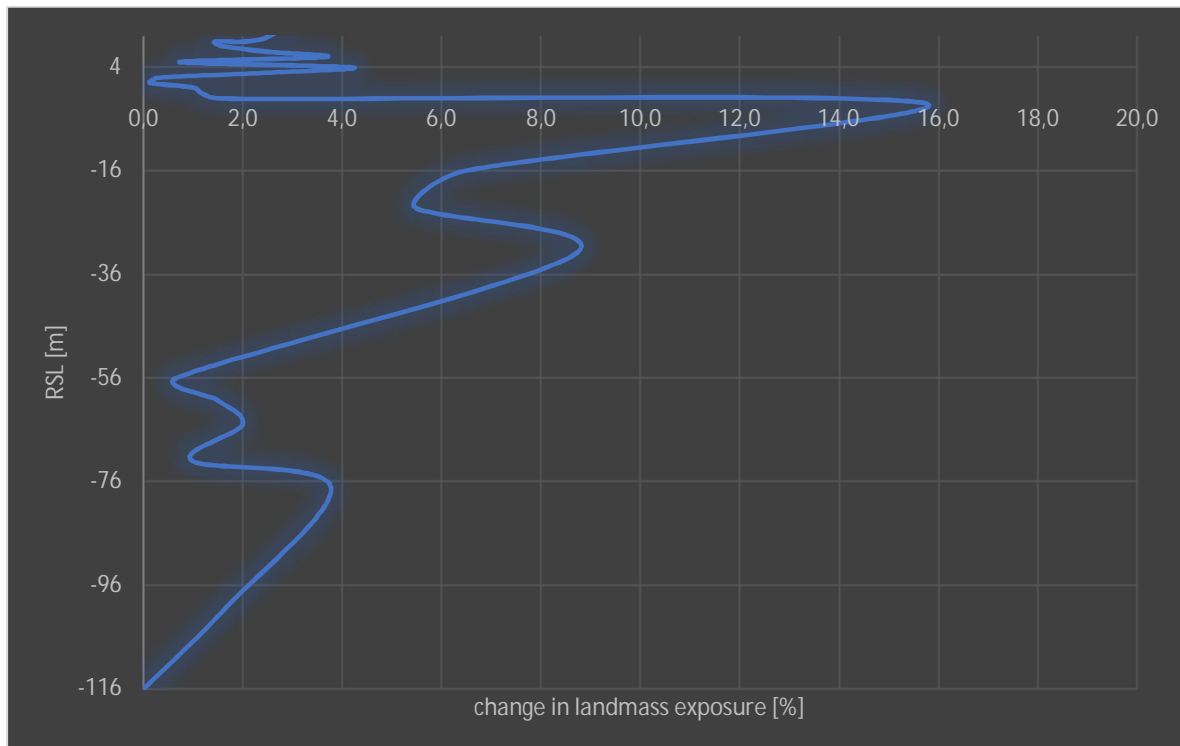
The proposed present-day hydraulic head of the Ayeyarwady Delta according to the paleo-reconstructive modelling efforts. Heads are relative to mean sea level, being 0 meters.

G5a: landmass exposed with respect to RSL



A percentual overview of the model's land/sea ratio. Example: an RSL of -16 meters (with respect to present sea level) coincides with 47% landmass exposure and a 53% ocean surface area.

G5b: percentual change in landmass exposure regarding RSLR



Each increment in RSL results in a unique associated decrease in landmass exposure. While from 0 to +1 m RSLR only results in a decrease of 0.1%, a RSLR of +4 m results in an increase of 4.2%.

G6a: Initial salinity distribution (paleo-reconstruction: 129,705 years)

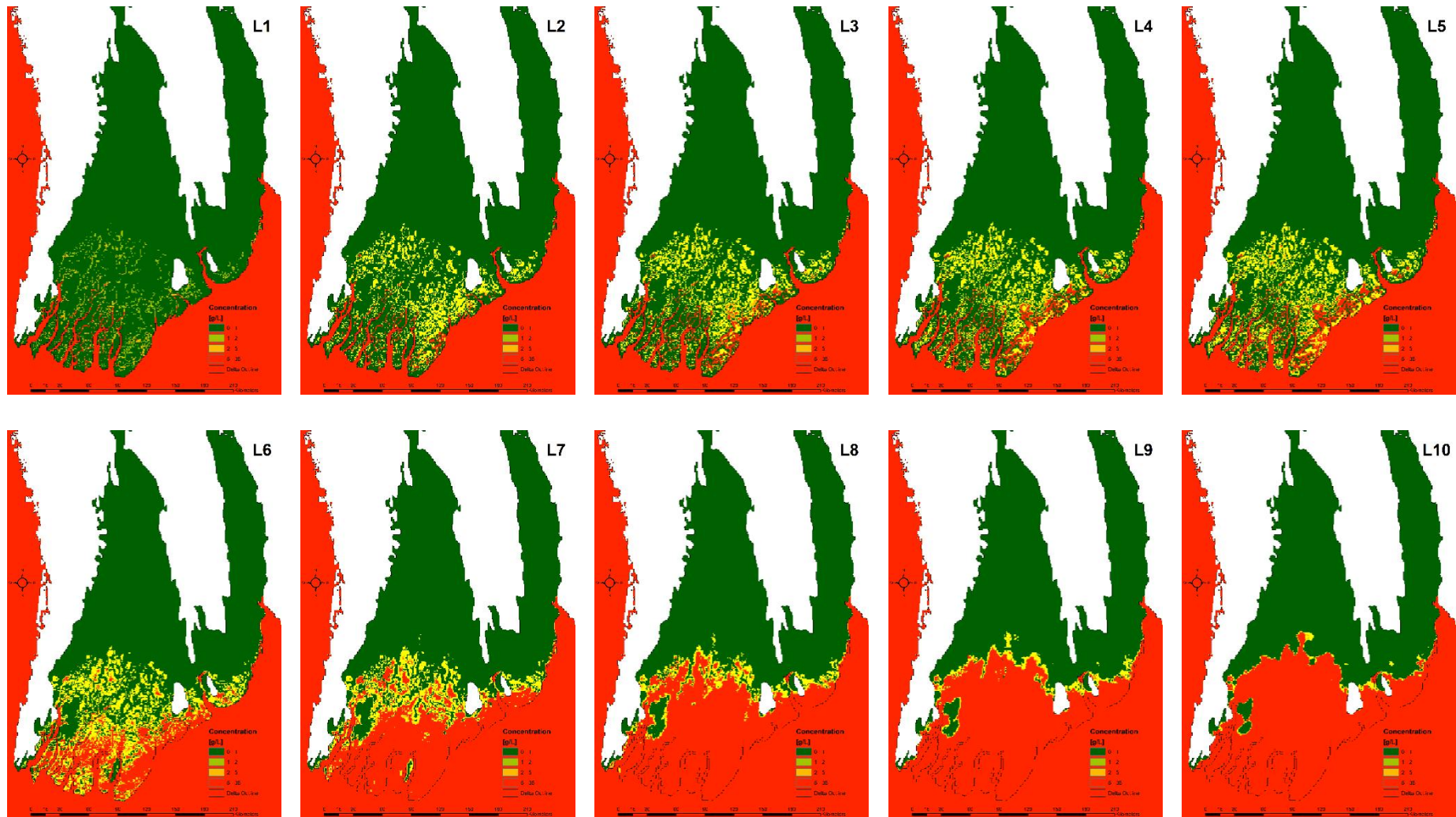
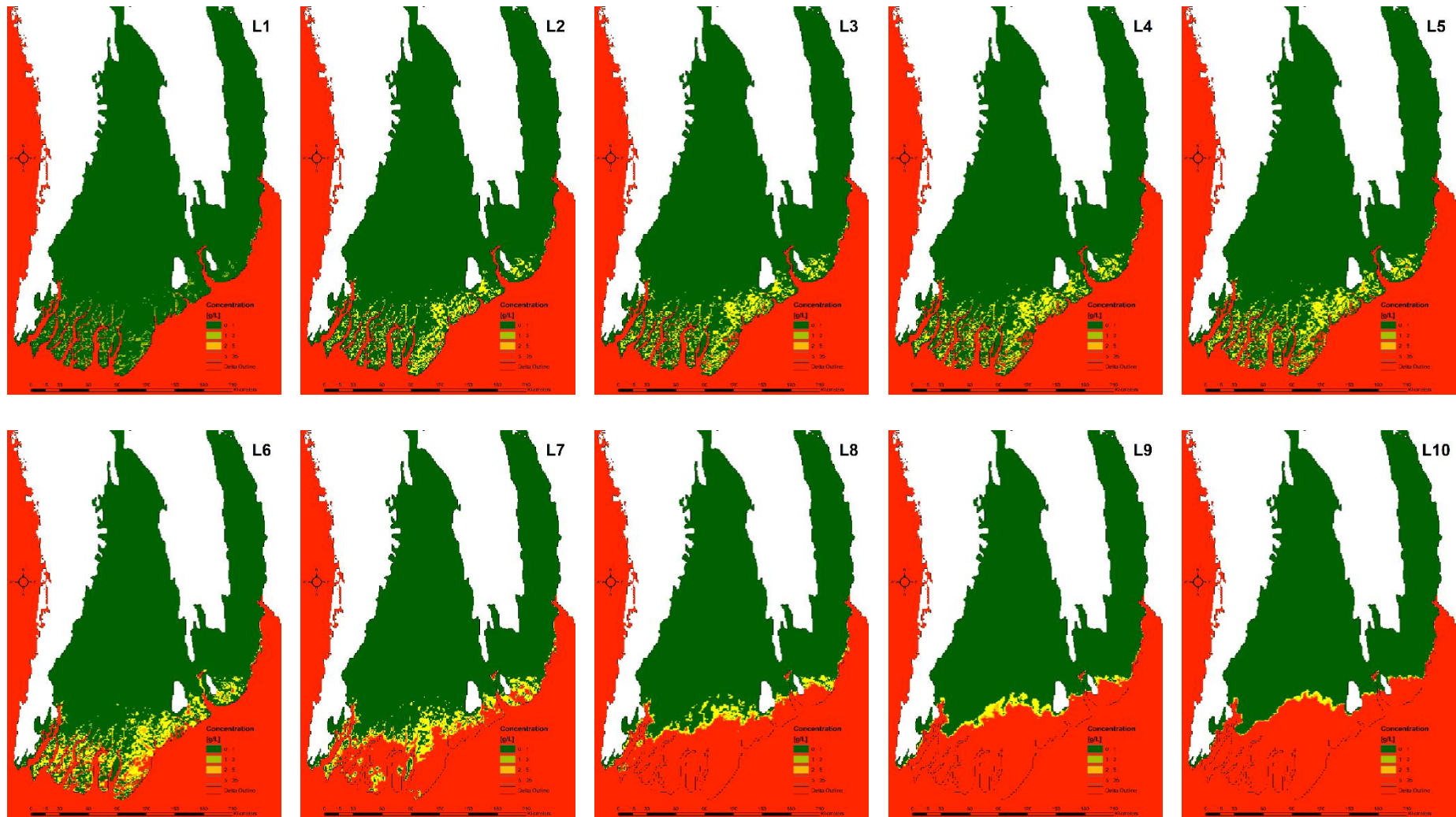


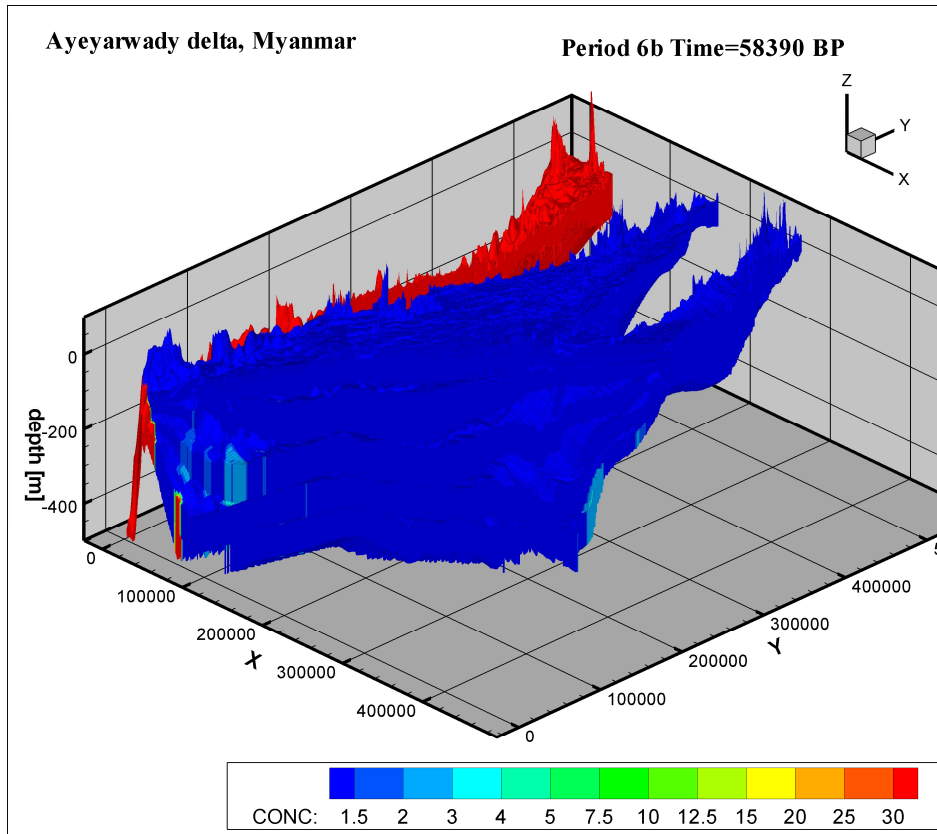
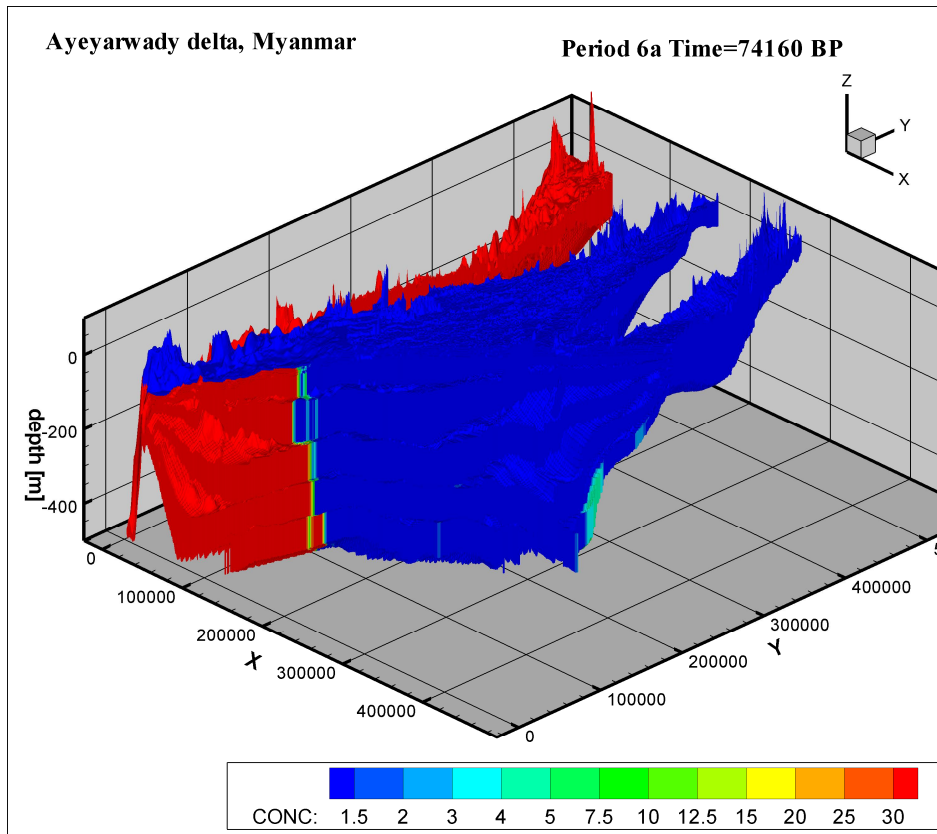
Figure 9: initial salinity distribution, as proposed by the paleo-reconstructive modelling results for each consecutive model layer. Concentrations are in g/L and are discretised by the colours dark green, light green, yellow and red for the ranges 0 – 1, 1 – 2, 2 – 5 and 5 – 35 g/L, respectively.

G6b: initial salinity distribution (present-day sea level: 130,000 years)



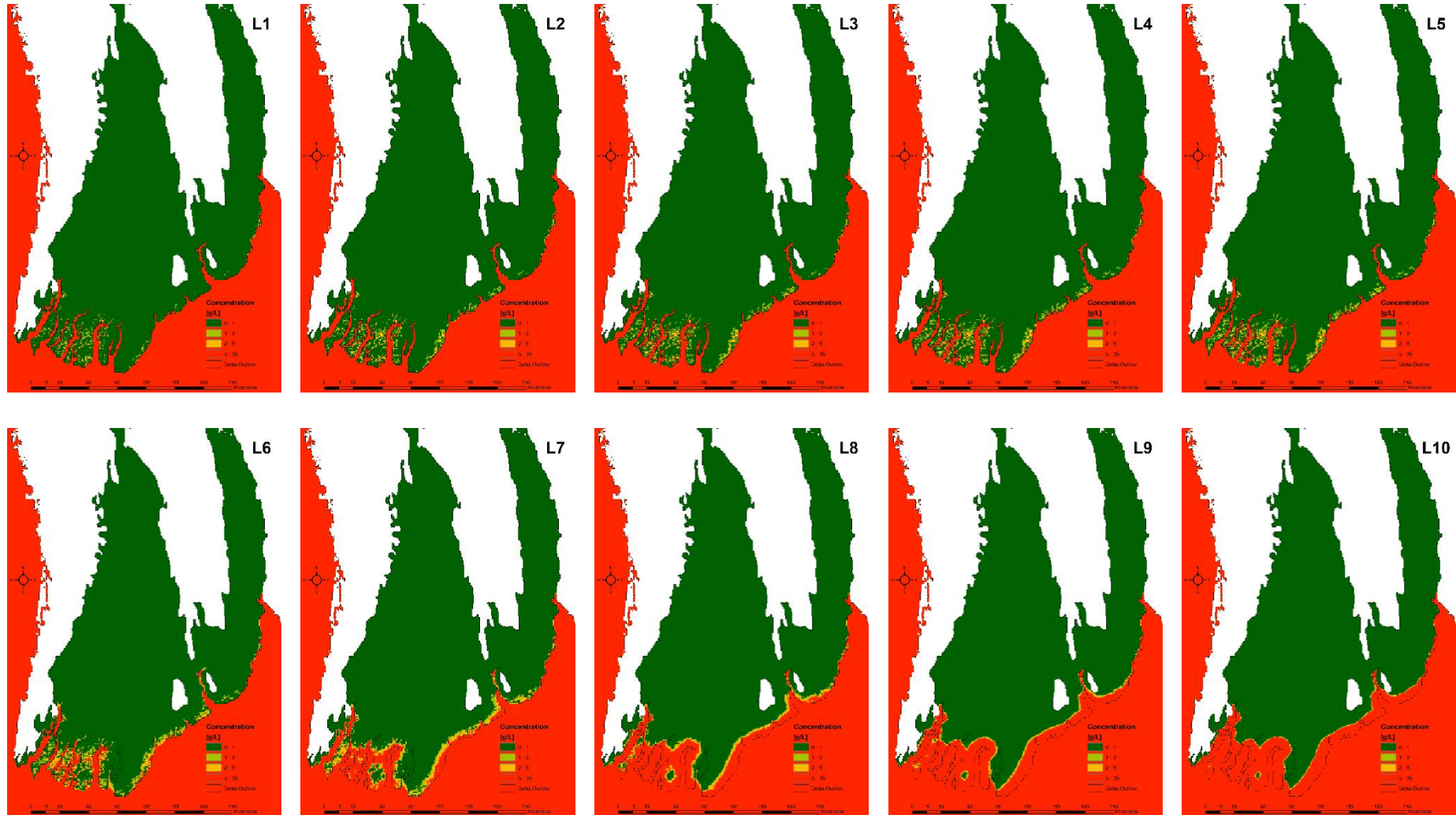
Initial salinity distribution, according to the equilibrium modelling results for each consecutive model layer. Concentrations are in g/L and are discretised by the colours dark green, light green, yellow and red for the ranges 0 – 1, 1 – 2, 2 – 5 and 5 – 35 g/L, respectively.

G7: groundwater "freshening"



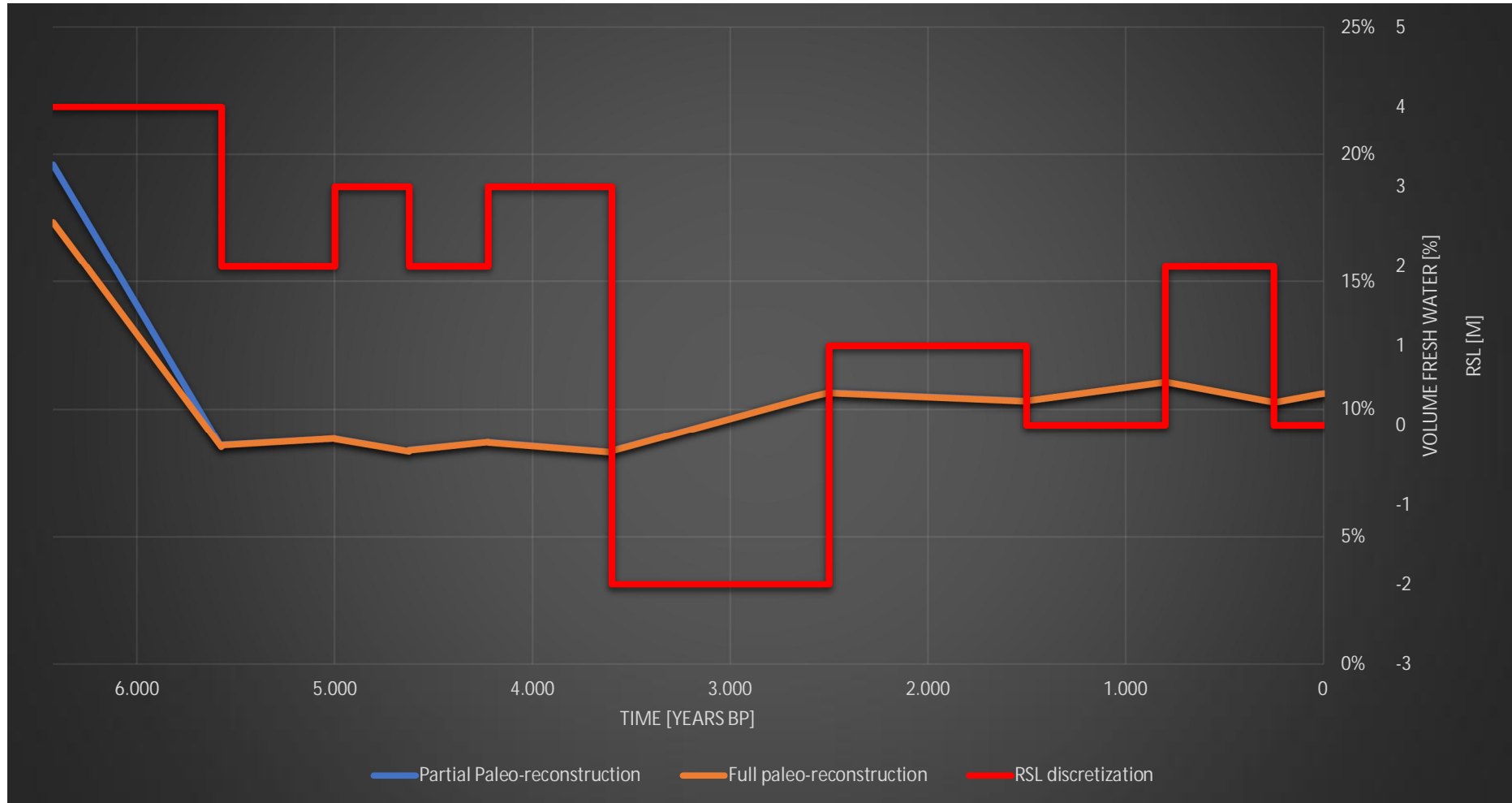
When the period of regression is long enough, the initially salt groundwater (red, upper figure) can be flushed-out almost entirely (blue, lower figure). In this example after 15,770 years.

G8: Initial salinity distribution (paleo-reconstruction: 6,425 years BP)



Initial salinity distribution as proposed by the paleo-reconstructive modelling results (6425 years) for each consecutive model layer. Concentrations are in g/L and are discretised by the colours dark green, light green, yellow and red for the ranges 0 – 1, 1 – 2, 2 – 5 and 5 – 35 g/L, respectively.

G9: Fresh groundwater volume differences between the full and the partial paleo-reconstructive modelling run



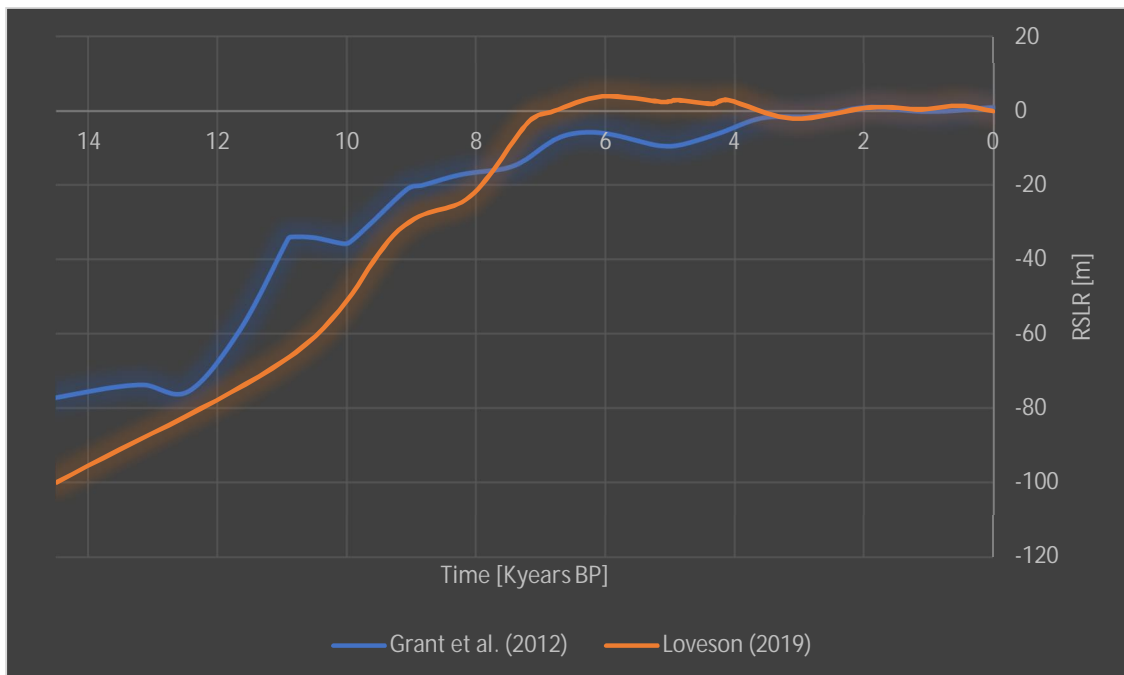
The figure above provides a comparison of the proposed fresh groundwater volumes of the Ayeyarwady Delta by the full paleo-reconstructive modelling run of 129,705 years (orange) compared to the partial paleo-reconstructive modelling run of 6,425 years (blue). The figure suggests an almost identical end result.

H1: wells located in the model's inactive area

Location	Well-IDs	Depth to "X"	Depth to Bedrock [m]
Hinthada District	A18	-150	-170
	A24	-156	-156
	A25	-128	-174
	A26	-152	-176
Yangon City	B0913	-89	-124
	B1705	-101	-101
	B2604	-16	-117
South Yangon	G8	-84	-320
	G9	-86	-261
	G12	-143	-292
	G22	-140	-299
Pathein District	F52	-87	-146
	F53	-86	-146
	F54	-87	-146
	F68	-124	-124
	F70	-61	-61
	F74	-86	-86

An overview of the wells that had their registered lithological sequence taken into account when modelling the 3D hydrogeological model, whilst being located outside of the actively modelled area. Depths are in meters below sea level.

H2: RSLR-curve discrepancies



An overview of the discrepancies between the two RSLR-curves used for paleo-reconstructive modelling for the period 14500 BP until present.

H3a: agricultural well extractions

Agriculture	
No. wells	14044
Avg. extraction per well	28.4

Layer No.	Q_Sum [m3/d]
Layer 6	283056
Layer 7	71688
Layer 8	25223
Layer 9	9146
Layer 10	9798
Total	398911

The total volume of groundwater extracted, specified per model layer, for the benefit of agriculture use.

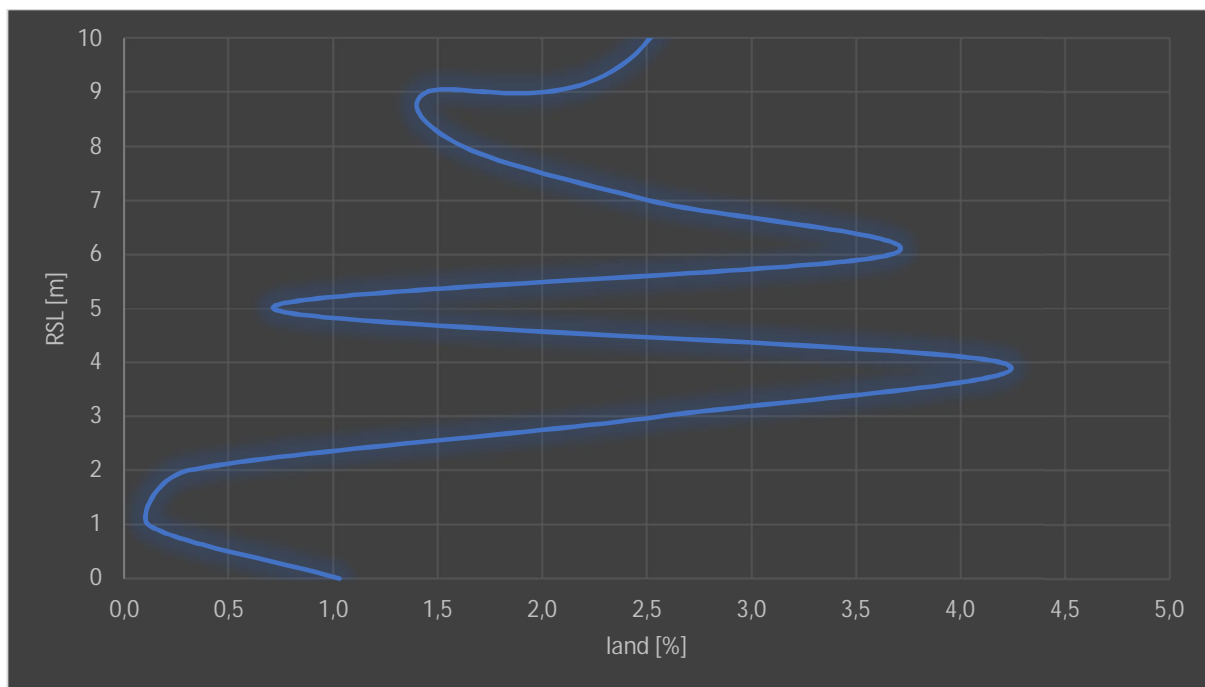
H3b: domestic well extractions

Domestic	
No. wells	349110
Avg. extraction per well	0.4

Layer No.	Q_Sum [m3/d]
Layer 6	82210
Layer 7	36356
Layer 8	11199
Layer 9	4424
Layer 10	5455
Total	139644

The total volume of groundwater extracted, specified per model layer, for the benefit of domestic use.

I1: change in landmass exposure regarding RSLR - zoomed



Each increment in RSL results in a unique associated decrease in landmass exposure. While from 0 to +1 m RSLR only results in a decrease of 0.1%, a RSLR of +4 m results in an increase of 4.2%.